5-2012

In Vitro Alterations of a Putative Phospholipid Translocase, *Atp10c*, and Its Role in Glucose Metabolism

Sarah Elizabeth Hurst
shurst6@utk.edu

To the Graduate Council:

I am submitting herewith a dissertation written by Sarah Elizabeth Hurst entitled "*In Vitro* Alterations of a Putative Phospholipid Translocase, *Atp10c*, and Its Role in Glucose Metabolism." I have examined the final electronic copy of this dissertation for form and content and recommend that it be accepted in partial fulfillment of the requirements for the degree of Doctor of Philosophy, with a major in Comparative and Experimental Medicine.

Madhu Dhar, Major Professor

We have read this dissertation and recommend its acceptance:

John Biggerstaff, Guoxun Chen, Carla Sommardahl

Accepted for the Council:

Carolyn R. Hodges

Vice Provost and Dean of the Graduate School

(Original signatures are on file with official student records.)

In Vitro Alterations of a Putative Phospholipid Translocase, *Atp10c*, and Its Role in Glucose Metabolism

A Thesis Presented for the
Doctor of Philosophy
Degree
The University of Tennessee, Knoxville

Sarah Elizabeth Hurst
May 2012

DEDICATION

Once upon a time, chemist and physicist Marie Curie said,

“I am among those who think that science has great beauty.

A scientist in his laboratory is not only a technician:

He is also a child placed before natural phenomena

which impress him like a fairy tale.”

This dissertation is dedicated to the child in all of us

who are still fascinated by the fairy tale that is science.

ACKNOWLEDGEMENTS

There are many people that deserve acknowledgement and thanks for their help in the completion of this thesis dissertation. First and foremost, I must thank my Heavenly Father for all the wondrous blessings He bestows on me from day to day. I am truly thankful for His grace and mercy, which is sufficient for a sinner like me. Secondly, I'd like to acknowledge my parents, W. Dale and Judy Hurst, and my grandparents, Gerald and Virginia Hurst and John and Lelia Woodruff. Their pride in my accomplishments motivates me and pushes me onward to future goals. I also must thank my friends for their unfailing love and support. I wouldn't have made it through the past few years without it!

Without hesitation, I'd like to thank my advisor and mentor, Dr. Madhu Dhar. During my time here at the University of Tennessee-Knoxville, I came to respect her as both a mentor and friend, and as a skilled scientist and researcher. She is definitely one of the most dedicated and generous people that I have ever had the privilege to work with, and to know. She believed in me in times when I needed it the most and took a chance on me when no one else would. For that I dedicate the work in this dissertation to her. I am truly grateful for all you have done in my life.

I would also like to acknowledge the assistance and guidance from the remaining members of my dissertation committee, Drs. John Biggerstaff, Guoxun Chen, and Carla Sommardahl. Their willingness and dedication to my graduate research experience was greatly appreciated. I am very thankful for all their help and encouragement over the last few years. I would also like to give a special thanks to several generous collaborators,

Drs. Sujata Agarwal, Steven Minkin, John Dunlap, Nolan Hoffmann, Jeffrey Elmendorf, and Ling Zhao, and Mr. Keith Prater for their help in learning and running real-time PCR experiments, in immunofluorescence techniques and imaging, and lastly, in procuring the L6-G4myc samples and the mouse tissue samples from the DIO and *ob/ob* mice. Without these individuals, I truly would have been lost and this project would not have ended as it has done.

Last, but not least, I would like to give a heartfelt thanks to all the faculty and staff in the Department of Large Animal Clinical Sciences, especially Ms. Catheryn Hance and Ms. Linda Beets. Their help was immediate and much appreciated! I also need to thank the Comparative and Experimental Medicine Program and the University of Tennessee Veterinary Medical Center, and its associated faculty and staff. Ms. Kim Rutherford and Ms. Misty Bailey proved invaluable assistance when asked and always provided a smiling face and a kind word when it was most needed. Moreover, the work in this dissertation would not have been possible without the funding agencies, The American Diabetes Association, The University of Tennessee Center of Excellence in Livestock Diseases and Human Health, and the University of Tennessee Obesity Research Center. Additional thanks to the unsung heroes, Ms. Nancy Neilson, Ms. Sarah Elliot, the soon-to-be Dr. Erin Bartley, and Ms. Lisa Amelse, who have helped me so much along the way!

ABSTRACT

Atp10c/ATP10C is a putative aminophospholipid translocase or "flippase" that encodes for a type 4 P-type ATPase. Based on previous research, we hypothesize that *Atp10c*/ATP10C due to its flippase nature plays a role in diet-induced obesity and type 2 diabetes as *Atp10c* heterozygous mice display this phenotype.

For purposes of this dissertation, *Atp10c*/ATP10C was characterized both generally and biologically to gleam information about its molecular weight, cellular location and possible biological roles and/or functions. Multiple experiments, both *in vitro* and *in vivo*, were performed in order to accomplish these characterizations and are discussed at length.

Essential results from this dissertation work include the validation of ATP10C's expected molecular weight (~165 kD), the localization of ATP10C to the plasma membrane, its possible co-localization with GLUT4, and the high expression of *Atp10c* in key tissues (skeletal muscle and adipose tissue) of two mice models, one a model of diet-induced obesity mice and another a genetic model (*ob/ob*).

To identify molecular and cellular targets of ATP10C, *Atp10c* expression was altered *in vitro* in C2C12 and L6-G4myc skeletal muscle myotubes. Functional outcomes of GLUT4 translocation and glucose uptake assays were performed resulting in the significant alteration of normal GLUT4 regulation and a significant decrease in glucose uptake. Additionally, when the expression of *Atp10c* was altered both experimentally and genetically, significant up-regulation of native and activated mitogen-activated protein kinases, p38, and ERK1/2 were observed. These results demonstrate that *Atp10c*-

silencing does affect these main mitogen-activated protein kinase proteins and in turn, glucose metabolism via both insulin-independent and insulin-dependent manners.

Taken together, all these results presented in this dissertation indicate that *Atp10c*/ATP10C has an important role in the regulation of glucose metabolism, at least in part via the mitogen-activated protein kinase pathway, and as such, plays a significant role in the development of insulin resistance and type 2 diabetes.

TABLE OF CONTENTS

LIST OF FIGURES

LIST OF ABBREVIATIONS

2-DOG	2-Deoxy [3H] Glucose
α-MEM	Alpha-Modified Eagle Media
ABC	ATP-Binding Cassette Transporters
APLT	Aminophospholipid Translocase
AS	Angelman Syndrome
BCA	Bovine Calf Albumin
BCS	Bovine Calf Serum
BMI	Body Mass Index
DAPI	4', 6-Diamidino-2-Phenylindole, Dilactate
DIO	Diet-Induced Obesity
DMEM	Dubecco's Modified Eagle Media
DMSO	Dimethyl Sulfoxide
ECL	Enhanced Chemiluminescence
ER	Endoplasmic Reticulum
ERK	Extracellular Signal Regulated Kinases
FBS	Fetal Bovine Serum
GLUT	Glucose Transporters
GLUT1	Glucose Transporter 1
GLUT4	Glucose Transporter 4
GSV	Glucose Storage Vesicles
HBSS	Hank's Balanced Salt Solution
HDL-C	High-Density Lipoprotein Cholesterol

HEK293T	Human Embryonic Kidney Cells 293T
HEPES	4-(2-Hydroxyethyl)-1-Piperazineethanesulfonic Acid
HRP	Horseradish Peroxidase
IR	Insulin Resistance
IRS	Insulin Receptor Substrate
JNK	c-Jun NH_2-terminal Kinases
KRP	Krebs-Ringer
L6-G4myc	Rat L6 Overexpressing GLUT4-myc
LDL-C	Low-Density Lipoprotein Cholesterol
MAPK	Mitogen-Activated Protein Kinase
NAFLD	Non-Alcoholic Fatty Liver Disease
NASH	Non-Alcoholic Steatohepatitis
PAGE	Polyacrylamide Gel Electrophoresis
PC	Phosphatidylcholine
PE	Phosphatidylethanolamine
PI3K	Phosphatidylinositol-3-Kinase
PI	Phosphatidylinositol
pi	Protease Inhibitors
PS	Phosphatidylserine
qPCR	Real Time Polymerase Chain Reaction
RIPA	Radioimmunoprecipitation Assay
RISC	RNAi Induced Silencing Complex
RNAi	RNA Interference

RT	Room Temperature
SDS	Sodium Dodecyl Sulfate
siRNA	Small Interfering RNA
T2D	Type 2 Diabetes Mellitus
TBST	Tris-Buffered Saline and Tween 20
TRITC	Tetramethyl Rhodamine Iso-Thiocyanate

CHAPTER I

INTRODUCTION

Disease Epidemics

The incidence of type 2 diabetes mellitus (T2D) and diet-induced obesity (DIO) is increasing rapidly and reaching epidemic proportions throughout the world populations. Although the cause of T2D remains unclear, it is known that insulin resistance (IR) is closely related to the development of the disease. IR is also linked with other metabolic syndromes and it is considered to be a major contributing factor to diseases including hypertension, atherosclerosis and coronary heart failure. IR is characterized by a failure of the hormone, insulin, to result in efficient glucose disposal, and particularly produce its normal increase in glucose transport in peripheral tissues namely skeletal muscle and adipose tissue. Defective glucose uptake in skeletal muscle and adipose tissues plays a major role in causing IR and glucose intolerance symptoms associated with T2D. Under normal conditions for humans and most other mammals, skeletal muscle accounts for approximately 80% of the glucose uptake impacting overall glucose homeostasis; adipose tissue accounts for only 5-20 % of glucose disposal. The rate-limiting step in glucose uptake is glucose transport mediated by the facilitative glucose transporter 4 (GLUT4), which is mainly expressed in skeletal muscle, cardiac muscle, and adipose tissues. In response to insulin, GLUT4 translocates from the cytoplasm to the cell membrane and mediates the transport of glucose into the cell [1, 2, 3, 4]. Defects in any part of the insulin signaling pathway have been shown to contribute in the pathogenesis of IR. How impaired glucose uptake and defective insulin signaling in skeletal muscle contributes to whole body IR remains unanswered. As such, defining the molecular nature of these

processes has become an important research and therapeutic goal for the prevention and treatment of IR and T2D.

Genetics, Environment or Factors of Both

It is clear that the molecular etiology of IR involves multiple genetic and environmental mechanisms contributing to the final disease state [5]. *Atp10c*, a type 4 P-type ATPase, is a putative aminophospholipid transporter (APLT) identified as a strong candidate for DIO and T2D. Previous data from our laboratory suggest that the heterozygous deletion, along with maternal inheritance of the chromosomal region on mouse chromosome 7 containing the single gene *Atp10c*, resulting in the manifestation of DIO, T2D and non-alcoholic fatty liver disease (NAFLD) [2]. Although the exact mechanism and biological role of ATPases, like *Atp10c*, are still poorly understood, extensive research in yeast shows that these ATPases are important in protein trafficking primarily in endocytic and exocytic pathways [6, 7]. The hypothesis of this dissertation is that there is an association between the type 4 ATPase, *Atp10c*, and cell signaling and intracellular protein trafficking with regards to those pathways involved in glucose metabolism. To investigate this believed association, the specific muscle cell lines, murine C2C12 and rat L6 overexpressing GLUT4-myc (L6-G4myc), were used as *in vitro* models of myogenesis and non-insulin and insulin stimulated cell signaling. Western immunoblotting in conjunction with immunofluorescence analysis and real-time polymerase chain reaction (qPCR) experimental techniques were used to monitor changes in gene and protein expression after *Atp10c*/ATP10C-silencing using RNAi technology. Alterations in gene and protein expression were also measured before and after insulin

stimulation. These experiments helped identify key molecular and cellular targets of *Atp10c* in glucose metabolic pathways. Additionally, functional assays of glucose uptake and GLUT4 translocation were conducted in order to elucidate *Atp10c*/ATP10C's role in pathways involved in these processes namely the phosphatidylinositol-3-kinase (PI3K) and the mitogen-activated protein kinase (MAPK) pathways as well as the endocytosis/exocytosis of GLUT4. Basic characterization of *Atp10c*/ATP10C involved the use of HEK293T cell line and an *Atp10c*/ATP10C-overexpression plasmid.

CHAPTER II

LITERATURE REVIEW

Insulin Resistance (IR) and Type 2 Diabetes (T2D)

In 2010, the global prevalence of diabetes was 284 million, or 6.4% of the world population. Projections for the year 2030 estimate that the prevalence will be almost double (439 million) comprising roughly 7.7% of the world population [8]. Diabetes, whether type 1 or 2, is a disease in which the body does not produce or properly use insulin, a hormone needed to convert sugar, starches, and other foods into energy. The most common form, T2D, is characterized by IR primarily of skeletal muscle and adipose tissue in combination with decreased to no pancreatic β-cell activity. Skeletal muscle is responsible for the majority of insulin-stimulated glucose clearance in the body and insulin's effects are achieved via the stimulation of glucose uptake into targeted tissues. In T2D, there is a failure to increase glucose disposal into peripheral tissues in response to insulin, leading to chronically elevated levels of glucose (hyperglycemia) in the circulation followed by a compensatory rise in insulin (hyperinsulinemia). The elevated glucose and insulin levels, in turn exacerbate IR, contributing significantly to the pathogenesis of the disease [9].

IR is often associated with metabolic syndrome, an assemblage of symptoms including obesity, glucose intolerance, and dyslipidemia. Metabolic syndrome too has reached epidemic proportions in the Western world [10]. Problems arise more often as metabolic syndromes are undiagnosed and allowed to progress. As a result of this failure to diagnose, patients may experience persistent hyperinsulinemia, resulting in detectable apoptosis of pancreatic β-cells and full T2D [11].

Another often referenced co-morbidity of T2D is DIO. The two are so often associated with each other that the term "diabesity" has been coined to describe the concurrence of both diseases. Obesity is defined as excessive adiposity in relation to lean body mass, which may involve both altered body fat distribution and enlarged adipose depot size. DIO is the result of an imbalance in energy homeostasis, whereby excessive food intake is not balanced by energy expenditure [12]. Declared a major health problem by the World Health Organization as early as 1985, DIO is a growing epidemic. Although excess fat storage is not a contagious disease in a literal sense, the epidemic metaphor is used to capture the rapidly rising levels in many nations [13]. DIO, like T2D, is a complex, multifactorial syndrome that is influenced by genetic as well as non-genetic factors. The etiology of obesity involves complex interactions among excessive caloric dietary habits, sedentary lifestyles, and genetic background [12]. Despite the obvious assumption that the recent rise in obesity has predominantly environmental and nutritional causes, around 40% of obesity can be attributed to hereditary factors [14]. Weight-gaining predispositions (i.e., the differences between individuals) are considered by geneticists to be highly heritable with as much as 70-80% of weight variation attributed to genetic factors; the only trait with higher heritability than weight-gain predisposition in humans is height. Accordingly, scientists and public health officials recognize that there must be a complex array of factors at play in weight gain and DIO [12]. The characterization of such factors in the population, which could be inherited or acquired during life, would be a huge step in scientific research and healthcare. The need for personalizing and improving healthcare is one important factor that has driven the search for new predictive biomarkers. Biomarkers are used to identify the risk, presence,

and/or susceptibility to disease, and also to guide diagnostic and therapeutic interventions and to individualize the treatment of distinct conditions within clinically similar populations, including DIO and T2D [12].

T2D has several more co-morbidities that are equally as harmful as obesity, if not more so. Adult patients with T2D, especially those with poor glycemic control, additionally experience hypertension, dyslipidemia, and non-alcoholic fatty liver disease (NAFLD), as well as having an increased risk for vascular complications. Moreover, these disorders may be present before the diagnosis of T2D and, like T2D, are associated with excessive weight. Although data in children and adolescents with T2D is limited, results suggest that they too are at increased risk for the same vascular complications similar to those seen in adults [15].

Hypertension is defined by experts as systolic and/or diastolic blood pressure greater than 130/80 mmHg as measured on three or more separate occasions. Treatment for hypertension calls for changes in lifestyle (dietary and physical) as well as pharmaceutical intervention. Such treatment also involves the diagnosis and treatment of any and all underlying causes of hypertension like T2D and/or its related co-morbidities [15].

Another common co-morbidity of T2D, dyslipidemia, often requires specialized treatment. Dyslipidemia is defined as a lipoprotein disorder that promotes the development of atherosclerosis and includes increased low-density lipoprotein cholesterol (LDL-C), decreased high-density lipoprotein cholesterol (HDL-C), and increased triglycerides. In patients with T2D, IR, relative insulin deficiency, and obesity are associated with hypertriglyceridemia, low serum HDL-C, and, occasionally, high serum

LDL-C concentration. Although dyslipidemia is not as common in children as in adults with T2D, a substantial proportion of young patients with T2D have abnormal serum lipids. Like hypertension treatment, non-pharmacologic therapy (diet, exercise, improved glycemic control, and weight reduction) is recommended as the first intervention for dyslipidemia. If the goals of reduction in all symptoms are not met, then medications are required for alteration of lipid levels [15].

DIO and T2D are associated with a clinical spectrum of liver abnormalities collectively known as NAFLD. NAFLD is the most common cause of liver disease in children, and is particularly common in children with T2D. Abnormalities include hepatic steatosis (increased liver fat without inflammation) and nonalcoholic steatohepatitis or NASH (increased liver fat with inflammation). NASH may lead to fibrosis, cirrhosis, and liver failure if left untreated. However, for patients with simple steatosis or mild steatohepatitis, the likelihood and risk factors for progression to more severe liver disease are unknown. Following the common theme of treatment, non-pharmacologic therapy (diet, exercise, improved glycemic control, and weight reduction) is initially used to manage NAFLD. Pharmacologic invention is reserved for patients over 10 years of age, who fail non-pharmacologic invention, have elevated LDL-C (>160 mg/dL, 4.14 mmol/L), and/or other cardiovascular risk factors [15].

Based on the staggering numbers presented, there is a desperate call for new research to examine the relationship between T2D and its co-morbidities. To understand the underlying causes and to clarify unknown players in metabolic pathways related to these disorders is an important goal in T2D research. Problems arise in the study of such complex disorders as searching for genes related to IR and T2D presents with major

issues, mainly genetic and environmental components. The genetic component of these diseases is based on multiple, single genes that act together with one or more genes which may be exposed to specific environmental factors. As early as the 1990s, geneticists were able to argue that human obesity genotypes are complex polygenic systems with networks of gene-gene and gene-environment interactions. As such, the growing number of obesity-related or obesity-causing genes does not bode well for the single gene hypothesis [12], nor does a single-gene hypothesis work for complex metabolic disorders like IR and T2D. Furthermore, if research focuses specifically on a single gene and its effect on IR and T2D while failing to examine and manage for other known as well as unknown genes and environmental factors involved, results of experimental and clinical studies become difficult to interpret. Since these factors are difficult to control in human subjects, polygenic diseases can be more easily studied in cell culture models. Information gleamed from these studies conducted in this dissertation as well as numerous research performed by other laboratories can then be translated into animal models and ultimately extrapolated into human homologs and phenotypes.

Cell Culture Models to Study IR and T2D

In vitro cell culture models have been used extensively in research to investigate numerous disease states. Using *in vitro* cell culture models allows the manipulation of target genes, which can aid investigators in recognizing biological functions without having to deal with the complexities involving whole animals or human subjects. As skeletal muscle is the target tissue of interest for glucose clearance and as such a desirable object of study in regards to IR and T2D, cell culture models used must exhibit

similar characteristics and behaviors of the tissue under investigation. These include the murine skeletal muscle cell line C2C12 and the altered rat L6 overexpressing a GLUT4-myc tag (L6-G4myc).

Mouse C2C12 cells are well-characterized murine skeletal muscle cell lines [16] that have been frequently utilized. Several investigators have reported that insulin stimulated the glucose uptake in C2C12 under differentiated conditions, thus simulating the *in vivo* status [17, 18]. Unlike C2C12 myoblasts which express only the non-insulin sensitive GLUT1, fully differentiated C2C12 myotubes express GLUT4 and glucose uptake can be activated by insulin [19]. However, others reported that the cell line lacks sensitivity to insulin [20]. This discrepancy can be explained by the instability of C2C12 cells [18]. Some advantages of these cells include their ability to undergo phenotypic differentiation and cell fusion [16] easily and show relatively good differentiation in terms of sarcomere development compared with other established cell lines, such as the rat L6 [21]. Still, C2C12 myotubes have not been widely utilized to study insulin-stimulated glucose uptake because they express relatively low levels of GLUT4 [22] when compared to GLUT4 expression from L6 cell lines and primary skeletal muscle cultures from mice.

As such, a cell line of rat skeletal muscle, L6-G4myc, has been developed and widely used. L6 G4mycs offer the ability to undergo phenotypic differentiation and cell fusion, as well as afford the opportunity to compare GLUT4 translocation with glucose uptake in intact cell preparations, as required to assess possible changes in GLUT4 activity [9]. Skeletal muscle cell lines like rat L6 cells have been used to study insulin-induced glucose transport systems. However, problems can arise with these myoblast

cells as they need to be differentiated by replacing the calf serum with horse serum or by dexamethasone treatment [18]. Some researcher forego this step of differentiation and use myoblasts alone [9, 22, 23], but this protocol is controversial as myoblasts do not accurately represent mature myotubes and/or adult skeletal muscle. The same literature states that the GLUT4-myc tag is responsible for both basal and acute insulin-stimulated glucose uptake in L6-G4myc cells [9]. Thankfully, this cell line can still be used to study GLUT4 translocation as the L6-G4myc muscle cell line has detectable myc-GLUT4 translocation upon insulin stimulation [1].

Understanding the pros and cons of both cell lines and the limitations of *in vitro* research is crucial for investigating biological functions without having to deal with the complexities involving animal models. For the purpose of our research, our laboratory has chosen to utilize both cells lines in their undifferentiated and differentiated forms (myoblasts and myotubes) to study *Atp10c*/ATP10C, a putative phospholipid translocase that may be a major player in glucose and lipid metabolism.

P-type ATPases and *Atp10c*/ATP10C

Biological membranes exist of amphipathic lipid molecules that self-assemble into bilayers in an aqueous environment due to their intrinsic property of a hydrophilic head group and a lipophilic tail. Each membrane is composed of hundreds of lipids systematically distributed. In eukaryotic cells, the main lipids of cellular membranes phosphatidylcholine (PC), phosphatidylserine (PS), phosphatidylethanolamine (PE) and phosphatidylinositol (PI) all of which are glycerophospholipids. Other major classes of lipids are sphingomyelin and glycerosphingolipids, which are phosphosphingolipids.

Cholesterol, a steroid of fat, is also an essential structural component of mammalian cell membranes and is required to establish proper membrane permeability and fluidity. Lipids are asymmetrically arranged between the two leaflets of the plasma membrane, and this was first thought to be a static characteristic of membranes. However, it is now clear that the lipid topology results from a continuous bi-directional movement of lipids between the two leaflets or "flip-flop" in which specific membrane proteins have an essential role [24]. A phospholipid molecule can diffuse rapidly throughout one leaflet, but faces a substantial barrier to the "flipping" of its polar head group through the hydrophobic interior of the membrane to the other leaflet. Consequently, the two leaflets of a membrane can be completely different in phospholipid composition [25]. Asymmetry of the plasma membrane is made possible by lipid-translocation machinery that hydrolyses ATP to flip aminophospholipids against a concentration gradient i.e. the APLT [24, 26].

While lipids can freely diffuse in the lateral plane of the membrane, transverse, or flip-flop movement of lipids in the plasma membrane is very slow (from hours to days) [25, 27]. For the creation and maintenance of the asymmetrical distribution of phospholipids, eukaryotic cells have evolved an elaborate set of proteins, which must be actively maintained. These proteins are divided into three classes – "floppases", "flippases", and "scramblases". "Scramblases", facilitate a lipid- specific transverse movement of phospholipids in either direction. "Floppases" also known as the ATP-binding cassette (ABC) transporters maintain transbilayer distribution of phospholipids by translocating specific phospholipid species from the inner to the outer leaflet of the bilayer (flop) at the expense of ATP [7, 27]. The third class of proteins that facilitate

transverse transport of phospholipids across biological membranes are the APLT or "flippases" [27].

The first flippase activity was described in 1984 in human erythrocytes [7, 28]. Subsequent work by several laboratories defined the biochemical properties of this family of transporters and the identification of a new branch in the phylogenetic tree of the P-type ATPase superfamily -- the type 4 subfamily [7]. The P-type ATPase superfamily is an evolutionary conserved, large family of proteins members of which are widely expressed in both prokaryotes and eukaryotes, including bacteria, yeast, parasites, nematodes, insects, plants, and animals [6]. P-type ATPases in multicellular organisms show distinct tissue distribution and specific roles in development. In addition, P-type ATPases reside in multiple, often very specific, cellular compartments, from the plasma membrane to specialized secretory vesicles suggesting high spatial regulation of P-type ATPase function. As such, dysfunctional P-type ATPases can potentially influence the spatial and/or temporal availability of phospholipids, and thus the distribution and activity of proteins [29].

As integral transmembrane proteins, P-type ATPases are important in the generation of cation gradients which make these proteins indispensable in the regulation of cell volume, excitability of nerve cells, muscle contraction, intracellular pH, acid secretion in the stomach, uptake of substrates, and signaling pathways [6]. The core of all P-type ATPases contains a conserved stretch of seven amino acids with the P-type signature sequence FDKTGT [L, I, V, M] [T, I, S] [6]. This motif includes an aspartic acid residue, which is essential in the reaction cycle of the protein. The mechanism via which substrates are pumped is based on the E1E2 model, in which ATP-mediated

phosphorylation, substrate binding, and subsequent dephosphorylation of the invariant aspartic acid are coupled to a conformational change of the transporter. The phosphotransfer reaction drives the transport cycle of these proteins, hence the name P-type ATPase [6].

The type 4 P-type ATPases form a separate group based on sequence divergence (approximately six subclasses) [28, 29] and their assumed role involves the translocation of phospholipid molecules across biological membranes rather than cations [6, 28]. The members of this subfamily have 10 -12 predicted transmembrane domains with an NH2- and COOH-termini protruding into the cytoplasm, and a large intracellular loop harboring P-type ATPase-specific sequences and an ATP-binding site [6, 24, 27]. Type 4 P-type ATPases differ from the cation-transporting P-type ATPases in that they lack negatively charged residues involved in ion transport [24]. Over 100 members of the type 4 P-type ATPases subfamily have been identified, all of which are exclusively found in eukaryotic organisms, including approximately a dozen human isoforms [28]. The type 4 P-type ATPases are proposed to catalyze the flippase activity that restricts PS and PE to the cytosolic leaflet of the plasma membrane. Slow flop of phospholipids without head group specificity, combined with rapid flip of PS and PE, is thought to establish the observed membrane asymmetry [29].

In mammalian plasma membranes, the aminophospholipids, PS and PE are stationed to the inner leaflet of the membrane bilayer, while PC and sphingolipids are found in the outer leaflet. APLTs translocate PS and/or PE from one leaflet of the membrane bilayer to the other, and seem to be responsible for concentrating PS and PE on the cytosolic leaflet of biological membranes [30]. The highly organized and

maintained distribution of phospholipids is crucial for many physiological processes. Some of these processes include signal transduction, cell morphology, cell movement, activity of membrane proteins, and vesicle biogenesis. Conversely, the ability for phospholipid randomization is essential in initiating processes like phagocytosis, platelet activation, and apoptosis. Therefore, to continue the asymmetric flux of the phospholipid bilayer, proteins that translocate the phospholipids are necessary.

Much of the present knowledge on the cellular function of type 4 P-type ATPases has been gained from studies of *Saccharomyces cerevisiae* as the yeast genome has five type 4 ATPases. The founding member of this subfamily is the yeast *drs2* gene (an ortholog of mouse *Atp10c*). This particular gene has been shown to participate in ribosomal assembly, the formation of Golgi-coated vesicles, and in maintenance of bilayer asymmetry. These activities are indispensable for intracellular membrane and protein trafficking, fluid-phase and receptor-mediated endocytosis, processes that require lipid flipping to initiate budding and the fusion of membrane vesicles from or with other membranes [6, 26, 28, 30]. Studies in yeast strains defective in single or multiple type 4 ATPases have accumulated data implicating these proteins in the biogenesis of transport vesicles and thus the establishment of cellular polarity [6, 30]. Furthermore, these proteins act in distinct, yet overlapping pathways [6].

In humans, 14 type 4 P-type ATPase genes have been identified, all with mouse orthologs [7]. The study of type 4 P-type ATPase mutants has linked many of these enzymes to the maintenance of membrane structure, vesicle trafficking, and amphipath transport. At least two have been associated with human diseases [28]. *Atp10c*, located on mouse chromosome 7, is putative APLT and a novel type 4 P-type ATPase as it

contains three conserved motifs consistent with this family of ATPases. Heterozygous *Atp10c* mice represent a genetic, diet-induced polygenic model of T2D, in association with DIO. These heterozygous mice are hyperinsulinemic, have IR and have an altered insulin-stimulated response in peripheral tissues, namely skeletal muscle and adipose tissues. The phenotype of *Atp10c* heterozygous mice further strengthens their biological role in intracellular signaling and protein trafficking and suggests that metabolic pathways of glucose metabolism can be used to delineate this function.

Although a substantial amount of indirect evidence has implicated a number of proteins as "flippases," positive identification awaits their purification, reconstitution, and demonstration of transport activity [28]. Moreover, the molecular mechanisms by which these proteins act are not fully understood due to the difficulties that arise when developing reliable assays to study intramembranous transport [7]. The cellular consequences of defects in type 4 P-type ATPases vary from vesicle formation deficiencies to membrane structure/stability defects. These defects have secondary consequences, making it difficult to pinpoint the biochemical functions of the type 4 P-type ATPase family [27]. Studying these proteins is a challenge, but successful research will provide fundamental insight with regard to membrane dynamics and protein trafficking. In addition, it will clarify the molecular mechanisms which underlie severe human diseases [6] like T2D and its related disorders.

For now, only one inherited disorder has been directly linked to mutations in a type 4 P-type ATPase gene -- ATP8B1 [6]. Byler disease or PFIC1 is a rare autosomal recessive disorder first described in the Amish population. The disease primarily manifests as a chronic intrahepatic cholestasis which progresses to severe, end-stage liver

disease before puberty. A less severe clinical phenotype associated with mutations in ATP8B1 is benign recurrent intrahepatic cholestasis [6]. Five studies by four independent groups suggest that ATP8B1 plays a critical role in maintaining stability of the plasma membrane of polarized epithelial cells [27]. How exactly ATP8B1 stabilizes the plasma membrane is currently unknown, but could involve phospholipid translocation as well as recruitment of proteins involved in cytoskeleton dynamics. As observed in human erythrocytes, loss of phospholipid asymmetry also leads to morphological aberrations and is accompanied by dis-attachment of cytoskeletal elements from the membrane [27].

Numerous studies have been conducted on APLTs and lipid membranes. Results of these studies suggest their role or possible roles in insulin signaling, further solidifying the importance of type 4 P-type ATPases in cell biology and health and disease [7]. Studies using a similar protein from the same family as *Atp10c* also showed promising results. Researchers discovered that of the 15 inbred mouse strains available for research purposes, only the C57BL/6J strain contained a premature stop codon in ATP10D, resulting in a non-functional protein. It is interesting to note that C57BL/6J mice are predisposed to develop obesity, hyperglycemia, hyperinsulinemia, and hypertension when fed a high-fat diet [7]. Moreover, this protein was also proposed to be a candidate for the modulation of the HDL-C levels. Since ATP10C and ATP10D belong to the same class of type 4 P-type ATPases, they may be involved in similar pathways. Thus, both may play a role in trafficking routes implicated in glucose and lipid metabolism [30, 31].

Additional type 4 P-type ATPase genes have been implicated in association with multiple diseases. The *Atp8a2* gene was reported to be frequently deleted in tumorigenic

malignancies; however, no relation between defective phospholipid translocase activity and tumorigenesis has been demonstrated at this time. Recently, *Atp11c* has been mapped to a chromosomal region (Xq27) associated with X-linked inherited disorders including hypoparathyroidism, albinism, deafness, and thoracoabdominal syndrome. If and how this ATPase contributes to these disease phenotypes however remains to be demonstrated.

The focus of our research, *Atp10c*/ATP10C, has been studied by others in relation to several neurological diseases. *ATP10C*/ATP10C has been linked to the neurological disorders including Angelman syndrome (AS) and autism [32, 33]. AS sometimes referred to as "happy puppet" syndrome is a neurological disorder characterized by ataxia, mental retardation, hyperactivity, subtle dysmorphic facial features, epilepsy, and an apparently happy, social disposition, and is a disorder in which genetic imprinting plays a role. This syndrome has been associated with mutations and/or deletions in a maternally-derived, chromosomal region which includes the *ATP10C* and *UBE3A* genes. The *UBE3A* gene encodes the ubiquitin-protein ligase E3A, an enzyme involved in the ubiquitination of proteins. Surprisingly, *ATP10C* expression is nearly absent in patients with AS. One obesity phenotype of AS has been described in three-quarters of patients suggesting causation from a lack of *ATP10C* activity. For the remaining quarter of AS patients, no obesity phenotype has been described. Rationale for those patients is that mutations occur only in the *UBE3A* gene and that the *ATP10C* gene is intact [33]. It is highly likely that the syndrome relates to the *UBE3A* gene rather than to *ATP10C* as transgenic mice with the maternal *UBE3A* gene knocked out, phenotypically resembled human patients, and most importantly are not obese.

Autism is a developmental disorder characterized by three areas of abnormality -- impaired social interaction, communication, and restricted stereotyped pattern of interest or behavior. Impairment in all three areas is generally observed before 3 years of age and disrupted growth of the brain is implicated in the etiology of autism. Numerous studies have indicated a robust role of genetic factors in the development of both autism and AS, while no susceptibility gene has been elucidated [32]. Further confounding matters is that some individuals with autism have a maternal duplication of the AS region. However, paternal inheritance of the same duplication has no effect. Also, conflicting studies on the involvement of *ATP10C* in autism have arisen. Two notable studies by Nurmi et al. 2002 [34] and Kim et al. 2002 [35] did not observe a significant association between *ATP10C* /ATP10C and autism, while one by Kato et al [32] did. Rationale for *ATP10C* /ATP10C involvement comes as recycling of membrane from neuronal synapses plays a critical role in synaptic vesicle production. In addition, the recycling or polarized delivery to specific sites on the plasma membrane is essential for proper function of neurons and may contribute to long-term potentiation.

Atp10c /ATP10C has been implicated in several metabolic abnormalities, and as such, is an ideal candidate for DIO and T2D. As stated earlier, mice inheriting a maternal deletion of *Atp10c* are considered a model of DIO and T2D as these mice develop hyperinsulinemia, IR, increased adiposity, impaired glucose tolerance, and NAFLD compared to mice inheriting the same deletion paternally [7, 12, 28, 31, 36]. Research by Dhar et al. [2] showed that after a high fat diet for 12 weeks, higher insulin levels were measured in *Atp10c* heterozygous mice. These mice also had a hyperglycemic response in an insulin tolerance test and showed impaired glucose uptake in adipose tissue and the

soleus muscle. Interestingly, these mice showed altered expression of a set of genes involved in insulin-stimulated glucose uptake in peripheral tissues, including *Glut4*, which is required for glucose uptake into myocytes and adipocytes. Further validation can be observed in a mouse model of AS. Researchers using human subjects also identified a subset of AS patients with the additional phenotype of increased body mass index (BMI) suggesting that *ATP10C*/ATP10C may play an important role in obesity of multiple etiologies, in mice and humans, respectively.

Additionally, other groups of investigators other than us have been looking at the biological role of *ATP10C* gene or its cognate protein, ATP10C, in metabolism. Several independent reports suggest that the epigenetic background of individuals may depend on a number of genetic and environmental factors acquired over ones' life or inherited from the parents. In a recent study by Milagro et al [12], researchers looked at whether or not changes in dietary patterns including hypocaloric diets and weight loss were able to alter the methylation profile of different genes. Results from this study revealed that some metabolically relevant genes were hypomethylated before any intervention. For *ATP10C*, significant differences between low and high responders were observed before the intervention. Diet-induced changes in fat mass and BMI were also observed confirming that it could be a reliable marker of successful response to the hypocaloric diet [12]. These results show that changes in dietary patterns, including hypocaloric diets and weight loss, are able to alter the methylation profile of different genes one of them being *ATP10C*, again validating its possible role in DIO and T2D. These results and the extensive research described above lead to the need to investigate the pathways involved

in glucose metabolism to find roles for ATPases like *Atp10c* /ATP10C in these metabolic disorders.

Glucose Metabolism Pathways and Insulin Resistance

Glucose transporters (GLUT) are known to play pivotal roles in energy metabolism. Many different eukaryotic GLUT isoforms have been identified and well characterized. They possess 12 transmembrane helical segments with the N- and C-termini and a large central loop exposed to the cytoplasm. GLUTs have distinct antigenic C-terminal regions, and are subject to different metabolic and developmental regulations. GLUT1 is located primarily in the plasma membrane in most tissues, whereas GLUT4 is found predominantly in intracellular membranes in insulin-sensitive tissues such as adipose tissue and skeletal muscles [37, 38, 39]. Glucose transport activity is affected by changes in the intrinsic activity, intracellular trafficking, and stability of the GLUTs. A number of mechanisms are involved in regulating the expression of GLUTs. GLUT expression can be regulated by the transporter itself, by other GLUTs, or other transcription factors. For instance, GLUT4 may interact with appropriate signal transducers which in turn regulate the level of functional transcription factors [37]. In the absence of stimulation, GLUT4 is almost completely excluded from the plasma membrane. The addition of insulin causes GLUT4 to shift from its intracellular location to the plasma membrane [40]. Several observations indicate that GLUT4 has a crucial role in whole body glucose homeostasis. Insulin stimulated glucose transport is an important rate-limiting step for glucose metabolism in both skeletal muscle and adipose tissue, and is severely disrupted in T2D. Disruption of GLUT4 expression in mice results

in IR, while an overexpression of GLUT4 showed improved diabetes in a genetic mouse model of T2D (*db/db*) [40]. Because skeletal muscle is the principal target tissue for glucose clearance and is the main tissue involved in insulin-stimulated glucose uptake, the GLUT4 protein content of skeletal muscle is of the utmost importance [39].

A key event in insulin-stimulated glucose transport is the translocation of the facilitative GLUT4 to the plasma membrane [4]. In mammals, GLUT4 is of particular relevance to insulin action because its expression is confined to insulin-sensitive cell types such as skeletal muscle, adipose tissue, and cardiac muscle [41]. In response to the activity of insulin, GLUT4-containing storage vesicles (GSVs) rapidly translocate towards the plasma membrane. Myotubes also express GLUT1, which can undergo translocation by insulin, but is more often responsible for basal or non-insulin stimulated glucose uptake. Responsible for majority of insulin-stimulated glucose uptake into peripheral tissues is GLUT4, a 12-transmembrane domain protein that mediates transport of glucose in the direction of the glucose gradient [40]. GLUT1 contributes only a small extent to the stimulated glucose transport as described by Bazuine et al [41]. Treatment with the GLUT4 inhibitor rottlerin reduced insulin-stimulated glucose transport to near-basal levels of transport. The concentration of GLUT4 in the plasma membrane determines the rate of glucose metabolism in adipose and muscle cells, which in turn contributes to whole-body glucose homeostasis [4]. In normal cells, GLUT4 is distributed among the plasma membrane and various intracellular membrane compartments. Insulin stimulation significantly increases the exocytic rate of GSVs while inhibiting GLUT4 endocytosis [42, 43, 44]. While GLUT1 may be found both

inside and outside the cell, GLUT4 vesicles have rarely, if ever, been found at the plasma membrane of un-stimulated muscle or fat cells [40].

Maintenance of lipid asymmetry has been implicated in membrane bending and the biogenesis of endocytic and secretory vesicles. An excess of lipid on one side causes the lipid bilayer to bend, and this process then contributes to the formation of transport vesicles. Although APLT activity may enhance vesicle formation, this activity alone is not enough to drive this process [26, 27]. Several investigators have shown that ATPases participating in distinct trafficking pathways and that these proteins are important for the biogenesis of exocytic and endocytic transport vesicles. In fact, membrane bending and the generation of a lipid imbalance across the bilayer is a prerequisite for vesicle budding. Phospholipids can rapidly cross the bilayer in both directions and the assembly of a protein coat sufficient to deform the bilayer into a bud is not a problem when adopting a transbilayer lipid arrangement permissive for vesicle formation. However, in the plasma membrane, the free 'flip-flop' of phospholipids across the bilayer is constrained and therefore a problem for vesicle budding without assistance of ATP-driven flippases [24, 43]. Direct participation of ATP-driven flippases in vesicle formation is supported by the observation that inward translocation of PS and PE by APLT in the plasma membrane of human erythroleukemia cells stimulates endocytosis. Intriguingly, yeasts lacking type 4 P-type ATPases genes, *Dnf1p*, *Dnf2p* and *Drs2p* display a general defect in endocytosis. Conversely, overexpression of ABC transporters with outward directed lipid translocase activity causes a defect in endocytosis. This suggests that lipid translocation is required to either generate a membrane environment permissive for vesicle formation or perhaps to help deform the membrane during vesicle budding. Further biochemical analysis of

these proteins will be required to better assess their role in protein trafficking [29, 30]. Collectively, all these results suggest a functional link between lipid transport and vesicle formation [24]. Several groups have demonstrated that these proteins participate in distinct intracellular vesicular trafficking pathways and are important for the biogenesis of exocytic and endocytic transport vesicles. Importantly, these functions are closely linked to the flipping of phospholipids or phospholipid analogues [31]. The formation of GSVs is mandatory for the translocation of GLUT4 and as a result, is necessary requirements for insulin-stimulated glucose uptake.

Additional evidence that GLUT4 is essential in the maintenance of normal glucose homeostasis is that mice carrying a muscle-specific deletion of the *Glut4* gene developed severe IR and glucose intolerance. Another study using an adipose-specific *Glut4* knockout mouse model also showed that these mice developed IR and glucose intolerance [1].

IR is a key feature of T2D. In particular, it has been argued that elevated levels of glucose (hyperglycemia) and insulin (hyperinsulinemia) are major factors for the development of IR, but the molecular mechanisms remain obscure [9]. The compensatory increase in insulin during the insulin resistant state initially offsets insulin's reduced ability to stimulate GLUT4 translocation and glucose uptake. However, both *in vivo* and *in vitro* studies demonstrate that the hyperinsulinemic state has a negative effect on insulin action. Insulin strongly promotes GLUT4 incorporation into the cell surface, and this translocation appears to fail in IR accompanying T2D [5].

Understanding the regulation of GLUT1 and GLUT4 has proved to be extremely challenging, principally because it involves several signal-transduction pathways that are

superimposed on a complex series of vesicle transport processes. The rate of glucose uptake in skeletal muscle and adipose tissue is limited by the total number of facilitative glucose transport proteins inserted into the plasma membrane. Acute insulin treatment activates not only glucose transport activity, but also the translocation of some GLUT1 and all GLUT4 transporters from intracellular sites to the plasma membrane. Multiple studies show that GLUT transport activity can be modulated, directly or indirectly, by protein–protein interaction, post-translational modification of the transporter, and/or changes in cellular environment [38, 41]. Insulin binds to a surface receptor on muscle and fat cells triggering a cascade of signaling events that culminates in GLUT4 translocation. In the absence of insulin, GLUT4 is largely excluded from the plasma membrane and is retained within endosomes, the trans-Golgi network, and tubular-vesicular compartments. Insulin triggers the redistribution of GLUT4 from intracellular compartments to the plasma membrane. This action increases the total number of transporters localized to plasma membrane and thus the maximal rate of glucose transport into cells. When insulin is removed, GLUT4 is rapidly cleared from the plasma membrane back into intracellular compartments, where it is recycled for use in subsequent stimulations [44].

Studies of this process of GLUT4 translocation have been carried out using two approaches. The first is an "outside–inside" approach that focuses on mapping the insulin-specific signaling pathway, PI3K, in skeletal muscle and fat cells with the view to identifying downstream targets that directly control GLUT4 translocation. Conversely, the second approach is an "inside–outside" one used to map the intracellular transport

itinerary of GLUT4 with the aim of identifying insulin-regulated steps [40] which may or may not be regulated by MAPK.

Phophatidylinositol-3-kinase (PI3K) pathway

Insulin furthermore initiates several signal transduction pathways in the cytoplasm of the cell [1, 41]. Years of research has shown that insulin activates downstream signal transduction cascades by binding to its receptor, thus activating it. On a cellular level, metabolic IR is known to display a reduced strength of signaling via the PI3K pathway. In almost all cases of IR there is a decline in PI3K activity. Two complementary mechanisms have emerged as potential explanations for the reduced strength of the PI3K signaling pathway. The first explanation is that the PI3K activity is minimized secondary to serine phosphorylation of insulin receptor substrate (IRS) proteins, specifically IRS-2 in skeletal muscle. A disruption in the balance between the amounts of the PI3K subunits may also explain the development of IR. PI3K consists of a regulatory subunit, p85, and a catalytic subunit, p110. As this heterodimer is responsible for PI3K activity, any increase or decrease in p85 expression could inversely lead to increased or decreased PI3K activity. In a study following acute overfeeding, human females displayed reduced whole body insulin sensitivity and showed an increase in total p85expression in skeletal muscle. This increase in p85 expression was inversely correlated with PI3K activity [45].

When insulin binds to its receptor, the occupied insulin receptor then undergoes auto-phosphorylation and phosphorylates IRS [41]. A key component of an insulin signaling cascade is the activation of PI3K and its downstream kinases such as Akt. Akt

kinase activity is dependent on its phosphorylation at Thr308 and at Ser473 [46]. Akt is known to mediate many of the physiological effects of insulin including GLUT4 translocation by phosphorylating downstream substrates [1, 4, 46]. Akt is often regarded as the most important substrate in the insulin signaling pathway because many physiological effects of insulin stimulation are mediated by Akt kinase activity. There are three Akt isoforms, but only the Akt2 isoform has been shown to be necessary for insulin-stimulated GLUT4 translocation and glucose uptake in skeletal muscle and adipose tissue. Furthermore, Akt2 knockout mice have impaired muscle and fat glucose uptake [41]. This trafficking process is in part mediated by AS160, an AKT substrate that is critically involved in insulin-stimulated regulation of GLUT4 trafficking. Interestingly, AS160 activation is reduced in patients with T2D [4]. AS160 has also been shown to associate with GLUT4 containing vesicles. Immunohistochemical analysis of AS160 indicated that it has a wide intracellular distribution that partially overlaps with GLUT4 and that it is absent from the plasma membrane. Unlike GLUT4 which is located in only insulin-sensitive tissues, AS160 has a widespread tissue distribution [47, 48]. Recently, studies using an *in vitro* fusion assay of intracellular vesicles that contain GLUT4 with plasma membranes showed that insulin modulates targets in both the vesicle and the plasma membranes. Therefore, this data supports the notion that there are several signaling pathways that join different aspects of GLUT4 transport [40]. Consequently it can be hypothesized that the development of IR induced by chronic exposure to glucose and insulin is at least not exclusively mediated products of the PI3K pathway alone but might also involve other signaling pathways [4]. One such pathway is mitogen activated protein kinase (MAPK) pathway. Therefore, the data from all these studies show the

importance of the PI3K pathway in glucose metabolism and its exploration alone and in conjunction with the MAPK pathway warrants further investigation.

Mitogen activated protein kinase (MAPK) pathway

Chronic inflammation and metabolic dysregulation are prominent features of T2D, cardiovascular disease, and several other disease states. The pathological stress underlying these conditions trigger persistent fluctuations through multiple intracellular signaling pathways that amplify the diseased state. As master regulators of gene expression and metabolism, MAPK proteins have been shown to couple cellular stress with an adaptive or maladaptive response in skeletal muscle.

Numerous studies have concluded that insulin stimulates glucose uptake via the rapid recruitment of GLUT4 to the surface of skeletal muscle and adipose tissue. However, many studies have shown that the extent of GLUT4 recruitment to the cell surface in response to an acute insulin challenge is less than the extent of the increase in glucose uptake [48, 49]. This discrepancy between glucose uptake and GLUT4 translocation may be reconciled if the intrinsic activity of GLUT4 were also elevated by insulin. Taken together, these observations suggest that GLUT4 at the cell surface may require activation by some critical mechanism before it can transport glucose to its maximum capacity [48, 49, 50]. It has been suggested by various researchers that insulin increases glucose uptake by first increasing GLUT4 translocation and then further activating the additional transporters in a separate pathway from the PI3K pathway. It is hypothesized that after translocation toward the plasma membrane, there is a secondary, MAPK-dependent step, leading to enhancement of insulin induced glucose uptake [41].

Recent work has demonstrated that the MAPK protein, p38, is necessary for insulin-stimulated glucose uptake. Inhibition of p38 can prevent insulin-stimulated glucose uptake, but not GLUT4 translocation, suggesting that p38 may regulate this yet to be discovered activation step. Thus, in acute situations, p38 is beneficial to GLUT4-mediated glucose uptake. However, when chronically exposed to insulin, p38 also contributes to the development of IR, as inhibition of p38 improved GLUT4 protein levels and insulin-stimulated glucose uptake. The detrimental effects of p38 activation are further supported by the observation that constitutive activation of the p38 pathway decreased GLUT4 messenger RNA and protein levels as well as insulin-stimulated glucose uptake [9, 50].

These signaling modules consist of a three-tiered kinase core where a MAPKKK activates a MAPKK that activates a MAPK [51, 52, 53]. The MAPK family of proteins is composed of distinct signaling modules in skeletal muscle including extracellular signal regulated kinases (ERK) 1 and 2, p38, and c-Jun NH2-terminal kinases (JNK). These MAPK branches are stimulated by cytokines, growth factors, and cellular stress [54]. MAPK proteins are 60-70% identical to each other, yet differ in their activation loop sequences and sizes. Downstream substrates of MAPK include mitogen-activated protein-kinase-activated protein kinases and transcription factors, the phosphorylation of which, either directly or indirectly, regulate gene expression at several points, including transcription, nuclear export, and mRNA stability and translation [55]. Much scientific evidence suggests that unrestrained signaling perpetuates IR and protein catabolism. As such, MAPK represents exciting targets for pharmacological interventions aimed at preventing or improving T2D and muscle wasting [54].

The ERK pathway was the first MAPK pathway to be identified. The ERK pathway is activated by numerous stimuli, including growth factors, cytokines, viral infection, and carcinogens [53, 54, 55]. ERK1 (p44) and ERK2 (p42) are co-expressed in virtually all tissues but with a remarkably variable relative abundance [56]. ERK1 and ERK2 MAPKs are activated by phosphorylation on threonine and tyrosine residues by the dual specificity kinase MEK1, which induces their translocation into the nucleus where they activate or repress a variety of transcription factors [57]. The functional consequence of ERK pathway activation includes cell-cycle regulation, proliferation, and cell survival [55]. Studies have demonstrated that in pancreatic β-cells, glucose is known to activate ERK1/2 and that glucose-induced ERK1/2 activity remains in the cytoplasm and participates in the regulation of insulin secretion in MIN6 cells [57].

The JNK family of enzymes is inflammation and stress-activated MAPKs involved in the regulation of cell proliferation, survival, and apoptosis, but the underlying mechanisms of actions in these processes are unclear [52]. Three mammalian isoforms, JNK1, JNK2, and JNK3, are encoded by distinct genes that are highly homologous, but differ in tissue expression. JNK1 and 2 are ubiquitously expressed, while JNK3 is more restricted to the central nervous system, heart, and testes [54].

As a separate signaling component of the MAPK network, p38 MAPK consists of four isoforms (p38 α, p38 β, p38 Δ, and p38 χ). Tissue-selective expression is observed, with p38 χ found predominantly in skeletal muscle, p38 Δ in the testes, pancreas, and small intestine. In contrast, p38 α and β are more ubiquitously expressed [49, 54, 55]. Significant amino acid sequence homology is observed among the 4 isoforms, with 60-75% overall sequence homology. Dually activated by phosphorylation on tyrosine and

threonine residues, p38 is capable of regulating many cellular processes including cell morphology, differentiation, apoptosis, as well as expression of numerous target genes. In one study, research showed that p38 is necessary for the full differentiation of preadipocytes into adipocytes [56]. Interestingly, studies also show that p38 contributes to insulin-mediated glucose uptake in adipocytes [10, 50]. These results support the tenet that p38 MAPK may be a regulator of glucose uptake and is altered in states of IR [9]. For this reason, the role of the MAPK pathway, specifically p38 involvement, in regulating skeletal muscle differentiation has been studied extensively, but the results have been mixed [58].

The molecular mechanisms involved in the induction of myoblast differentiation and fusion are complex and to date, remain unclear. A coordinate induction of muscle-specific gene products occurs along with morphological changes of differentiation. Members of the MyoD family of muscle-specific transcription factors (*MyoD, myogenin, Myf-5, MRF4*) are involved in these processes, and their ectopic expression in a variety of non-muscle cells can promote myogenesis [16]. Studies revealed that modulating the p38 pathway with chemical or upstream kinase activators or inhibitors regulated the activity of the promoters of muscle-specific marker genes such as *myogenin* and *MyoD* [52]. MyoD triggers differentiation of myoblasts by activating the expression of the fourth and last muscle regulating factor implicated in myogenesis: *myogenin* [58]. Investigators showed that *in vitro* blocking the p38 pathway seriously perturbed cytoskeletal organization during the terminal stages of myogenesis [52]. Researchers conducting this study also observed data that suggested an interaction between the p38 and the PI3K pathway. Controversy arises as the differentiation of an *in vitro* cell line of mouse

skeletal muscle, C2C12 cells was not accompanied by any activation or inhibition of ERK2. Moreover, inhibitor PD098059, which prevents activation of the MAPK pathway, had no apparent effect on myotube formation or on the expression of differentiation markers such as *myogenin* or *MyoD*. Instead, SB203580, a specific inhibitor of p38 blocked myotube formation and the expression of muscle-specific proteins [57, 58]. The literature on the response of ERK1/2 and JNK activity to differentiation in C2C12 myoblasts is mixed, from decreased to unchanged to increased [58] so the roles of these proteins remains yet to be solved. Data from all the studies discussed above serve as evidence that the MAPK pathway is an important pathway in many vital biological processes and as such, its role in glucose metabolism warrants further investigation.

Gene/Protein Modification Techniques

RNAi interference (RNAi)

With the advent of synthetic silencing RNA (siRNA) technology, RNA interference (RNAi)-based gene silencing in cultured cells has been extremely valuable in dissecting elements crucial for the cell signaling pathways. RNAi is a post-transcriptional gene silencing technique that was first coined in 1998 to describe the observation that double-stranded RNA could be used to block gene expression. siRNA is a class of double stranded RNA molecules generally 19 to 25 nucleotides in length, which act to interfere with the expression of mRNA. These siRNAs are either generated *in vitro* by cleavage of double-stranded RNA using the enzyme Dicer or generated synthetically and introduced into the cell experimentally. Routinely, commercially available and synthesized siRNA

is transfected into cells to form a complex with the RNAi-induced silencing complex (RISC). After the duplex or plasmid unwinds, a single antisense strand guides RISC to the messenger RNA (mRNA). Binding of the strand at the complementary sequence results in cleavage of the targeted mRNA, thus the final outcome is targeted silencing of a particular gene of interest [59]. Due to the endogenous expression of proteins at the time of transfection and subsequent mRNA silencing, some protein has already been translated, so complete silencing or knockdown of the protein of interest may not be possible at this level, but should be greater than 70% at the mRNA level for transfection to be deemed efficient.

Gene silencing by siRNA in cultured mammalian cells is being used as an effective way to quickly test if a specific gene is required for a biological function. It is additionally being used in high throughput screens to determine if there are any genes within a large set of genes required for a particular function. The use of RNAi is definitely an important experiment to conduct before more expensive experiments to generate transgenic mice are undertaken.

Overexpression

Overexpression of a particular cDNA and its product is another effective way to characterize a gene and to study possible biological function of its cognate protein. The process of overexpressing a particular gene/protein of interest involves a complicated procedure of cloning and subcloning. Cloning is the process of moving a gene from the natural occurring chromosome to an independently replicating vector. During this process, the DNA is removed from select cells and manipulations of the DNA are carried

out before the DNA is then put back into cells. Because the bacteria E. coli is so well characterized, it is usually the cell of choice for manipulating DNA molecules. Once the appropriate combination of vector and cloned DNA/construct has been made in *E. coli*, the construct can be put into other cell types for further experimental use [60]. Often times after cloning a gene of interest, researchers analyze the gene's characteristics by overexpression analysis of the gene of interest into various cell types [61]. For the purpose of analyzing insulin-stimulated glucose transport, the most commonly selected cell lines are skeletal muscle and adipose tissue. However, the introduction of DNA or genes of interest into these insulin-responsive tissues by standard transfection protocols are very inefficient and time consuming [61, 62]. As such, many times investigators will use another cell line to perform these overexpression studies. Human embryonic kidney cells, also known as HEK293 cells, have been grown in tissue culture for many years and are very widely used as they are relatively easy to grow and transfect readily. An important variant of this cell line is the HEK293T cell line that contains the SV40 large T antigen, which allows for replication of transfected plasmids containing the SV40 origin of replication. This benefit allows for amplification of transfected plasmids and extended expression of the desired gene products **[**63, 64**]**.

Research Project Overview

Although there is a consensus on the physiological function of flippases in intracellular signaling and protein trafficking, their precise biological roles are poorly understood. The hypothesis of this project is that there is an association between type 4 ATPase mediated phospholipid translocase activities, cell signaling and intracellular

protein trafficking. Based on the phenotype of *Atp10c* heterozygous mice, these processes can be studied in metabolic pathways of glucose metabolism. Since *Atp10c*/ATP10C is a novel product and as such, little is known regarding its function, the purpose of our research is to explore both the PI3K and MAPK pathways measuring changes in the expression of key proteins when *Atp10c*/ATP10C expression is altered via experimental gene and protein modification techniques. RNAi will be used to alter the expression of *Atp10c*/ATP10C *in vitro* and a commercially available plasmid construct containing ATP10C cDNA coupled with a GFP cDNA will be used in a similar fashion for this project to characterize *Atp10c*/ATP10C and hopefully, identify its location within the cell, thus estimating possible biological functions. The skeletal muscle cell lines, murine C2C12 and rat L6-G4myc were used as the *in vitro* systems to investigate the biological role of *Atp10c*/ATP10C in PI3K, MAPK, and endocytosis/exocytosis of GLUT4. Specific experiments and the corresponding results will be discussed in greater detail throughout the remainder of this dissertation.

CHAPTER III

EXPERIMENTAL INVESTIGATIONS

General Characterization

Abstract

Atp10c is a putative phospholipid "flippase" that encodes for a type 4 P-type ATPase. Based on previous research, we hypothesize that ATP10C due to its flippase nature plays a role in DIO and T2D as *Atp10c* heterozygous mice display this phenotype. For our investigation, we characterized *Atp10c*/ATP10C in order to gleam information about its biological role and/or function. In order to do this, an ATP10C-GFP plasmid construct was commercially obtained and transfected into HEK293T cells. Results showed a band at the expected molecular weight, about 165 kD. Next, immunolocalization by fluorescence confocal microscopy was employed, and we were able to show that the ATP10C-GFP fusion protein localized to the plasma membrane of HEK293T cells; also we see some co-localization of ATP10C with GLUT4 (about 81%). Finally, the expression of *Atp10c* in two mice models, one DIO and the other genetic (*ob/ob*) was measured. Results from these experiments revealed a high expression in all the tissues tested. The expression of *Atp10c* was highest in fat for the *ob/ob* mice (2.94 fold). For the DIO mice, the expression of *Atp10c* was higher in the skeletal muscle (3.78 fold). All the results presented strengthen *Atp10c*'s role in glucose and lipid metabolism.

Introduction

Due to the staggering numbers of new incidents of DIO and T2D reported each year, there is a desperate call for new research to examine the relationship between T2D and its co-morbidities, to understand the underlying causes those diseases, and to clarify unknown players in metabolic pathways related to T2D and other related disorders. However, problems arise in the study of such complex disorders as searching for genes related to IR and T2D presents with major issues, mainly genetic and environmental components. The genetic component of these diseases is based on multiple, single genes that act together with one or more genes which may be exposed to specific environmental factors. As early as the 1990s, geneticists were able to argue that human obesity genotypes will be complex multigenic systems with networks of gene-gene and gene-environment interactions. As such, the growing number of obesity-related or obesity-causing genes does not bode well for the single gene hypothesis [12]. Nor does a single-gene hypothesis work for complex metabolic disorders like IR and T2D. Furthermore, if research focuses specifically on a single gene and its effect on IR and/or T2D while failing to examine and manage for other known as well as unknown involved genes and environmental contacts, then results of experimental and clinical studies become difficult to interpret. Since these factors are difficult to control in human subjects, polygenic diseases can be more easily studied in cell culture models. HEK293 cells have been grown in tissue culture for many years and are very widely used as they are relatively easy to grow and transfect readily. An important variant of this cell line is the HEK293T cell line that contains the SV40 large T antigen, which allows for replication of

transfected plasmids containing the SV40 origin of replication. This benefit allows for amplification of transfected plasmids and extended expression of the desired gene products [63, 64]. For our investigation, we decided to use this cell culture model, HEK293T to look at *Atp10c*/ATP10C, a putative phospholipid translocase or "flippase", in order to gleam information about its biological role and/or function in glucose metabolism. We hypothesize that as a putative flippase, *Atp10c*/ATP10C should be localized in or around the plasma membrane. Moreover, we believe that *Atp10c*/ATP10C plays a role in DIO and T2D as mice heterozygous for *Atp10c*/ATP10C display this phenotype and should be highly expressed in tissues responsible for glucose metabolism.

Materials and Methods

HEK293T, a commercially-available cell line, was purchased from Open Biosystems (Thermo Fisher Scientific, Waltham, MA). Dulbecco's modified Eagle's medium (DMEM) supplemented with 5% heat-inactivated FBS (fetal bovine serum), 100 units/ml penicillin and 100 μg/ml streptomycin, radioimmunoprecipitation assay (RIPA) buffer, and ABsolute Blue SYBR Green ROX quantitative PCR mix were also from Thermo Fisher Scientific (Waltham, MA). DMEM with 1% antibiotics and 10% FBS is furthermore referred to as the complete growth media. The protease inhibitor (pi) cocktail in dimethyl sulfoxide (DMSO) was obtained from Sigma Aldrich (St. Louis, MO). A Bicinchoninic Acid Kit (BCA) and an Enhanced Chemiluminescence (ECL) Western Blotting Detection Kit were purchased from Pierce Biotech Inc. (Rockford, IL) and used in protein experiments. Primary antibodies, β-tubulin, Calnexin, and Rab5, as well as the secondary antibody, horseradish peroxidase (HRP)-conjugated anti-rabbit IgG, were

obtained from Cell Signalling Technology (Danvers, MA). All immunofluorescence materials (protein blocks [normal rabbit], negative control [normal rabbit] and antibody diluent) were purchased from BioGenex (San Ramon, CA). Secondary antibody specific for immunofluorescence application, Alexa Fluor 568 donkey anti-rabbit, as well as Prolong Gold Anti-fade reagent and wheat-germ-agglutinin (WGA) were purchased from Invitrogen (Carlsbad, CA). RNeasy Mini Kit and QuantiTect primer assays for *Atp10c* were from Qiagen (Valencia, CA). Quantitative PCR primers specific for mouse glyceraldehyde 3-phosphate dehydrogenase (*Gapdh*) were designed using the Primer 3 program (http://primer3.sourceforge.net) and were commercially obtained from Operon (Huntsville, AL). The iScript cDNA synthesis kit was acquired from Bio-Rad Laboratories (Hercules, CA). The ATP10C-GFP plasmid and TurboFectin along with anti-DDK monoclonal antibody and peroxidase conjugated affinity purified goat anti-mouse IgG were purchased from OriGene Technologies, Inc (Rockville, MD). The GLUT4- expression plasmid was generated and graciously obtained by our lab from Dr. Jeffrey Pessin (University of Iowa, Iowa City, IA). Glass bottom culture dishes from MatTek Corporation (Ashland, MA) were also used for immunofluorescence experiments.

Cell Culture

HEK293T cells were cultured as described elsewhere [62, 63, 64]. Roughly 1.0 x 10^3cells were seeded in either a 60-mm dish. They were then maintained at 37°C and 5% CO_2 in complete growth media. At the appropriate confluency, cells were harvested for use in subsequent experiments.

Mouse Treatment and Sample Collection

DIO mice as well as *ob/ob* and their control littermates were purchased from the Jackson Laboratory (Bar Harbor, ME). For DIO mice, male C57BL/6J mice were fed a high-fat diet (60% kcal % from fat) (Research Diets, New Brunswick, NJ) or regular chow diet for 20 weeks before being euthanized at 26 weeks of age. Male *ob/ob* and their controls were fed a chow diet for 8 weeks before being euthanized at 14 weeks of age. The mouse studies were approved by the Institutional Animal Care and Use Committee (IACUC) at the University of Tennessee.

RNA, cDNA synthesis, and qPCR

The following procedures were performed as described elsewhere [2, 65, 66]. Cells were washed with ice cold 1X HBBS and total RNAs were isolated using RNeasy Mini RNA kit (Qiagen), according to the manufacturer's instructions. Single-stranded cDNA was synthesized using the iScript cDNA synthesis kit (Bio-Rad), and amplified using gene-specific primers by qPCR with mouse *Gapdh* as the housekeeping gene. All mRNA expressions were achieved by qPCR using ABsolute SYBR Green ROX quantitative PCR mix on the Strategene Mx3005P with MxPro analysis software under the following PCR conditions: 1 cycle of 50°C for 15 min and 95°C for 2 min, followed by 40 cycles of 95°C for 25 s, 52°C for 25 s and 72°C for 1 min. The relative abundance of target gene expression was calculated using the 2-ΔΔCT and standard curve method, with ΔΔCT being the difference between CT of the target gene normalized with respect to the *Gapdh* CT [67].

Transfection of ATP10C plasmids

TurboFectin is a transfection reagent optimized for nucleic acid delivery into eukaryotic cells. Its proprietary formulation of lipid/histone blend is supplied in 80% alcohol [68]. TurboFectin has been tested and shown to be very effective in the delivery of cDNA clones for gene overexpression like the ATP10C-GFP and GLUT4-RFP plasmids. As TurboFectin was used as the transfection reagent, standard protocol provided by the manufacturer was followed. Briefly, two days before transfection, HEK293T cells were plated at a density of 1.0 x 10^3 cells/dish in complete growth medium and grown to obtain 50-70% confluency. Cells were then incubated overnight and transfection proceeded the following day. To form the transfection complex of reagent and DNA, 100 uL of serum free medium plus the appropriate amount of TurboFectin (2-6 uL per 1 ug DNA based on manufacturer's instructions) were added to a tube. After mixing completely by gentle pipetting, this solution was incubated at RT for 5 min before the addition of the respective plasmid DNA (1-3 ug per well) to the TurboFectin-containing media prepared above. The two solutions were gently mixed and allowed to incubate at RT for 30 min. During this incubation period, the cells were removed from the incubator and the spent medium replaced with 2 mL of fresh complete medium per dish. Upon complex formation, the solution was added to the seeded cells drop-wise and distributed evenly throughout the dish. Cells were cultured for 24 and 48 hours before either harvesting for RNA and/or protein, or undergoing immunofluorescence analysis.

Preparation of cellular extracts, immunoblotting, and immunofluorescence

Total cell lysates were isolated using RIPA buffer according to standard methods [65, 66, 69]. Briefly, cells were washed twice with 1X HBBS and lysed in RIPA buffer containing pi at 4°C for 30 min. Lysates were centrifuged at 16,000*g* for 10 min at 4°C. Protein estimation was performed using the BCA kit (Pierce Biotech) with an internal standard, according to the manufacturer's instructions. Immunoblot analysis was carried out according to standard procedures [65, 66, 69]. Equal concentrations (25−100 μgs) of proteins were resolved on 10% SDS-PAGE, using 5X Laemmli sample buffer containing Tris-HCL (375 mM, pH 6.8), glycerol (48%), SDS (6%), β-mercaptoethanol (6%), and bromophenol (0.03%). Cell lysates were denatured by heating before being applied to SDS-PAGE gel. After electrophoresis, proteins were transferred to nitrocellulose membranes, blocked for 1 h in blocking solution (1-5% BSA in TBST buffer), and incubated with specific primary antibodies overnight at 4°C. Primary antibodies were detected with HRP-conjugated secondary antibodies, and antibody-protein complexes were visualized using ECL (Pierce Biotech).

For immunofluorescence, 2.0 x 10^4 cells were seeded onto glass bottom culture dishes (MatTek) and subjected to the appropriate treatments as described in the relevant sections. Immunofluorescence assays were carried out according to standard methods as described by others [17, 70]. Briefly, cells were fixed with 1% paraformaldehyde in 0.1 M sodium phosphate buffer, pH 7.3 for 10 min at RT. Cells were washed in 1X HBBS, permeabilized by incubating with 0.01% Tween-20/HBBS for 10 min, and then washed again with 1X HBBS. After the last wash, cells were blocked using blocking buffer (1% BSA, 2% normal serum, 0.1% Tween-20 in PBS) for 30 min; blocking solution contained

normal serum from the animal in which the primary antibody was generated. Once blocking was complete, the cells were incubated with specific primary antibodies overnight at 4°C. Bound antibody was visualized under the microscope (Leica SP2 confocal laser-scanning microscope, Leica Microsystems, Wetzlar, Germany) by incubating for 1 h with secondary antibody labelled with Alexa Fluor 568 [Tetramethyl Rhodamine Iso-Thiocyanate (TRITC)]. To visualize the nucleus, cells were exposed for 5 min at RT to a concentration of 300 nM DAPI (4', 6-diamidino-2-phenylindole, dilactate) in HBBS. DAPI was prepared and diluted based on manufacturer's instructions (Invitrogen). After washing, cells were mounted using ProLong Gold Antifade reagent (Invitrogen). Dishes were sealed and allowed to dry overnight before imaging. Additionally, both positive and negative controls were prepared and imaged alongside the samples to correct for any background fluorescence and to serve as controls for quantitative analysis. Images were captured using confocal microscopy (Leica SP2 confocal laser-scanning microscope, Leica Microsystems) with a 63x oil objective lens (NA 1.32) and an automated stage.

Immunofluorescence quantitation

Immunofluorescence images were analyzed using NIS-Elements software (AR v. 3.1) (Nikon Instruments). For each sample, image stacks (z-series) were acquired for 3 fields with a step size of 0.5 µm. The percentage of co-localization was calculated using Pearson's correlation with a perfect correlation of 1 as compared to the internal control.

Results and Discussion

HEK293T cells are frequently used to exogenously express target proteins for analyses of protein-protein interactions, subcellular localization, etc. Two days prior to transfection, cells were cultured in complete growth media under standard conditions [62, 63, 64] and a plasmid containing ATP10C and GFP (Origene) was transfected into HEK293T cells using TurboFectin transfection reagent (Origene). For the GLUT4 co-localization, a GLUT4-RFP plasmid was co-transfected along with the ATP10C-GFP plasmid. Without a good antibody available for ATP10C, this technique allowed us to finally show a protein band at the expected molecular weight, about 165 kD (cDNA of *Atp10c* is approximately 4.5 kb) (Figure 1).

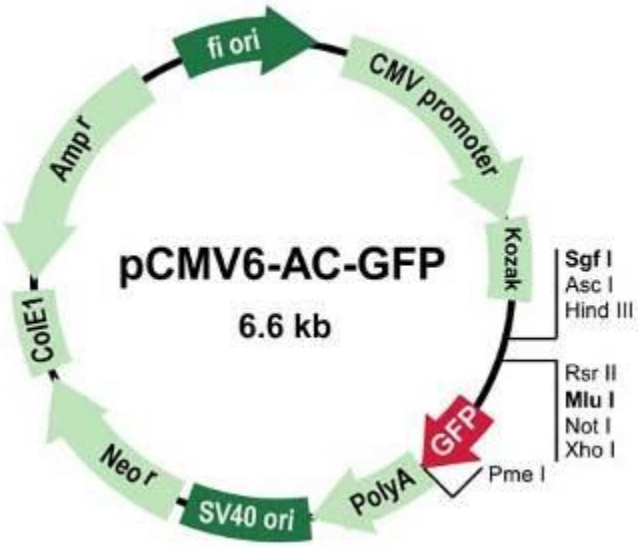

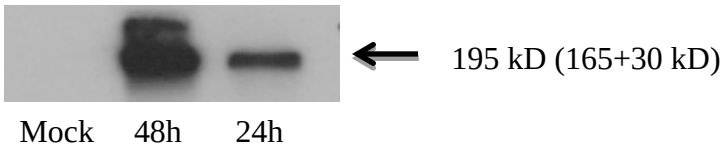

Figure 1: ATP10C-GFP expressed in HEK293T cells

ATP10C expression was examined by Western immunoblotting using HEK293T-ATP10C-GFP total proteins collected in RIPA buffer at 24 h and 48 h post-transfection. The 30kD molecular weight corresponds to the GFP fragment of the plasmid, while the 165 kD molecular weight is the expected size of ATP10C. *Modified from "Turbofectin", Origene Technologies, Inc [68]*.

Using immunofluorescence and confocal microscopy, we were able to show that the ATP10C fusion protein localized to the plasma membrane of HEK293T cells (Figure 2). Similar studies using confocal immunofluorescence microscopy showed that ATP8B1, ATP8B2 and ATP8B4, all members of the same ATPase family as ATP10C, localized primarily at the plasma membrane. Additionally, ATP8A1 displayed a peri-nuclear staining and co-localized with the Golgi-marker formiminotransferasecyclodeaminase indicating expression in the Golgi complex. When expressed at very high levels, these type 4 ATPases also showed nuclear-envelope and reticular staining that coincided with the endoplasmic reticulum (ER) marker protein, disulfide isomerase [26].

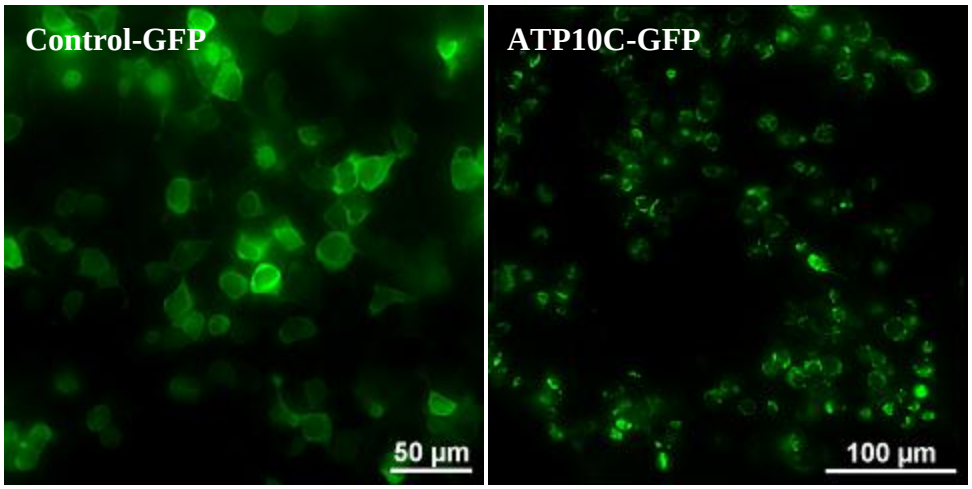

Images courtesy of J. Dunlap, Advanced Microscopy and Imaging Center, UTK.

Figure 2: Localization of ATP10C-GFP in HEK293T cells

ATP10C localization was determined by immunofluorescence microscopy using HEK293T-ATP10C-GFP cells. HEK293T cells were transfected with an ATP10C-GFP expression plasmid; a control-GFP plasmid (pMax) was also transfected into HEK293T cells to serve as a positive control. All samples were fixed at a designated time point (48 h). Confocal images were captured on a Leica SP2 laser scanning confocal microscope (Leica Microsystems, Wetzlar, Germany) with a 63x oil objective lens (NA 1.32). For each sample, image stacks (z-series) were acquired for 3 fields with a step size of 0.5 µm.

Based on these findings, we sought to co-localize ATP10C with known subcellular markers from a subcellular localization antibody kit (Cell Signaling). Currently, none of the antibodies tested co-localized with ATP10C suggesting that ATP10C does not localized in the microtubules (β-tubulin), the ER (Calnexin), or the endosome (Rab5) (Figure 3). This makes sense as these proteins are expressed solely in specialized compartments of the cell and not around the plasma membrane or in the Golgi network. Based on these results it does not appear that like many other ATPases, ATP10C localizes to the ER or endosomes. When we co-transfected ATP10C-GFP with a GLUT4 expression plasmid, it appears as though there is some overlap in their localization (Figure 3). It is difficult to quantify this co-localization as the transfection of both plasmids into the HEK293T has relatively low efficiency. As such, this procedure needs to be optimized for maximum transfection efficiency before any further conclusions can be made. However, by measuring a particular region of interest (ROI) within a given field, we were able to calculate percentage of co-localization of ATP10C and GLUT4. Pearson's correlation of the two proteins yielded an 81% co-localization. This value was obtained when comparing the image with significant overlap with an image that had none (0.1% co-localization). Future work to see if ATP10C co-localized with any of the known Golgi, VAMP, and SNARE markers should be conducted. Unfortunately, we cannot use the HEK293Tcells to perform these experiments as these cells are non-responsive to insulin and therefore, do not contain the machinery necessary to form and/or translocate glucose storage vesicles (GSVs). As such, another transfectable *in vitro* cell models must be found and optimized for these experiments.

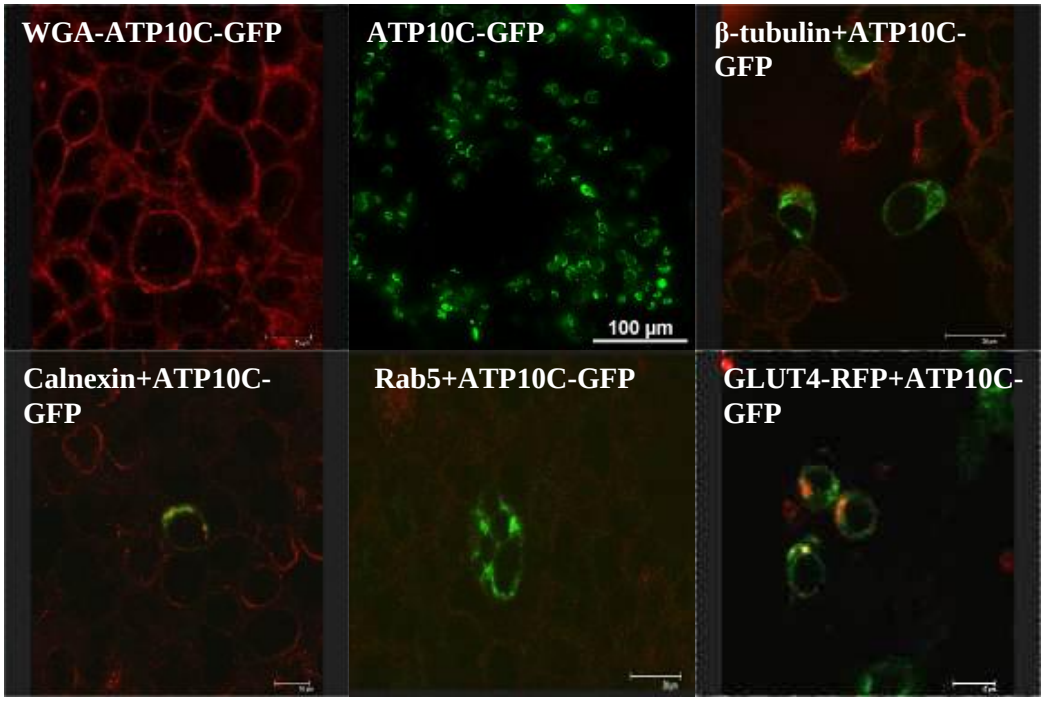

Images courtesy of J. Dunlap, Advanced Microscopy and Imaging Center, UTK.

Figure 3: Co-localization of ATP10C-GFP with known protein markers

ATP10C localization was determined by immunofluorescence microscopy using HEK293T-ATP10C-GFP cells, or HEK293T cells co-transfected with both plasmids, ATP10C-GFP and GLUT4-RFP. Cells transfected with the ATP10C-GFP plasmid only were immunostained with primary polyclonal antibodies and labeled using the appropriate secondary antibodies conjugated with TRITC. Confocal images were captured on a Leica SP2 laser scanning confocal microscope (Leica Microsystems, Wetzlar, Germany) with a 63x oil objective lens (NA 1.32). For each sample, image stacks (z-series) were acquired for 3 fields with a step size of 0.5 µm.

Given the significant results of the ATP10C, GLUT4 co-localization, we wanted to explore further the possible interaction of these proteins and their plausible joint role in DIO and T2D. As a possible consequence and/or cause of DIO, insulin increases triglyceride storage in adipocytes, inhibits of the breakdown of fat, and stimulates adipocyte differentiation, thus increasing the level of adipose tissue [71, 72]. An increase in adiposity additionally raises various secreted adipokines which in turn cause secondary effects in liver and skeletal muscle. An aberration in any of these processes will result in IR. IR resistance in skeletal muscle like adipose tissue can be caused by alterations in insulin binding and signalling that effect glucose and lipid metabolism. Insulin sensitivity improves when insulin binds to its membrane bound receptor, eliciting downstream effects that lead to the uptake of glucose from the blood.

Based on previous results from our laboratory, *Atp10c*-heterozygotes represent a novel model of DIO and T2D, to further validate this model, we examined the expression of *Atp10c* in two mice models of obesity, one genetic and one diet-induced. Since we hypothesize that *Atp10c*/ATP10C plays a role in DIO and T2D, we wanted to examine its expression in key tissues (skeletal muscle, adipose and liver tissues) responsible for glucose homeostasis. As shown in Figure 4, there is relatively high change of expression in the skeletal muscle (3.78 fold) as compared to adipose and liver tissues in the DIO model. In the *ob/ob* mice, *Atp10c* expression was highest in fat (2.94 fold), then skeletal muscle (2.44 fold) when compared to their age and sex matched wild type controls as indicated in Figure 5. While none of these tissues show significant expression of *Atp10c* when compared to their age and sex-matched controls, we are still assured that given the expression profiles of the skeletal and fat tissues, this novel gene is important in both

DIO and T2D and its functional investigation involving these disease processes is not only warranted, but is necessary.

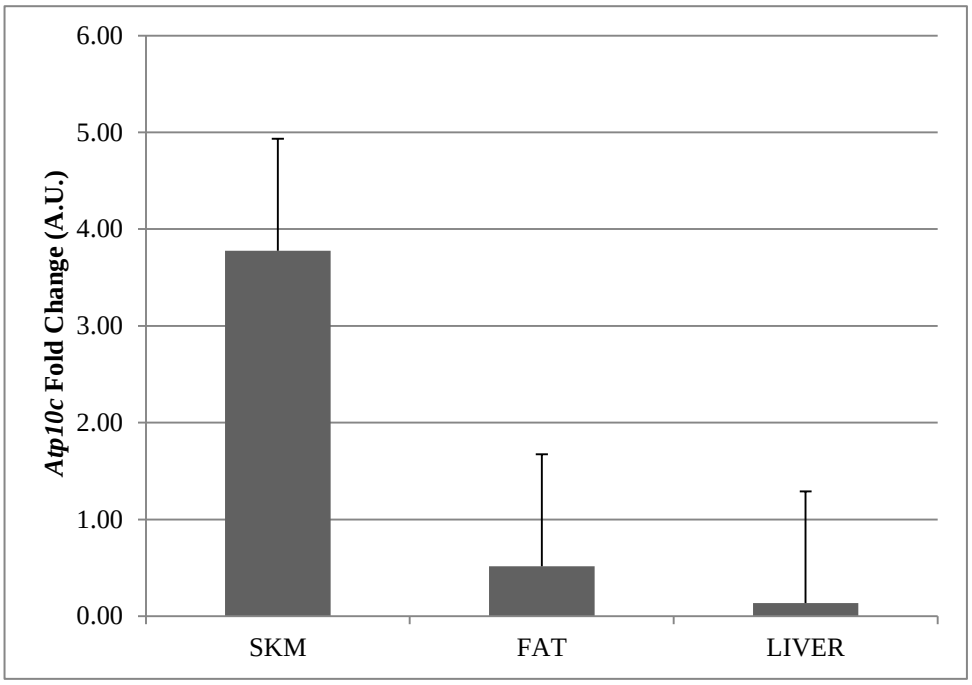

Figure 4: *Atp10c* mRNA is expressed in a DIO mouse model

Atp10c expression was examined by qPCR in mouse skeletal muscle (SKM), in mouse epididymal fat (FAT), and in mouse liver (LIVER) tissues after 20 weeks on a high fat diet. *Gapdh* served as an internal control. The expression of *Atp10c* is denoted as an arbitrary unit (A.U.) and is represented normalized to *Gapdh.*

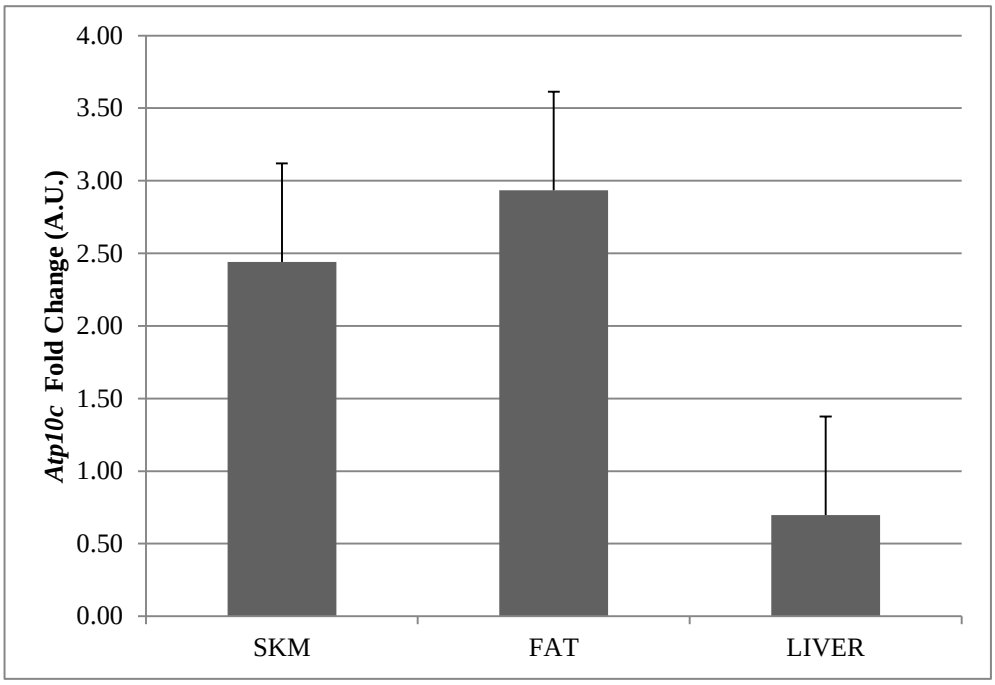

Figure 5: *Atp10c* mRNA is expressed in a genetic mouse model of obesity (*ob/ob*)

Atp10c expression was examined by qPCR in mouse skeletal muscle (SKM), in mouse epididymal fat (FAT), and in mouse liver (LIVER) tissues. *Gapdh* served as an internal control. The expression of *Atp10c* is denoted as an arbitrary unit (A.U.) and is represented normalized to *Gapdh.*

Overall, in the genetic model of obesity (*ob/ob*), *Atp10c* expression was highest in adipose tissue (2.94 fold) suggesting that this gene may play an important role in adiposity. This pronounced effect on the fat can then in turn affect various other tissues in the body such as skeletal muscle and the liver. Studies in our laboratory have further demonstrated that *Atp10c* encodes an APLT and is a type 4 P-type ATPase related to lipid trafficking and maintenance of the phospholipid asymmetry and fluidity of the plasma membrane. Moreover, *Atp10c* seems to be involved in modulating body fat. Evidence continues as mice inheriting a maternal deletion of *Atp10c* are considered a model of DIO and T2D, since they develop more hyperinsulinemia, IR, and NAFLD than mice inheriting the same deletion paternally. Similarly, simulations of maternal deletion of *Atp10c* indicated an anabolic metabolism consistent with the known clinical phenotypes of obesity [12].

For the DIO mice, the expression of *Atp10c* was higher in the skeletal muscle (3.78 fold), so changes in diet appear to effect the expression of *Atp10c* validating its role in DIO and other disorders that can arise like IR and T2D. Moreover, these results demonstrate that the diet induced greater responses in skeletal muscle than it does in fat tissue. In a 2004 study, Dhar et al [72] showed that when these mutant mice were placed on a high-fat diet (45% energy), body weight, adiposity index, and plasma insulin, leptin and triglyceride concentrations were significantly greater in the mutants compared with their age and sex-matched control mice fed the same diet. Additionally, glucose and insulin tolerance tests were performed on these mice, and the mutants had altered glucose tolerance and insulin response compared with controls resulting in IR. Moreover, routine gross and histological evaluations of the liver, pancreas, adipose tissue, and heart were

performed and histological evaluation showed micro and macrovesicular lipid deposition within the hepatocytes that was more severe in the *Atp10c* mutant mice than in age-matched controls.

Importantly, the 2004 Dhar et al study [72] focused primarily on the obesity issues and therefore, studies were exhaustive for adipose tissue. Future work on these *Atp10c*-mutant mice needs to be conducted to focus on the skeletal muscle consequences of this genetic aberration as our results from this study and numerous others show that skeletal muscle is a vital player in both glucose and lipid metabolism. Moreover, all these results give direct evidence from the *Atp10c* mutant mice demonstrating the significance of both genetics and environmental conditions in the disease states of DIO and T2D.

Conclusions

Atp10c/ATP10C is a putative phospholipid translocase that *Atp10c* plays a role in the maintenance of the phospholipid asymmetry and fluidity of the plasma membrane. As such, loss of *Atp10c*/ATP10C function upsets the normal membrane environment and perturbs glucose and lipid metabolism. To understand the role of type 4 P-type ATPases, it is important not only to study the cellular consequence when they are non-functional, but also to elucidate the specific conditions required for their activation as well as their (subcellular) localization [27]. Our results concluded that ATP10C, a 165 kD protein, localizes in or around the plasma membrane and appears to co-localize with GLUT4 as well. In view of the data presented here and the literature discussed, we are encouraged in using this model to dissect metabolic pathways involved in glucose and lipid metabolism thus gaining a better understanding of the underlying molecular mechanisms through

biological characterization. Also, in the present study, we established the legitimacy of our gene as a good candidate for DIO and T2D, as demonstrated by *Atp10c*'s increased expression in two mice models of obesity, one a genetic model and the other an environmental one. Specific targeted experiments to generate adipose tissue and skeletal muscle-specific transgenic mice and to then, assess protein expression of target genes are projects that should be initiated in the future.

Biological Characterization

Abstract

Atp10c/ATP10C is a strong candidate gene for DIO and T2D. To identify molecular and cellular targets of ATP10C, *Atp10c* mRNA expression was altered *in vitro* in C2C12 and L6-G4myc skeletal muscle myotubes transiently by transfection with an *Atp10c*-specific siRNA. During basal and insulin-stimulated conditions, results show that several MAPK proteins are altered both *in vitro* and *in vivo*. The PI3K pathway was also shown to be effected as key proteins in that pathway were also altered during both experimental states. Additionally, GLUT1 was significantly up-regulated; no changes in GLUT4 expression were observed. Glucose uptake assays revealed that insulin stimulation caused a significant 2.54-fold decrease in 2-DOG uptake in transfected cells. Results from GLUT4 translocations assays show that silencing of *Atp10c* is altering normal GLUT4 regulation, most likely playing a role in GLUT4 endocytosis. The involvement of MAPK proteins was confirmed using the specific inhibitor SB203580, which down-regulated the expression of native and phosphorylated MAPK proteins in transfected cells without any changes in insulin-stimulated glucose uptake. Taken together, all these results indicate that *Atp10c* regulates glucose metabolism, with strongest evidence supporting its action on the MAPK pathway, specifically p38, and thus, plays a significant role in the development of IR and T2D.

Introduction

The incidence of T2D and DIO is increasing rapidly and reaching epidemic proportions throughout the world populations. Although the cause of T2D remains unclear, it is known that IR is closely related to the development of the disease. IR is characterized by a failure of the hormone, insulin, to result in efficient glucose disposal, and particularly produce its normal increase in glucose transport in target tissues namely skeletal muscle and adipose tissue. Defective glucose uptake in skeletal muscle and adipose tissues plays a major role in causing IR and glucose intolerance symptoms associated with T2D. In humans, skeletal muscle accounts for nearly 40% of the body's mass and serves as the main tissue involved in glucose uptake during insulin stimulation. Several researchers have established that glucose consumption in skeletal muscle decreases with T2D. This reduced glucose consumption can be the result of impaired transduction of insulin signals, such as IRS phosphorylation; PI3K activity; MAPK activity; insulin-responsive glucose transporters, namely GLUT4; and/or other insulin-independent mechanisms [18]. Therefore, a detailed analysis of insulin signaling at the cellular and molecular level is critical to understand the pathogenesis of T2D associated with DIO. Cell culture models have been used extensively in research to investigate numerous disease states including IR and T2D. As skeletal muscle is the target tissue of interest for glucose clearance and as such a desirable object of study in regards to IR and T2D, the cell culture models used must exhibit similar characteristics and behaviors of the tissue under investigation. For our experiments, two skeletal muscle models were chosen, murine C2C12 and rat L6. Specifically, rat L6 cells over-expressing a GLUT4-

myc tag were used for analysis of the PI3K pathway and its association with GLUT4 translocation.

Heterozygous *Atp10c* mice present with the disease states of IR and DIO, as well as a host of other related disorders, including hyperlipidemia and hyperinsulinemia. Previous research using these mice indicates that the *Atp10c* gene appears to be a strong candidate gene for DIO and T2D [72]. *Atp10c* is a putative phospholipid translocase or "flippase," which encodes for a type 4 P-type ATPase. *Atp10c* maps to the *p*-locus on mouse chromosome 7, to a region of a quantitative trait locus associated with body weight, body fat and diabetic phenotypes. The human ortholog, *ATP10C,* maps to the syntenic region on chromosome *15q12* and is also associated with an elevated BMI [36, 73]. Moreover, microarray gene profiling on *Atp10c* heterozygous mice indicated significant changes in the mRNA expression of factors involved in insulin dependent and insulin-independent glucose uptake [2].

Although flippases, like *Atp10c*, have been studied for many years, their exact character and function remain unclear. These proteins are believed to maintain the asymmetry of the lipid bilayer by translocating specific phospholipids from one leaflet to the other and vice versa [7], but they may also participate in the formation of transport vesicles [74]. Moreover, deficiencies in these proteins have been shown to cause defects in lipid metabolism and have been implicated in the disease states of DIO, T2D, and NAFLD [72]. Not much is known about the role of ATP10C in regulating IR in skeletal muscle, if any, and its possible molecular and cellular targets have not been investigated.

In view of the above literature, we hypothesized that the type 4 P-type ATPase, ATP10C has an important role in glucose metabolism. Since ATP10C is a

transmembrane protein it might exert its effect via multiple signaling pathways; (1) acting solely at the plasma membrane to maintain the non-random distribution of phospholipids, thus contributing to a proper membrane environment for normal protein sequestration and function, (2) acting at the plasma membrane affecting the biogenesis of membrane vesicles important for plasma membrane delivery and/or retrieval of glucose transporter proteins in basal and insulin-stimulated states, and (3) acting directly on the expression, translocation and/or function of glucose transporter proteins themselves. Based on the observed phenotype of glucose and lipid metabolic abnormality in *Atp10c*-heterzygous mice, we explored *Atp10c*/ATP10C's role in these important pathways to address its plausible function. Since the MAPK pathway is known to be a key signaling cascade which mediates glucose clearance/uptake by the skeletal muscle in presence or absence of insulin, we tested whether the MAPKs, in general, are the targets of ATP10C. To prove our hypothesis, specific objectives were to (a) establish a tissue culture systems of mouse skeletal muscle wherein endogenous expression of *Atp10c* could be monitored, (b) alter the endogenous level of *Atp10c* expression by siRNA and, (c) measure functional outcomes i.e. glucose uptake and GLUT4 translocation and assess changes in expression of MAPKs involved in this process. Moreover, since the MAPK pathway is known to be a key signaling cascades which mediate glucose clearance/uptake by the skeletal muscle in presence or absence of insulin, we tested whether the products of this pathway are potential targets of ATP10C, and whether or not the activity of the PI3K pathway, the insulin-dependent pathway, is altered by *Atp10c*-silencing.

Materials and Methods

Mouse skeletal muscle cell line C2C12, a commercially-available cell line, was kindly provided by Dr. Seung Baek, College of Veterinary Medicine, the University of Tennessee, Knoxville, TN, USA. Rat L6 muscle cells stably expressing GLUT4 with an exofacial myc-epitope (L6-G4myc) were commercially obtained from Dr. Amira Klip (The Hospital for Sick Children, Toronto, Canada). DMEM containing 4.5 mg/L glucose and 4.5 mM/L L-glutamine, antibiotics (100 IU/ml penicillin and 100 μg/ml streptomycin), ABsolute Blue SYBR Green ROX quantitative PCR mix, BCS, and RIPA buffer were from Thermo Fisher Scientific (Waltham, MA). DMEM with 1% antibiotics and 10% BCS is furthermore referred to as the complete growth media. Horse serum, 2-DOG, pi cocktail in DMSO solution, MAPK inhibitor SB203580, and human insulin solution (10 mg/mL in HEPES, pH 8.2) were from Sigma Aldrich (St. Louis, MO). α-Minimum essential medium (α-MEM) containing 5.5 mM glucose was obtained from Gibco (Grand Island, NY) and 10% FBS was purchased from HyClone Laboratories (Grand Island, NY). BCA and an ECL Western Blotting Detection Kit were purchased from Pierce Biotech Inc. (Rockford, IL) and used in protein experiments. Primary antibodies (p38, phospho-p38, JNK, phospho-JNK, ERK1/2, phospho-ERK1/2, phospho-Akt2 (Ser473) and phospho-Akt2 (Ser/Thr) referred hereafter as AS160) as well as the secondary antibody, HRP-conjugated anti-rabbit IgG, were obtained from Cell Signaling Technology (Danvers, MA). PY20 and its specific secondary antibody (goat anti-mouse) were purchased from BD BioSciences, Sparks, MD). Caveolin-1 was used as an immunoblot control and was purchased from Santa Cruz Biotechnologies (Santa Cruz, CA) along with primary antibodies for PI3K, Akt2, myc, GLUT1, and GLUT4. The

secondary antibody, HRP-conjugated anti-goat IgG, was also obtained from Santa Cruz Biotechnologies. HiPerfect transfection reagent, *Atp10c*-specific siRNA constructs, RNeasy Mini Kit and QuantiTect primer assays for *myogenin*, *MyoD* and *Atp10c* were from Qiagen (Valencia, CA). Quantitative PCR primers specific for mouse glyceraldehyde 3-phosphate dehydrogenase (*Gapdh*) were designed using the Primer 3 program (http://primer3.sourceforge.net) and were commercially obtained from Operon (Huntsville, AL). The iScript cDNA synthesis kit was acquired from Bio-Rad Laboratories (Hercules, CA). All immunofluorescence materials (protein blocks [normal goat], negative control [normal goat] and antibody diluent) were purchased from BioGenex (San Ramon, CA). All the immunocytochemistry materials (Odyssey Blocking Buffer and infrared-conjugated secondary antibody) were purchased from LI-COR Biosciences (Lincoln NE). Syto60 was purchased from Molecular Probes (Eugene, OR). Millicell EZ slides from Millipore (Billerica, MA) were used for the immunofluorescence studies. Secondary antibody specific for immunofluorescence application, Alexa Fluor 568 donkey anti-goat as well as Prolong Gold Antifade reagent were purchased from Invitrogen (Carlsbad, CA).

Cell culture and treatments

C2C12 myoblasts were cultured as described elsewhere [70]. Roughly 2.0 x 10^5 cells were seeded in a 60-mm dish or a single well of a 6-well plate. They were maintained at 37°C and 5% CO_2 in complete growth media. Cells at 70% confluency were differentiated in the presence of 2% horse serum-enriched media for 3–5 days. Completely differentiated myotubes (days 3–5) were either subjected to various

treatments described in the relevant sections or harvested for use in subsequent experiments. L6-G4myc cells were cultured as previously described [76]. Myoblasts were maintained and differentiated into multinucleated myotubes with the addition of 2% FBS. All studies with the L6-G4myc cells used myotubes between 4-6 days post-initiation of differentiation. Cells were serum starved for 30 min before all experiments. During the final 20 min of these incubations, cells were left in either the basal state or were acutely stimulated with 100 nM insulin.

Mouse treatment and sample collection

Mice containing radiation-induced chromosomal deletions of *Atp10c* on mouse chromosome 7 located at the *pink-eyed dilution* locus were generated and maintained [77, 78]. Heterozygous mice inheriting the deletion maternally that were fed a high-fat diet as were heterozygotes inheriting the *Atp10c*-deletion paternally which served as the controls. After feeding both sets of mice for 4 and 12 weeks, the mice were euthanized and tissues collected. The mouse studies were approved by the IACUC at the University of Tennessee.

siRNA transfection

Three different siRNA oligonucleotides against *Atp10c* were commercially obtained (Qiagen); one was generated from the sequence at the 3′ end of the *Atp10c* gene, SI00906220 (sense: r[CCU GGG UAU UGA AAC CAA A]dTdT and antisense: r[UUU GGU UUC AAU ACC CAG G] dTdG), the second, SI00906213, and third, SI00906206, were generated from the sequence at the 5′ end (sense: r[CGU CUU UGC UGC AAU

GAA A]dTdT and antisense: r[UUU CAU UGC AGC AAA GAC G]dGdA). C2C12 and L6-G4myc myotubes were transiently transfected with and *Atp10c*-specific siRNA using HiPerfect transfection reagent (Qiagen) according to the manufacturer's instructions. Myotubes transfected with siRNA were either harvested or treated with the reagents indicated in the relevant sections and/or used for functional assays.

In the first experiment, the optimum concentration and time of knockdown for each siRNA used was determined. Briefly, HiPerfect transfection regent and siRNAs were mixed at various concentrations (0, 50, 100, and 200 nM) to form a complex. The transfection complexes were then applied to designated cells and incubated for 24, 48, or 72 h before subsequent analysis. C2C12 and L6-G4myc myotubes demonstrating efficient *Atp10c* knockdown as quantitated by qPCR and, therefore, used in all further experiments were designated as C2*10c*/- and L6*10c*/-. Mock transfected (i.e. transfected with HiPerfect only) C2C12 and L6-G4myc myotubes (C2wt and L6wt respectively) were used as corresponding controls.

RNA, cDNA synthesis, and qPCR

The following procedures were performed as described elsewhere [2, 65, 66]. Cells were washed with ice cold 1X HBBS and total RNAs were isolated using RNeasy Mini RNA kit (Qiagen), according to the manufacturer's instructions. Single-stranded cDNA was synthesized using the iScript cDNA synthesis kit (Bio-Rad), and amplified using gene-specific primers by qPCR with mouse *Gapdh* as the housekeeping gene. All mRNA expressions were achieved by qPCR using ABsolute SYBR Green ROX quantitative PCR mix on the Strategene Mx3005P with MxPro analysis software under the following

PCR conditions: 1 cycle of 50°C for 15 min and 95°C for 2 min, followed by 40 cycles of 95°C for 25 s, 52°C for 25 s and 72°C for 1 min. The relative abundance of target gene expression was calculated using the 2-ΔΔCT and standard curve method, with ΔΔCT being the difference between CT of the target gene normalized with respect to the *Gapdh* CT [67].

Preparation of cellular extracts and immunoblotting

Total cell lysates were isolated using RIPA buffer according to standard methods [65, 66, 69]. Briefly, cells were washed twice with 1X HBBS and lysed in RIPA buffer containing pi at 4°C for 30 min. Lysates were centrifuged at 16,000*g* for 10 min at 4°C. Protein estimation was performed using the BCA kit (Pierce Biotech), with an internal standard according to the manufacturer's instructions.

Immunoblot analysis was carried out according to standard procedures [66, 69]. Equal concentrations (25−100 μgs) of proteins were resolved on 10% SDS-PAGE, using 5X Laemmli sample buffer containing Tris-HCL (375 mM, pH6.8), glycerol (48%), SDS (6%), beta-mercaptoethanol (6%), and bromophenol (0.03%). Cell lysates were denatured by heating before being applied to SDS-PAGE gel unless otherwise noted as in the case of GLUT1 and GLUT4 investigation. After electrophoresis, proteins were transferred to nitrocellulose membranes, blocked for 1 h in blocking solution (1-5% BSA in TBST buffer), and incubated with specific primary antibodies overnight at 4°C. Primary antibodies were detected with HRP-conjugated secondary antibodies, and antibody-protein complexes were visualized using ECL (Pierce Biotech). Results are expressed as the ratio of target protein expression to that of an internal loading control, caveolin-1.

Immunofluorescence and immunocytochemistry

For immunofluorescence, 2.0 x 10^4 cells were seeded onto 4-well chamber slides (Millipore) and subjected to the appropriate treatments as described in the relevant sections. Immunofluorescence assays were carried out according to standard methods as described by others [17, 75]. Briefly, cells were fixed with 1% paraformaldehyde in 0.1 M sodium phosphate buffer, pH 7.3 for 10 min at RT. Cells were washed in 1X HBBS, permeabilized by incubating with 0.01% Tween-20/HBBS for 10 min, and then washed again with 1X HBBS. After the last wash, cells were blocked using blocking buffer (1% BSA, 2% normal serum, 0.1% Tween-20 in HBBS) for 30 min. Blocking solution contained normal goat serum, the animal in which the primary antibody was generated. Once blocking was complete, the cells were incubated with specific primary antibodies overnight at 4°C. Bound antibody was visualized under the microscope (Nikon Ti-E Eclipse, Nikon Instruments, Melville, NY) by incubating for 1 h with secondary antibody labeled with Alexa Fluor 568 (TRITC). To visualize the nucleus, cells were exposed for 5 min at RT to a concentration of 300 nM DAPI in HBBS. DAPI was prepared and diluted based on manufacturer's instructions (Invitrogen). After washing, cells were mounted using ProLong Gold Antifade reagent (Invitrogen). Slides were sealed and allowed to dry overnight before imaging. Additionally, both positive and negative controls were prepared and imaged alongside the samples to correct for any background fluorescence and to serve as controls for quantitative analysis. Images were captured using an epifluorescence microscope (Nikon Instruments) with a 60x objective lens (NA 1.49) and an automated stage.

For immunocytochemistry, myotube GLUT4myc labeling was performed as previously described [76]. Briefly, myotubes were fixed with 2% paraformaldehyde/HBBS. After fixation, cells were left un-permeabilized and blocked in Odyssey Blocking Buffer (LI-COR Biosciences). The samples were then incubated in primary myc antibody (Santa Cruz Biotechnology) overnight, washed and incubated with an infrared-conjugated secondary antibody (LI-COR) for 1 h. Images were then taken and quantified for further analysis.

Glucose uptake

Glucose uptake in myotubes was measured as previously described [66]. Briefly, myoblasts were plated in 6-well cell culture plates at a density of 2 $x10^5$ cells/well and allowed to differentiate under normal conditions. After differentiation, cells were washed with IX HBBS and serum starved in DMEM only for 3−5 h. Cells were stimulated with 100 nM insulin in DMEM for 30 min at 37°C. Each 6-well plate was set up so that wells 1, 2, and 3 did not contain insulin and wells 4, 5, and 6 did contain insulin. Insulin induction was stopped by washing the cells twice with 1 ml Krebs-Ringer HEPES (KRP) (121 mM NaCl, 4.9 mM KCl, 1.2 mM MgSO4, 0.33 mM CaCl2, 12 mM HEPES) minus glucose at RT. Cytochalasin B (5 µl of 1 mM stock/1 ml cocktail) was used to normalize for non-specific glucose uptake. Glucose uptake was determined after the addition of 3H-2-deoxyglucose (1 µl of 10 Ci/mmol stock/1 ml cocktail) in KRP buffer at 37°C for 5 min. Incorporation was terminated by washing the cells twice with 1 ml ice cold KRP plus 25 mM glucose. Cells were lysed on ice for 30 min with RIPA buffer. Following incubation, 0.5 ml cell lysates were mixed with 10 ml scintillation fluid (Scintiverse) and

subjected to liquid scintillation counting. For protein quantitation (BCA method, Pierce Biotech), 250 µl of the lysate was used and processed according to the manufacturer's instructions. Glucose uptake was expressed as disintegrations per minute per microgram of total protein (dpm/µg). Data is reported as the glucose uptake stimulation expressed as the ratio of dpm/µg of total protein in presence of insulin to that in the absence of insulin.

Densitometry analysis

Relative densitometry analyses of the immunoblots were determined using Image J (http://rsb.info.nih.gov/ij/index.html) analysis software. By giving an arbitrary value of 1.0 to the respective control sample (caveolin-1) of each experiment, a ratio of relative density was calculated for each protein of interest.

Immunofluorescence and immunocytochemistry quantitation

Immunofluorescence images were analyzed using NIS-Elements software (AR v. 3.1) (Nikon Instruments). For each sample, 9 dual-channel images were captured and stitched together to form a large image (3x3). Mean fluorescence intensity per cell was calculated (MFI per cell = total image fluorescence/cell count). Cell count was determined using a nuclear stain (300 nM DAPI in HBBS).

For immunocytochemistry, images were collected and quantified with the Odyssey system as previously described [76]. Immunofluorescent intensity was normalized to intensity from Syto60, a fluorescent nucleic acid stain (Molecular Probes).

Statistical analysis

The data are expressed as mean ± SE. For comparison of two groups, *P* values were calculated using the two-tailed paired Student *t* test. In all cases $P < 0.05$ was considered statistically significant and $P < 0.10$ was indicative of a trend.

Results and Discussion

To alleviate whole-animal complexities, C2C12, a mouse skeletal muscle cell line as well as a rat skeletal muscle cell line, L6, overexpressing a GLUT4myc tag were chosen as *in vitro* models to identify molecular and cellular targets of *Atp10c*/ATP10C and then assess its biological role, if any, in insulin signaling and glucose metabolism [20, 21, 22, 23, 79]. Under permissive conditions, C2C12 and L6-G4myc myoblasts undergo differentiation to form myotubes. Differentiation of C2C12 myoblasts to myotubes was confirmed by visual inspection (Figure 6), as well as by monitoring the expression of skeletal muscle-specific mRNAs for *MyoD* and *myogenin* [80].

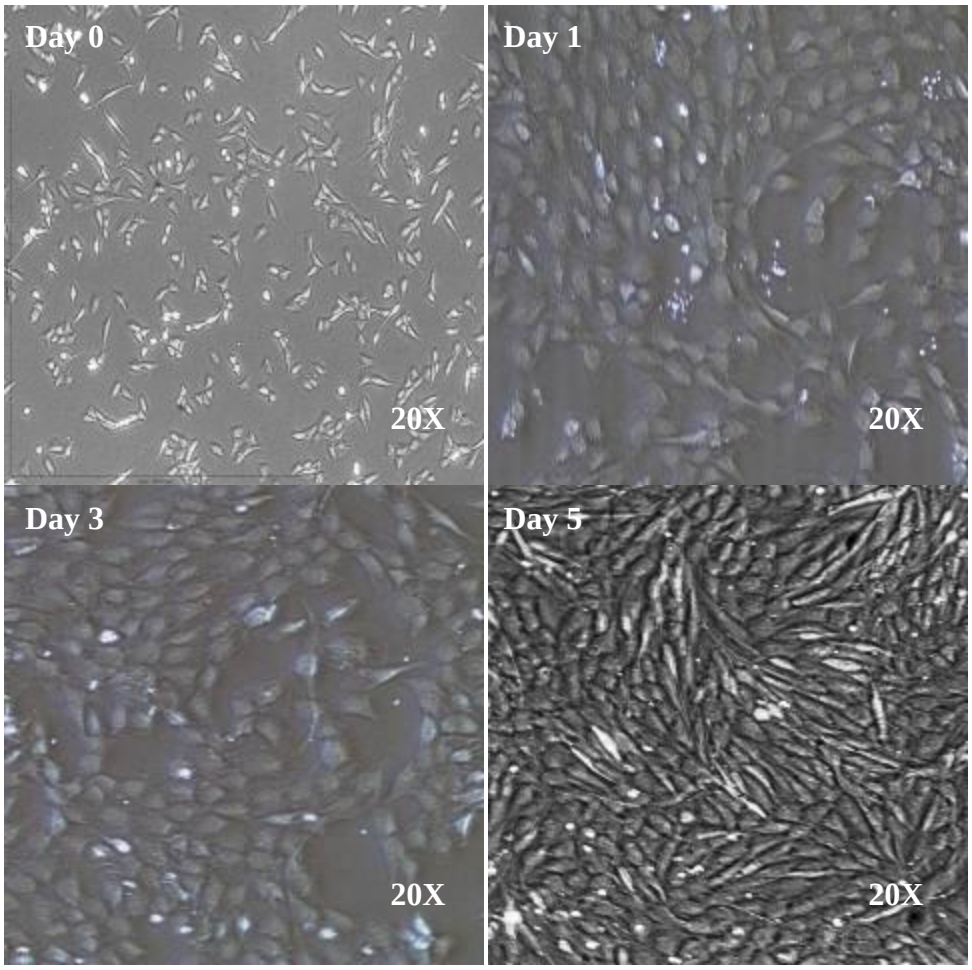

Figure 6: C2C12 myoblasts differentiate to myotubes

Skeletal muscle differentiation was examined in C2C12 cells. Cells were seeded into 60 mm dishes and allowed to attach. After 24 h, differentiation was stimulated via the addition of horse serum (2%) enriched media. Differentiation media was changed every 48 h until the process was complete (about 3-5 days). Images were produced on Digital USB2 Microscope (Westover Scientific Inc., Mill Creek, WA) using Micron imaging software.

C2C12 cells were collected on days 1, 3, and 5 during the differentiation process. Cells collected at day 1 represent the myoblasts, which are then stimulated to differentiate into myotubes by days 3-5. The activation of cell differentiation is characterized by the expression of myogenic regulatory factors including *MyoD* and *myogenin*. After proliferation, cells express *myogenin* which commits the myoblasts towards myogenic differentiation. This is followed by the expression of additional factors including but not limited to Myf-5 and MRF4, and permanent exit from the normal growth and proliferation cycles. As expected and shown in Figure 7, the expression of *myogenin* increased as C2C12 myoblasts were stimulated to differentiate (30% to 52%), and decreased when differentiation was complete (20%). Similarly, qPCR showed that *MyoD* expression increased dramatically on day 1 (172%), then steadily declined on days 3 and 5 (64% and 24%, respectively). Interestingly, *Atp10c* was expressed in both myoblasts and myotubes, and its expression increased upon differentiation (42% to 64%) and steadily decreased as myotubes were formed (47% on day 5). Changes in *Atp10c* expression with differentiation were similar, but, not as striking as that of *myogenin* and *MyoD*, ramifications of which are clearly beyond the scope of this study. The data thus demonstrated the expression of *Atp10c* mRNA in C2C12 cells, and gave us an opportunity to modulate its expression in both myoblasts and myotubes, both of which can have significant consequences in insulin signaling pathways.

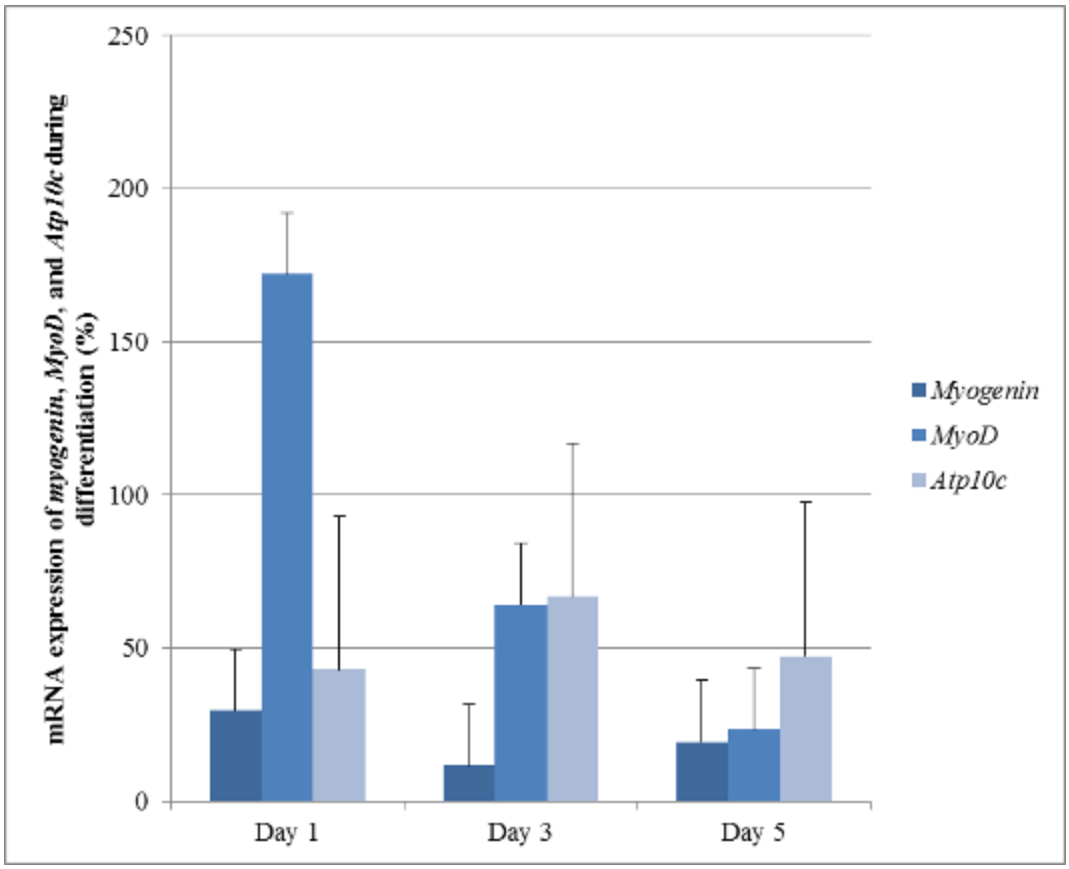

Figure 7: *Atp10c, myogenin,* and *MyoD* mRNA is expressed in C2C12 cells undergoing differentiation

Cells were collected at the above time points (Days 1, 3, and 5). *MyoD, myogenin* and *Atp10c* gene mRNA expression was analyzed using qPCR. The expression of *Atp10c, myogenin,* and *MyoD* is denoted as percentages (%) as normalized to *Gapdh.* Data represents three independent experiments with each sample repeated in triplicate.

One of the limitations of global gene-targeting and whole-animal approach is that adaptations over time might occur, possibly producing secondary phenotypes that are not directly linked to the mutation. In this case, the role of *Atp10c* could be shown either by generating knockout mice or using specific inhibitors against ATP10C. Since no inhibitors are available, and to avoid whole-animal complexities in transgenics, we modulated *Atp10c* expression *in vitro* in both C2C12 and L6-G4myc cells transiently by transfecting them with three independent and commercially available *Atp10c* specific siRNAs (Qiagen). ATP10C is a putative transmembrane domain protein and as such a good antibody against ATP10C has yet to be generated, making experiments to study ATP10C challenging. Therefore, in this analysis, changes in *Atp10c* expression were determined solely at the mRNA level by qPCR using QuantiTect primer assays (Qiagen). Out of the three siRNAs tested, only one, SI00906220, resulted in a significant knockdown of ≥70% (Figure 8 and Figure 9).

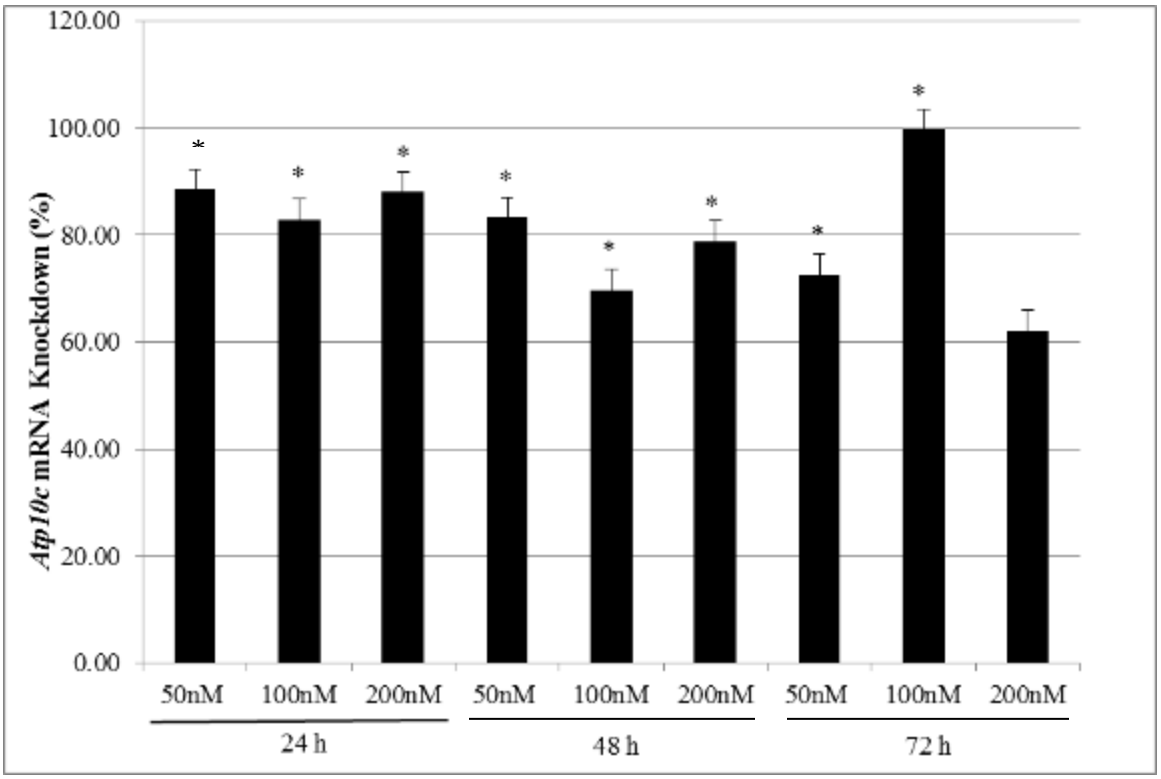

Figure 8: Optimization of siRNA in C2C12 myotubes at a concentration of siRNA (SI00906220) 50nM and a time point of 24 h gives the most efficient transfection condition.

C2C12 myoblasts were differentiated into myotubes. Myotubes were transfected at each concentration of siRNA (SI00906220) (0, 50, 100, and 200 nM) collected at the above time points (24, 48, and 72 h). *Gapdh* (housekeeping gene) and *Atp10c* gene mRNA expression was analyzed using qPCR. The percentage of knockdown was calculated at each concentration and time point based on the expression of the mock-transfected (0 nM) samples ($^{*}P < 0.7$ based on Qiagen recommendations). Data represents three independent experiments with each sample repeated in triplicate.

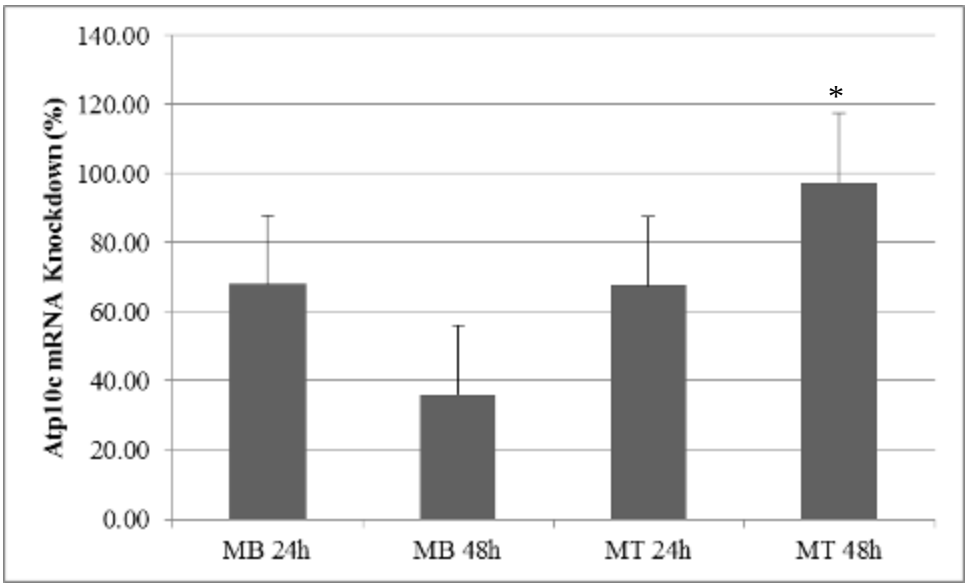

Figure 9: Optimization of siRNA in L6-G4myc cells at a concentration of siRNA (SI00906220) 50nM and a time point of 48 h gives the most efficient transfection condition.

L6-G4myc myoblasts and myotubes were transfected at each concentration of siRNA (SI00906220) (0 and 50 nM) collected at the above time points (24 and 48 h). *Gapdh* (housekeeping gene) and *Atp10c* gene mRNA expression was analyzed using qPCR. The percentage of knockdown was calculated at each concentration and time point based on the expression of the mock-transfected (0 nM) samples ($^{*}P < 0.7$ based on Qiagen recommendations). Data represents three independent experiments with each sample repeated in triplicate.

As shown in Figure 8, significant knockdowns (70 to 100%) were observed in all samples with the exception of 200 nM, 72 h for C2C12 myotubes. Higher concentrations and longer time periods resulted in cell death and poor quality of cells (as judged visually). Optimization of concentration and time of transfection results indicated that a concentration of 50 nM of siRNA (SI00906220) and a time point of 24 h be used for all subsequent experiments in C2C12 myotubes. Similarly, a siRNA (SI00906220) concentration of 50nM and a time point of 48 h were found to be optimal for the L6-G4myc myotubes (Figure 9). *Gapdh* was used as the housekeeping gene, and no significant mRNA changes in its corresponding expression in transfected cells were observed. Results thus suggest that changes in *Atp10c* expression after transfection with siRNA (SI00906220) were not an artifact, and there was no deleterious effect on C2C12 or L6-G4myc myotubes due to *Atp10c* silencing. All further experiments were carried out under these conditions in wild-type C2C12 (C2wt) and L6-G4myc (L6-G4myc wt) and *Atp10c*-silenced C2C12 and L6-G4myc myotubes (C2*10c/-*and L6-G4myc *10c/-*) simultaneously. Since these transfections are transient, *Atp10c* mRNA knockdown was confirmed in each and every experiment (data not shown).

Previous experiments in our laboratory have shown that on a high fat diet, there is a 35% decrease in glucose uptake in soleus muscle in *Atp10c* heterozygotes [2]. Based on this finding, we next determined whether down regulation of *Atp10c* expression had a similar effect *in vitro*. Glucose uptake was measured in C2wt and C2*10c/-* myotubes in basal (without insulin) and stimulated (100 nM insulin, 30 min) states. Fold change representing the glucose uptake stimulation/reduction between the C2wt and C2*10c/-* was compared. As shown in Figure 10, insulin stimulation caused a significant 2.54-fold

decrease in 2-DOG uptake in C2*10c*/- cells ($P < 0.05$). Data thus complement the *in vivo* findings, suggesting that *Atp10c* is necessary for insulin-stimulated glucose uptake in skeletal muscle and its knockdown renders the myotubes insulin resistant.

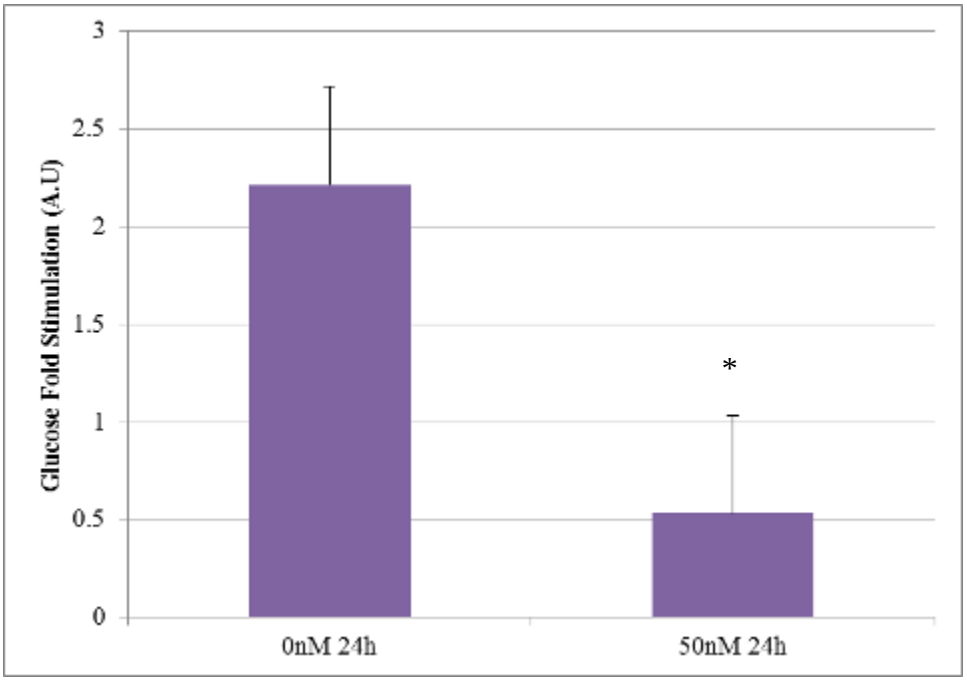

Figure 10: Glucose uptake in *Atp10c*-silenced C2C12 myotubes is decreased 2.5 fold

C2C12 myoblasts were differentiated into myotubes. Myotubes were transfected at each concentration of siRNA (SI00906220) (0 and 50 nM) at the designated time point (24 h). Cells were then stimulated with insulin (100 nM, 30 min), and a 2-DOG uptake was performed ($^{*}P < 0.05$). Data is reported as the glucose uptake fold stimulation which is expressed as the ratio of dpm/µg of total protein in presence of insulin to that in the absence of insulin and indicated as arbitrary units (A.U.).

Silencing *Atp10c* mRNA decreases cellular glucose uptake, which might be of consequence to impaired insulin signaling. Insulin-induced glucose uptake into muscle and adipose tissue involves a series of intracellular signaling cascades, culminating in glucose disposal and metabolism [81, 82, 83, 84, 85, 86]. The possible mechanisms include insulin-mediated activation of the insulin receptor and/or its downstream molecules, ultimately effecting GLUT4 expression and translocation. Since these processes are a complex interplay of a variety of proteins and because their changes have not been studied in *Atp10c*-silencing, we sought to identify changes in the key proteins of relevant signaling cascades, the PI3K and the MAPK pathway in the presence of any insulin stimulation. Specifically, in the present study, the effect of *Atp10c*-silencing was considered on three essential MAPKs: p38, JNK, and ERK1/2 in addition to PI3K key proteins PI3K, Akt2, phospho-Akt2 (Ser473) and AS160. Additionally, proteins up-stream of MAPK and PI3K, IRS-2, and IR-β, were examined. Total proteins isolated from C2wt, C2*10c/-*, L6-G4myc wt and L6-G4myc *10c/-* myotubes were subjected to immunoblot analysis while C2wt and C2*10c/-* myotubes were further analyzed using immunofluorescent techniques.

Under basal glucose uptake conditions for MAPK pathway analysis, results indicated significant up-regulation of p38 ($P = 0.02$) and ERK1/2 ($P = 0.04$), and a significant down-regulation of JNK ($P = 0.001$) and phospho-ERK1/2 ($P = 0.05$) in C2*10c/-* cells (Figure 11A-C). While not significant, results indicated a trend for an increase in phospho-p38 ($P = 0.1$) (Figure 13A) and phospho-JNK ($P = 0.06$) (Figure 11C). Besides these signal transduction proteins, there was significant up-regulation of

MyoD (P = 0.01), Actin (P = 0.02) (Figure 12A-B), and GLUT1 (P = 0.03) (Figure 13). Most importantly, there was no significant change in GLUT4 expression (Figure 13).

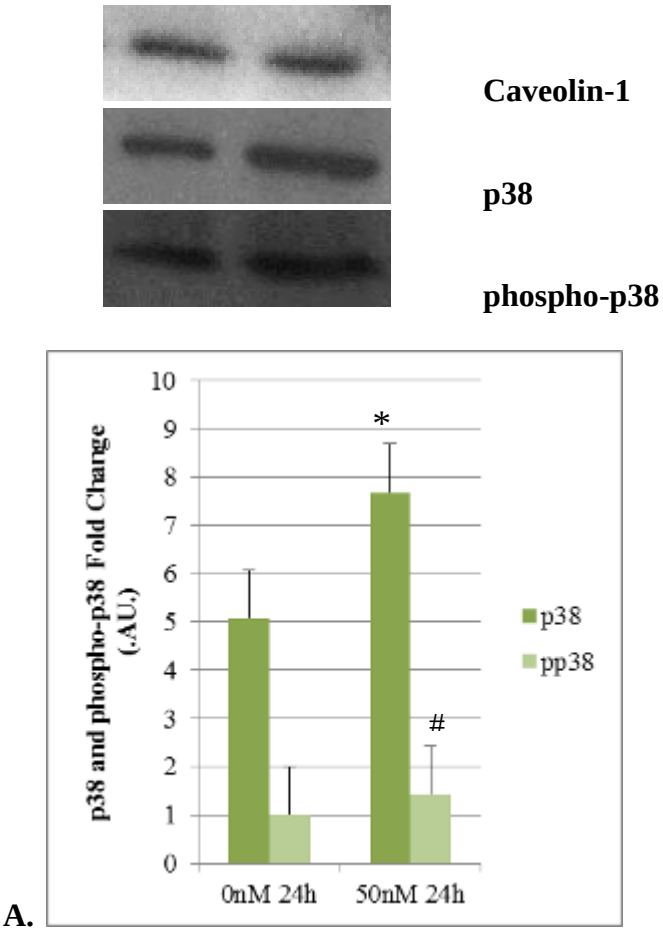

A.

Figure 11A: MAPK proteins, p38 and phospho-p38, are significantly up-regulated after *Atp10c*-silencing in C2C12 myotubes

C2C12 myoblasts were differentiated into myotubes, then transfected at each concentration of siRNA (SI00906220) (0 and 50 nM) and collected at the designated time point (24 h). Proteins were collected from these samples and subjected to immunoblot analysis. Data shown are representative of multiple independent experiments (n = 2 to 4), all analyzed in triplicate. The expression of p38 and phospho-p38 is denoted as arbitrary units (A.U.) and represented as the fold change normalized to Caveolin-1; **P*<0.05, #*P*<0.10.

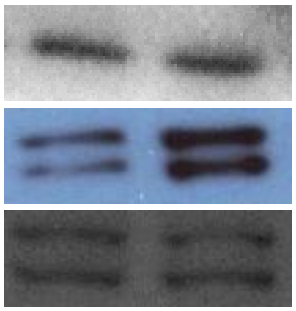

Caveolin-1

ERK1/2

phospho-ERK1/2

B.

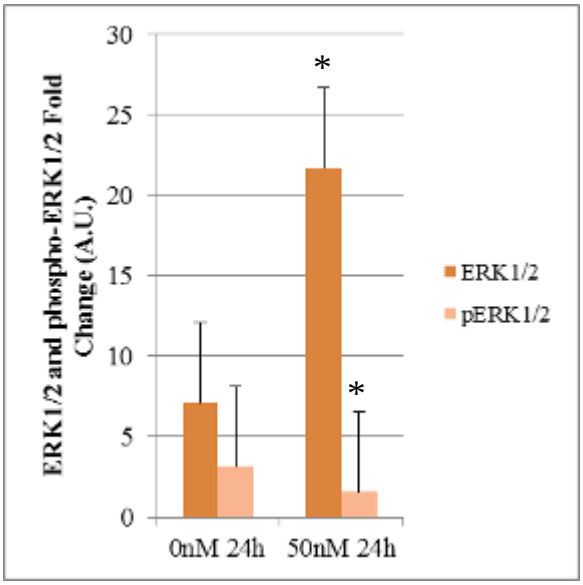

Figure 11B: MAPK proteins, ERK1/2 and phospho-ERK1/2, are significantly altered after *Atp10c*-silencing in C2C12 myotubes

C2C12 myoblasts were differentiated into myotubes, then transfected at each concentration of siRNA (SI00906220) (0 and 50 nM) and collected at the designated time point (24 h). Proteins were collected from these samples and subjected to immunoblot analysis. Data shown are representative of multiple independent experiments (n = 2 to 4), all analyzed in triplicate. The expression of ERK1/2 and phospho-ERK1/2 is denoted as arbitrary units (A.U.) and represented as the fold change normalized to Caveolin-1; *$P<0.05$.

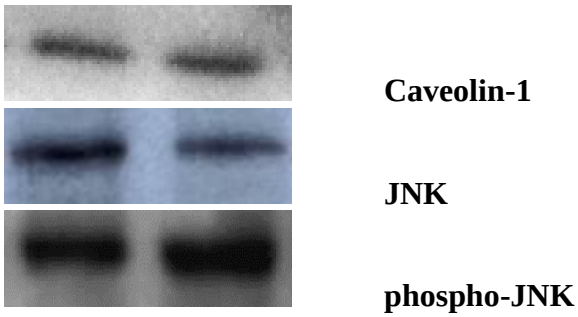

C.

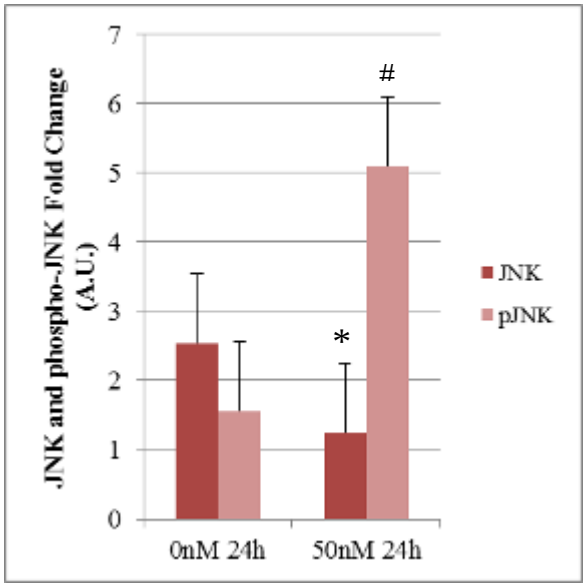

Figure 11C: MAPK proteins, JNK and phospho-JNK, are significantly altered after *Atp10c*-silencing in C2C12 myotubes

C2C12 myoblasts were differentiated into myotubes, then transfected at each concentration of siRNA (SI00906220) (0 and 50 nM) and collected at the designated time point (24 h). Proteins were collected from these samples and subjected to immunoblot analysis. Data shown are representative of multiple independent experiments (n = 2 to 4), all analyzed in triplicate. The expression of JNK and phospho-JNK is denoted as arbitrary units (A.U.) and represented as the fold change normalized to Caveolin-1; **P*<0.05, #*P*<0.10.

Caveolin-1

Actin

MyoD

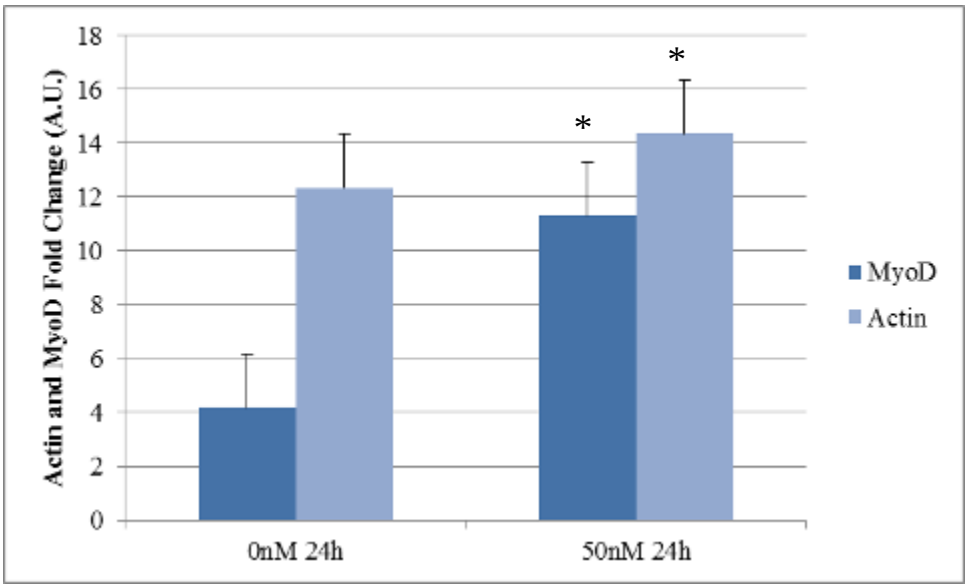

Figure 12: Actin and MyoD are significantly up-regulated after *Atp10c*-silencing in C2C12 myotubes

C2C12 myoblasts were differentiated into myotubes, then transfected at each concentration of siRNA (SI00906220) (0 nM and 50 nM) and collected at the designated time point (24 hours). Proteins were collected from these samples and subjected to immunoblot analysis. Data shown is representative of multiple independent experiments (n=2 to 4), all analyzed in triplicate. The expression of MyoD and Actin is denoted as arbitrary units (A.U.) and represented as the fold change normalized to Caveolin-1; *P<0.05.

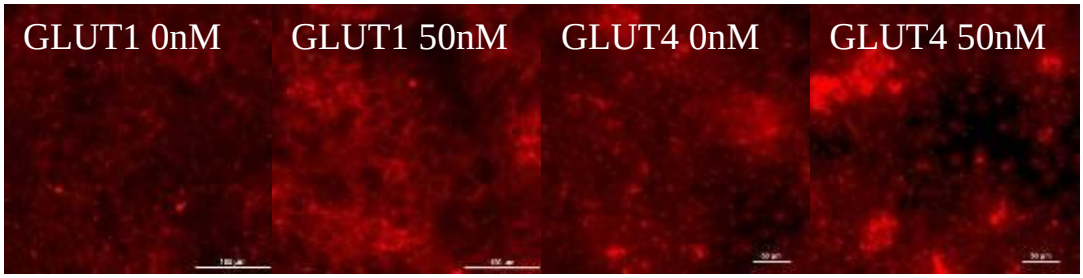

Images courtesy of S. Minkin, Environmental Biotechnology, UTK

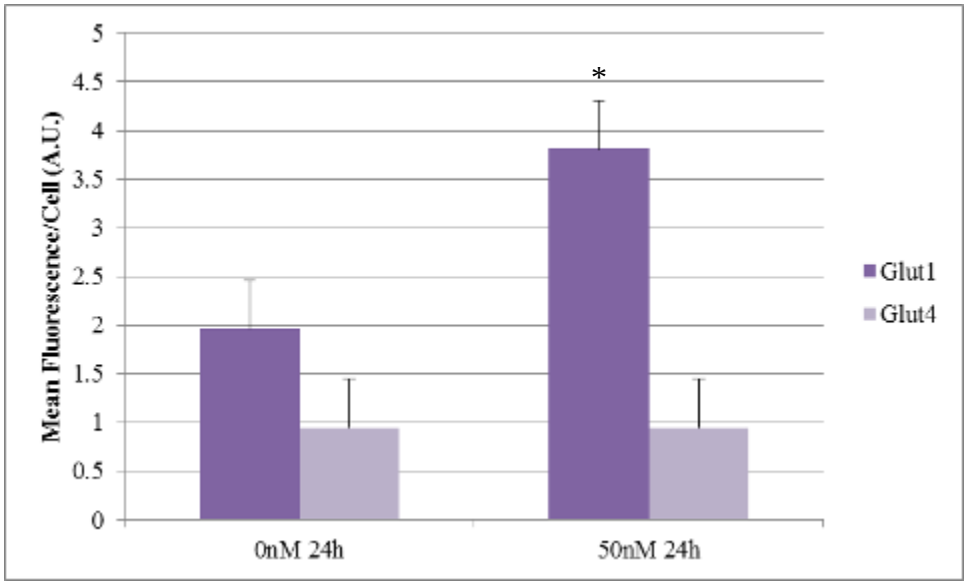

Figure 13: GLUT1 is significantly up-regulated in *Atp10c*-silencing C2C12 myotubes

C2C12 cells were seeded onto chamber slides and allowed to differentiate from myoblasts to myotubes. Myotubes were then transfected at each concentration of siRNA (SI00906220) (0 and 50 nM) and fixed at the designated time point (24 h). After transfections, cells underwent standard immunofluorescence processing and were imaged. Each sample was compared to negative and positive controls, which were used to quantify the image results. The expression of GLUT1 and GLUT4 is denoted as arbitrary units (A.U.) and represented as the mean intensity fluorescence normalized to isotype controls; $^{*}P < 0.05$.

Moreover, results from our *in vivo* data are complementary to our *in vitro* data as we see a significant up-regulation in the same MAPK proteins (Figure 14A-C) after 12 weeks on a high fat diet. Namely, MAPK proteins, p38 ($P = 0.02$) and phospho-p38 ($P = 0.001$) and well as ERK1/2 ($P = 0.02$ and 0.00004, respectively) and phospho-ERK1/2 ($P = 0.02$ and 0.01 respectively) are significantly up-regulated in *Atp10c* heterozygous mutants. For these samples, unlike *in vitro* conditions, we also observe an up-regulation of JNK ($P = 0.00007$) and phospho-JNK ($P = 0.0001$). Reasons for this aberration could be that the chronic stress conditions of DIO, T2D, hyperinsulinemia, hypercholesterolemia, and NAFLD as seen in these mice, result in a higher level of the stress-activated JNK and phospho-JNK proteins. Moreover, multiple studies show that obesity and T2D are inflammatory diseases, a state which in of its self is stressful on the tissues. This stress is not observed *in vitro* as the cells do not have to compensate for whole body abnormalities.

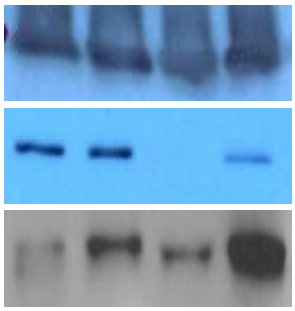

Caveolin-1

p38

phospho-p38

A.

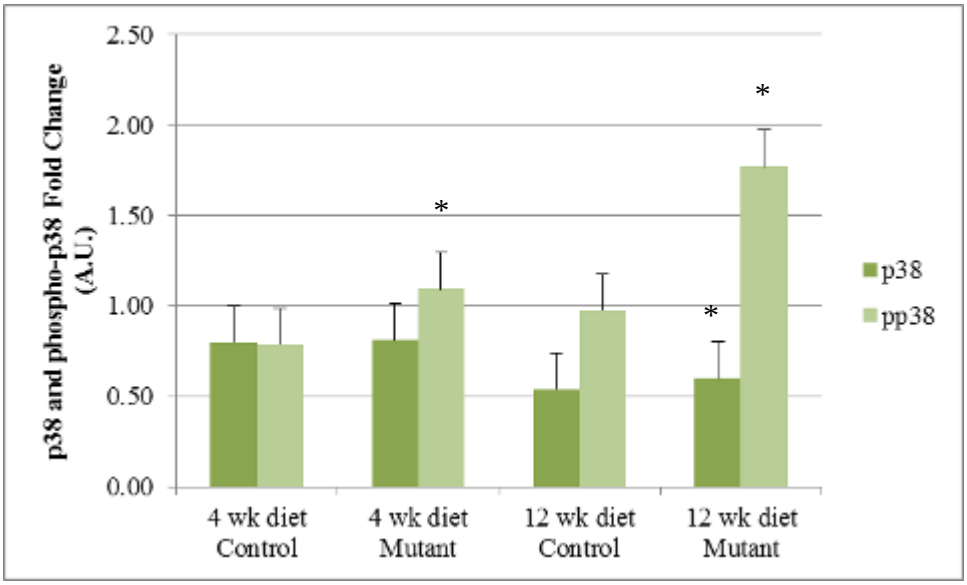

Figure 14A: MAPK proteins, p38 and phospho-p38 are significantly up-regulated in *Atp10c* heterozygous mutants at 12 weeks on a high fat diet

Atp10c heterozygous mice (n = 6 to 8) were fed a high-fat diet for 4 and 12 weeks, and then sacrificed. Proteins were collected from the skeletal muscle of these mice and subjected to immunoblot analysis. Data shown are representative of multiple independent experiments (n = 2 to 4), all analyzed in triplicate. The expression of p38 and phospho-p38 is denoted as arbitrary units (A.U.) and represented as the fold change normalized to Caveolin-1; *P<0.05.

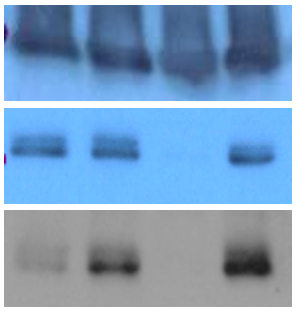

Caveolin-1

ERK1/2

phospho-ERK1/2

B.

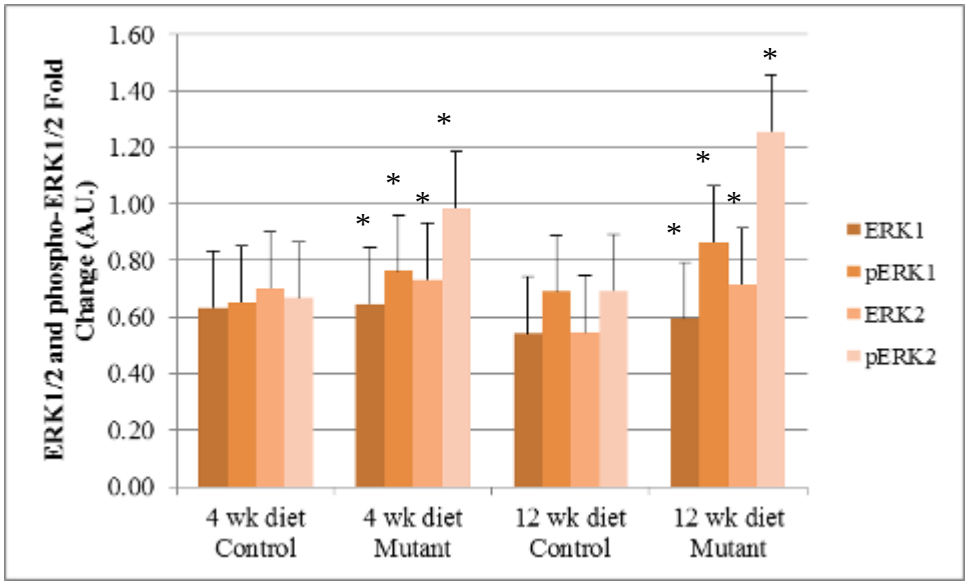

Figure 14B: MAPK proteins, ERK1/2 and phospho-ERK1/2 are significantly up-regulated in *Atp10c* heterozygous mutants at 12 weeks on a high fat diet

Atp10c heterozygous mice (n = 6 to 8) were fed a high-fat diet for 4 and 12 weeks, and then sacrificed. Proteins were collected from the skeletal muscle of these mice and subjected to immunoblot analysis. Data shown are representative of multiple independent experiments (n = 2 to 4), all analyzed in triplicate. The expression of ERK1/2 and phospho-ERK1/2 is denoted as arbitrary units (A.U.) and represented as the fold change normalized to Caveolin-1; **P*<0.05.

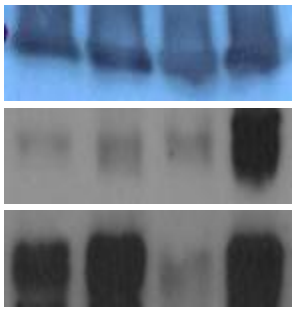

Caveolin-1

JNK

phospho-JNK

C.

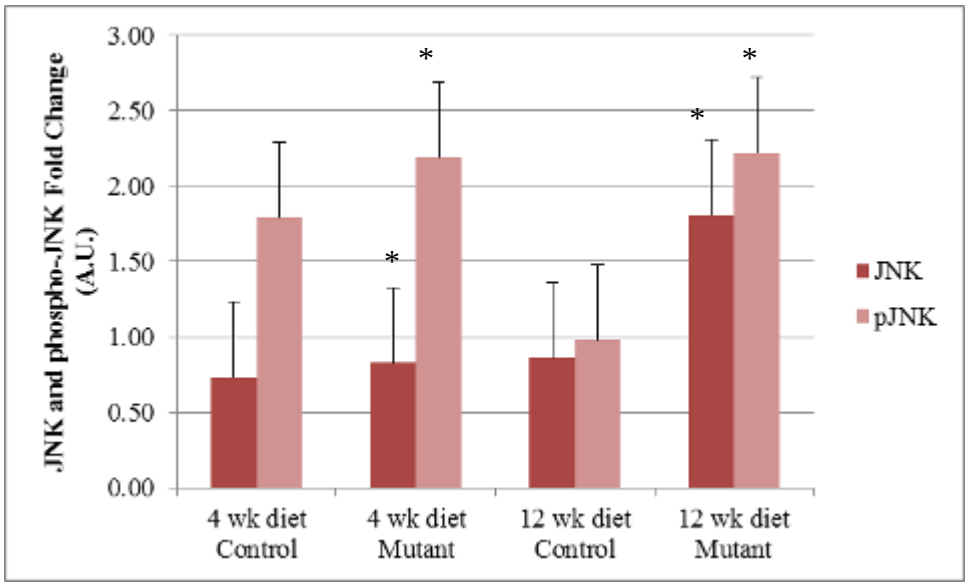

Figure 14C: MAPK proteins, JNK and phospho-JNK are significantly up-regulated in *Atp10c* heterozygous mutants at 12 weeks on a high fat diet

Atp10c heterozygous mice (n = 6 to 8) were fed a high-fat diet for 4 and 12 weeks, and then sacrificed. Proteins were collected from the skeletal muscle from these mice and subjected to immunoblot analysis. Data shown are representative of multiple independent experiments (n = 2 to 4), all analyzed in triplicate. The expression of JNK and phospho-JNK is denoted as arbitrary units (A.U.) and represented as the fold change normalized to Caveolin-1; *P<0.05.

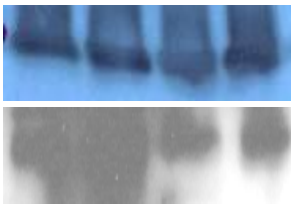

Caveolin-1

MyoD

D.

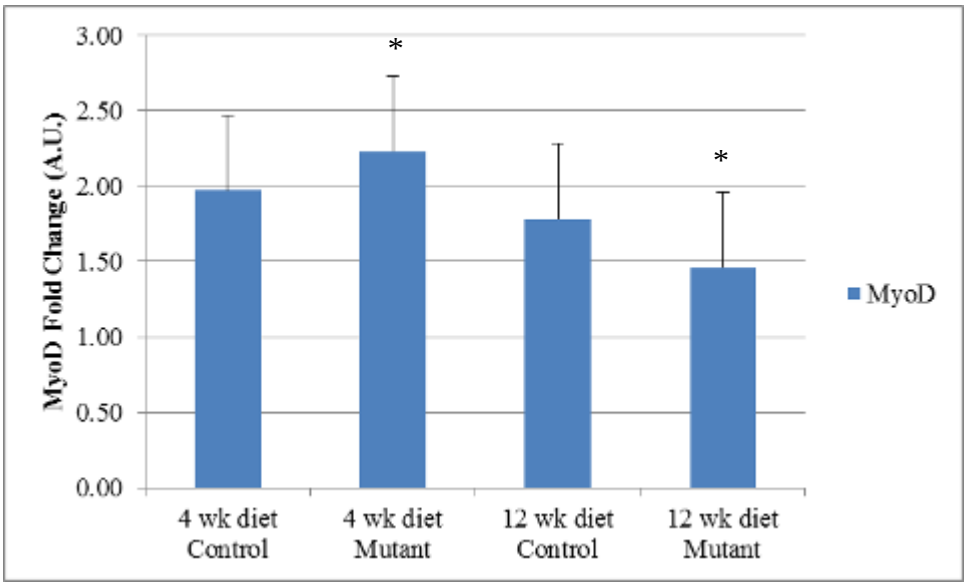

Figure 14D: MyoD is significantly altered in *Atp10c* heterozygous mutants at 12 weeks on a high fat diet

Atp10c heterozygous mice (n = 6 to 8) were fed a high-fat diet for 4 and 12 weeks, and then sacrificed. Proteins were collected from these mice and subjected to immunoblot analysis. Data shown are representative of multiple independent experiments (n = 2 to 4), all analyzed in triplicate. The expression of MyoD is denoted as arbitrary units (A.U.) and represented as the fold change normalized to Caveolin-1; *P<0.05.

Under acute insulin-stimulated glucose uptake conditions in C2*10c/-* cells, results indicated significant up-regulation of p38 ($P = 0.02$) and a significant down-regulation of phospho-38 ($P = 0.01$), JNK ($P = 0.0003$), and phospho-ERK1/2 ($P = 0.015$ and $P = 0.017$ respectively) (Figure 15A-C). It is our hypothesis based on the *in vivo* results of the MAPK proteins is that the *Atp10c*-mutants on a high-fat diet for 4 weeks give us a better representation of what would be going on in a pre-diabetic state before chronic IR and T2D has manifested. As such, this time point is better suited to compare with our *in vitro* data, as *Atp10c*-silenced cells would better represent an acute state of IR rather than a chronic one. As such, all the results from these experiments were performed with samples obtained from 4 week old mice on a high-fat diet. As such, results from our *in vivo* data are somewhat confusing when compared to our *in vitro* data. Complementary to our *in vitro* data, there is an up-regulation of p38 and ERK1/2, but not of significance (Figure 16A-C). The results are contradictory to our *in vitro* data in that there is up-regulation in phospho-p38 ($P = 0.005$), phospho-ERK2 ($P = 0.03$), JNK ($P = 0.1$) and phospho-JNK ($P = 0.007$). Reasons for these discrepancies could be as follows: (1) a time point of 4 weeks was not long enough to see marked changes in any of the proteins as the observed changes even when significant are small, (2) the insulin dose was not enough for the animals and therefore either a larger dose should be used, (3) a shorter treatment time (less than 30 min) for the insulin challenge should be used, (4) based on the standard error for these results, there is great variability between from animal to animal in response to an insulin challenge and/or (5) the fat from the high-fat diet did not contribute a substantial amount of calories to induce greater DIO consequences. This point can be corrected with greater numbers of mice. Future work using skeletal muscle

collected from these *Atp10c*-mutant mice after 12 weeks on high-fat diet needs to be performed in order to elucidate a more precise mechanism of action of *Atp10c in vivo*.

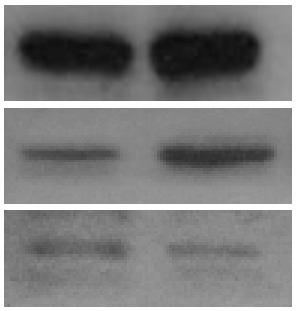

Caveolin-1

p38

phospho-p38

A.

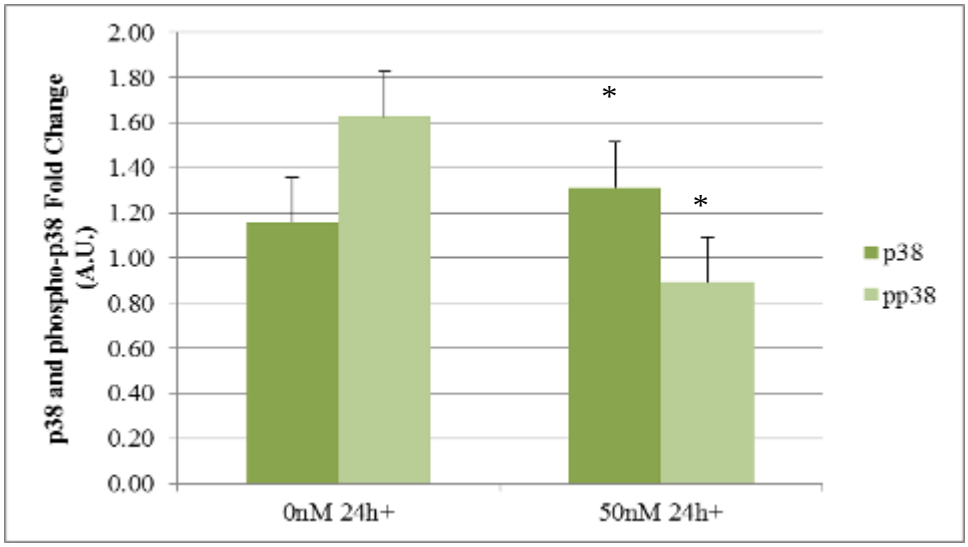

Figure 15A: MAPK proteins, p38 and phospho-38 are significantly altered after *Atp10c*-silencing and acute insulin stimulation in C2C12 myotubes

C2C12 myoblasts were differentiated into myotubes. Myotubes were transfected at each concentration of siRNA (SI00906220) (0 and 50 nM), stimulated with insulin (100 nM, 30 min) and collected at the designated time point (24 h). Proteins were collected from these samples and subjected to immunoblot analysis. Data shown are representative of multiple independent experiments (n = 2 to 4), all analyzed in triplicate. The expression of p38 and phospho-p38 is denoted as arbitrary units (A.U.) and represented as the fold change normalized to Caveolin-1; *P<0.05.

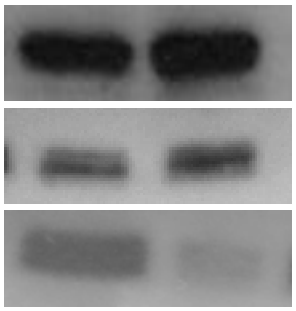

Caveolin-1

ERK1/2

phospho-ERK1/2

B.

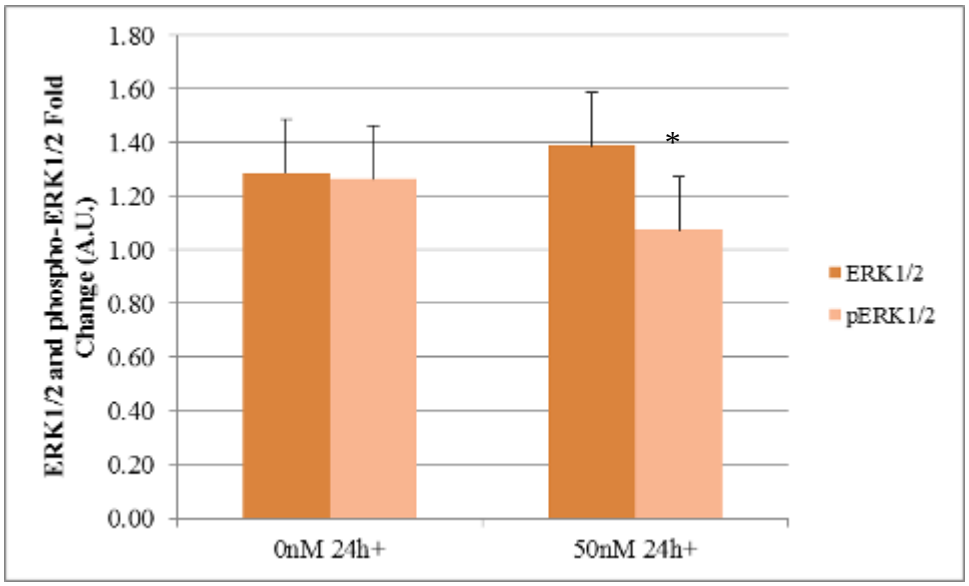

Figure 15B: A MAPK protein, phospho-ERK1/2, is significantly down-regulated after *Atp10c*-silencing and acute insulin stimulation in C2C12 myotubes

C2C12 myoblasts were differentiated into myotubes. Myotubes were transfected at each concentration of siRNA (SI00906220) (0 and 50 nM), stimulated with insulin (100 nM, 30 min) and collected at the designated time point (24 h). Proteins were collected from these samples and subjected to immunoblot analysis. Data shown are representative of multiple independent experiments (n = 2 to 4), all analyzed in triplicate. The expression of ERK1/2 and phospho-ERK1/2 is denoted as arbitrary units (A.U.) and represented as the fold change normalized to Caveolin-1; *P<0.05.

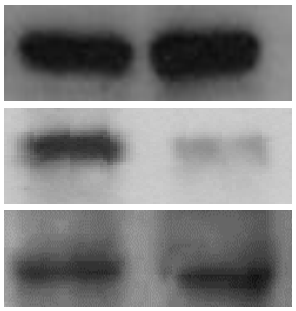

Caveolin-1

JNK

phospho-JNK

C.

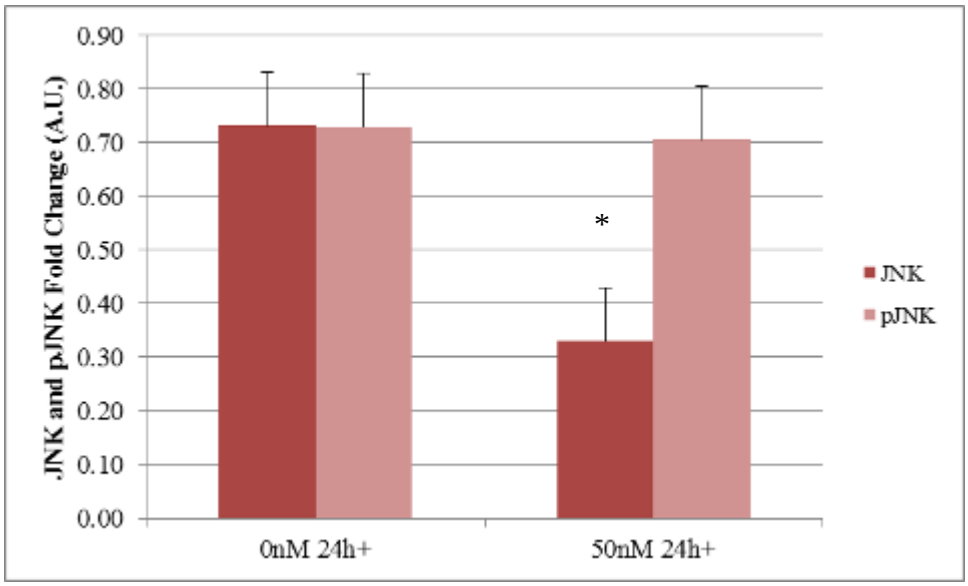

Figure 15C: A MAPK protein, JNK, is significantly down-regulated after *Atp10c*-silencing and acute insulin stimulation in C2C12 myotubes

C2C12 myoblasts were differentiated into myotubes. Myotubes were transfected at each concentration of siRNA (SI00906220) (0 and 50 nM), stimulated with insulin (100 nM, 30 min) and collected at the designated time point (24 h). Proteins were collected from these samples and subjected to immunoblot analysis. Data shown are representative of multiple independent experiments (n = 2 to 4), all analyzed in triplicate. The expression of JNK and phospho-JNK is denoted as arbitrary units (A.U.) and represented as the fold change normalized to Caveolin-1; *P<0.05.

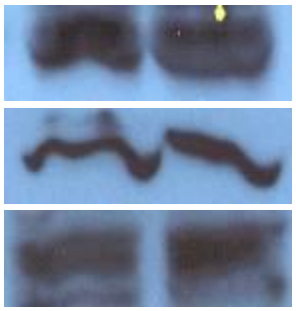

Caveolin-1

p38

phospho-p38

A.

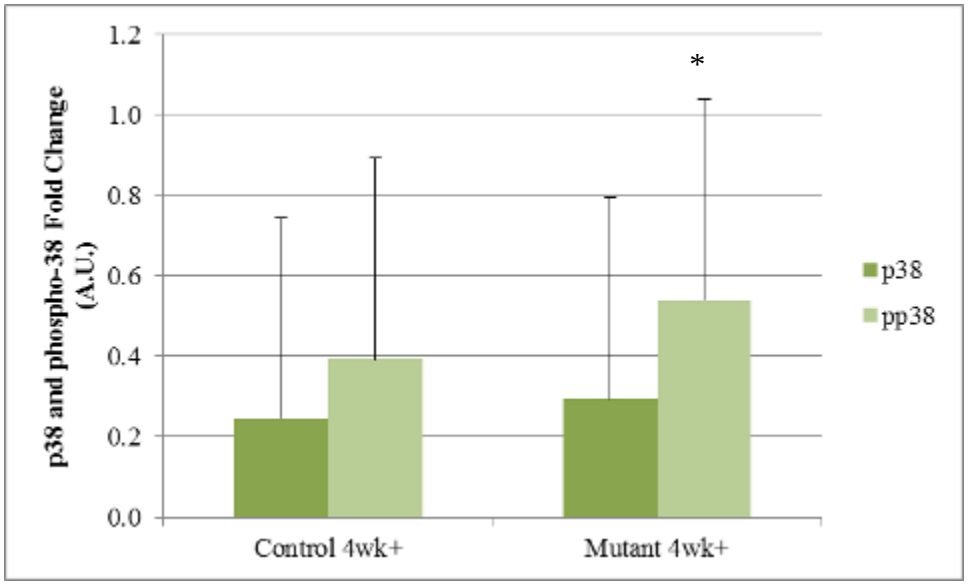

Figure 16A: A MAPK protein, phospho-p38, is significantly up-regulated after acute insulin stimulation in *Atp10c* heterozygous mutants

Atp10c heterozygous mice (n = 6 to 8) were fed a high-fat diet for 4 weeks, and then sacrificed. Proteins were collected from these mice and subjected to immunoblot analysis. Data shown are representative of multiple independent experiments (n = 2 to 4), all analyzed in triplicate. The expression of p38 and phospho-p38 is denoted as arbitrary units (A.U.) and represented as the fold change normalized to Caveolin-1; *P<0.05.

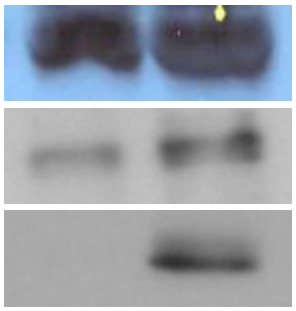

Caveolin-1

ERK1/2

phospho-ERK1/2

B.

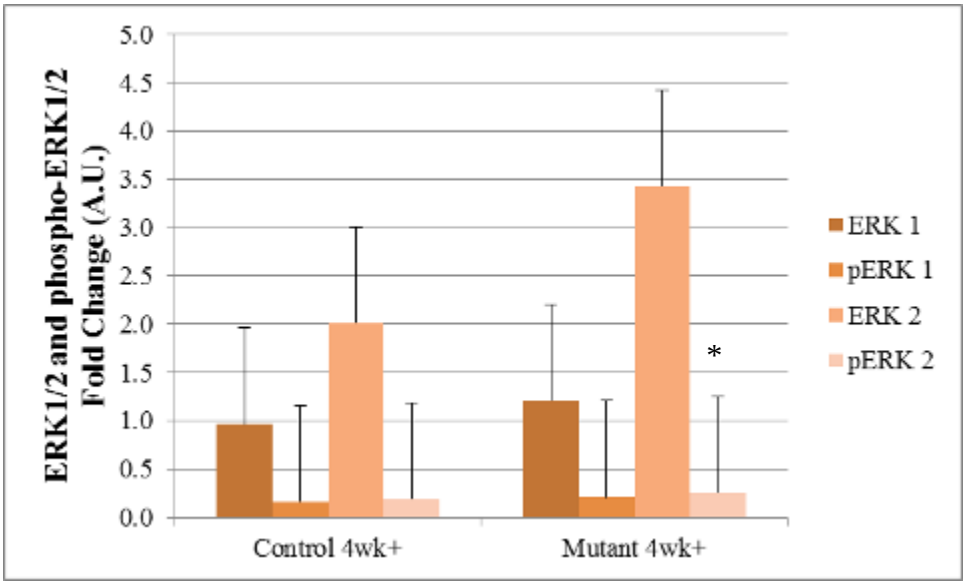

Figure 16B: A MAPK protein, phospho-ERK2, is significantly up-regulated after acute insulin stimulation in *Atp10c* heterozygous mutants

Atp10c heterozygous mice (n = 6 to 8) were fed a high-fat diet for 4 weeks, and then sacrificed. Proteins were collected from these mice and subjected to immunoblot analysis. Data shown are representative of multiple independent experiments (n = 2 to 4), all analyzed in triplicate. The expression of ERK1/2 and phospho-ERK1/2 is denoted as arbitrary units (A.U.) and represented as the fold change normalized to Caveolin-1; *$P<0.05$.

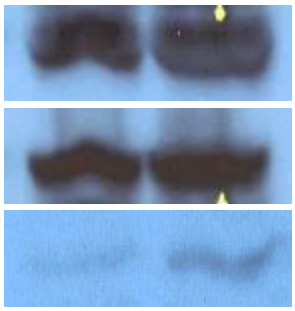

Caveolin-1

JNK

phospho-JNK

C.

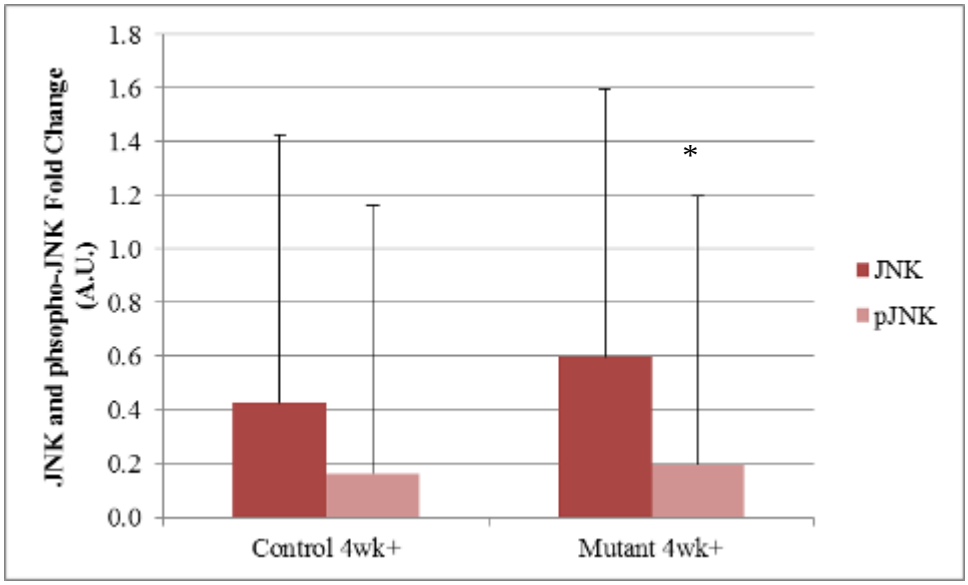

Figure 16C: A MAPK protein, phospho-JNK, is significantly up-regulated after acute insulin stimulation in *Atp10c* heterozygous mutants

Atp10c heterozygous mice (n = 6 to 8) were fed a high-fat diet for 4 weeks, and then sacrificed. Proteins were collected from these mice and subjected to immunoblot analysis. Data shown are representative of multiple independent experiments (n = 2 to 4), all analyzed in triplicate. The expression of JNK and phospho-JNK is denoted as arbitrary units (A.U.) and represented as the fold change normalized to Caveolin-1; **P*<0.05.

Since the PI3K/Akt pathway has been shown to be the most important pathway for insulin-stimulated glucose uptake and therefore, GLUT4 translocation, we used the rat L6-G4myc cells to examine both the PI3K pathway and its association with the translocation of GLUT4. For PI3K proteins, results indicated a significant decrease in PI3K at 48 h-post transfection ($P = 0.02$) (Figure 17A). Results from this analysis also show a significant down-regulation of Akt2 ($P = 0.03$) and phospho-Akt (Ser473) ($P = 0.01$) (Figure 17B). AS160 ($P = 0.008$), IR-β ($P = 0.02$), and IRS-2 ($P = 0.004$) are all up-regulated significantly 48 h post-*Atp10c* silencing (Figures 17A-B). While not significant, there was also an observed up-regulation of Actin ($P = 0.1$). Moreover, the expression of GLUT4 appears to be up-regulated in these cells ($P = 0.01$), but we attribute this increase due to the GLUT4 overexpressing nature of the L6-G4myc cells and not as a direct effect of *Atp10c*-silencing on these cells. Moreover, this result suggests that protein transcription and translation of GLUT4 are not being effected due to *Atp10c*-silencing and therefore, not a cause of the observed IR and T2D. Starting at the level of the IR-β, we observed an up-regulation here and downstream at IRS-2, and then a down regulation of phosphotyrosine associated PI3K activity, and Akt and its phosphorylation at Ser473. The usual pattern observed is that the acute effect of insulin will down regulate all these proteins [9]. As demonstrated by our results, *Atp10c* may play a role in the activation of these proteins further downstream in the pathway, a portion of which is still largely unknown. Moreover, the activation of Akt at Ser473 in response to insulin provides potential explanations for many abnormalities including IR. While it is known that Akt activation requires phosphorylation at both Ser473 and Thr308, Ser473 phosphorylation was shown to precede the phosphorylation of Thr308

and is in fact a prerequisite for Thr308 phosphorylation [1]. This can help explain why we see an up-regulation downstream at AS160 as it is not fully activated and thus is trying to compensate for the inactivity of Akt.

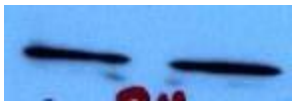

Caveolin-1

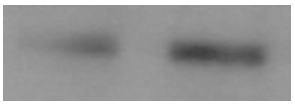

IR-β

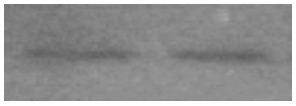

IRS-2

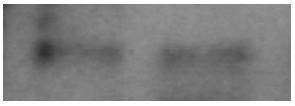

PI3K

A.

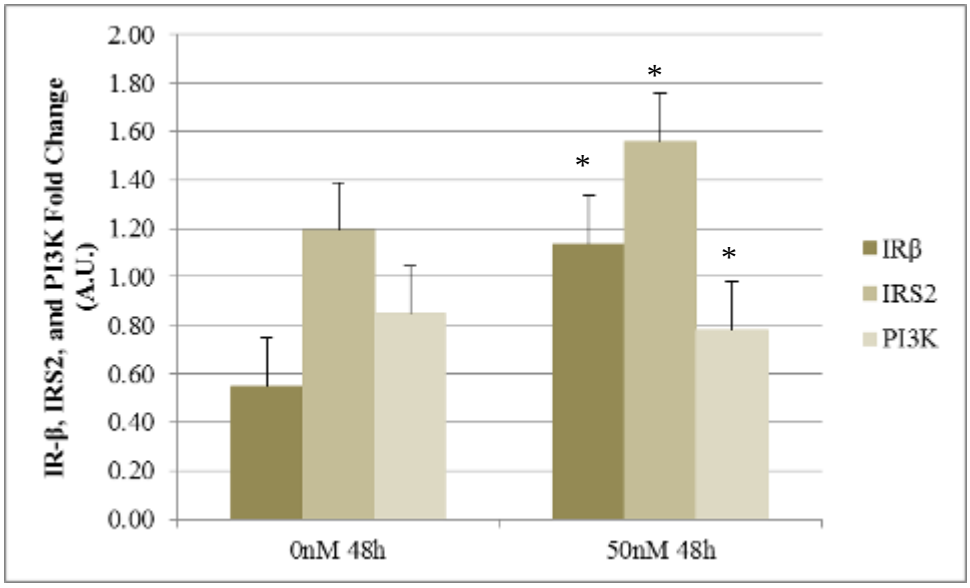

Figure 17A: PI3K, IR-β, and IRS-2 are significantly altered after *Atp10c*-silencing and acute insulin stimulation in L6-G4myc myotubes

L6-G4myc myoblasts were differentiated into myotubes. Myotubes were transfected at each concentration of siRNA (SI00906220) (0 and 50 nM), stimulated with insulin (100 nM, 30 min) and collected at designated time point (48 h). Proteins were collected from these samples and subjected to immunoblot analysis. Data shown are representative of multiple independent experiments (n = 2 to 4), all analyzed in triplicate ($^{*}P < 0.05$). The expression of PI3K, IRS-2, and IR-β is denoted as arbitrary units (A.U.) and represented as the fold change normalized to Caveolin-1.

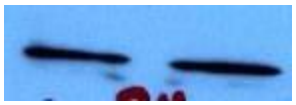

Caveolin-1

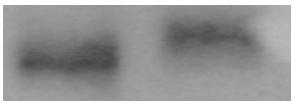

Akt2

phospho-Akt2

AS160

B.

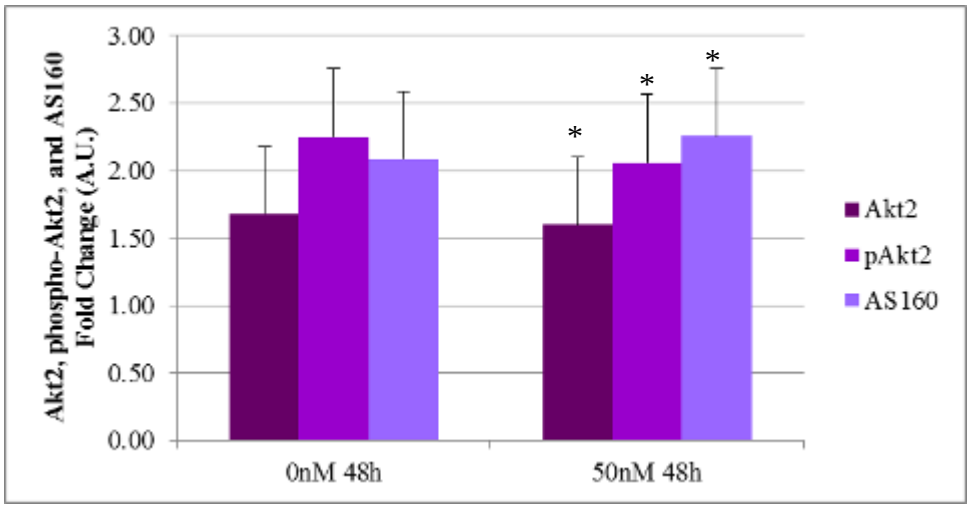

Figure 17B: PI3K proteins, Akt2, phospho-Akt, and AS160 are significantly altered after *Atp10c*-silencing and acute insulin stimulation in L6-G4myc myotubes

L6-G4myc myoblasts were differentiated into myotubes. Myotubes were transfected at each concentration of siRNA (SI00906220) (0 and 50 nM), stimulated with insulin (100 nM, 30 min) and collected at designated time point (48 h). Proteins were collected from these samples and subjected to immunoblot analysis. Data shown are representative of multiple independent experiments (n = 2 to 4), all analyzed in triplicate ($^{*}P < 0.05$). The expression of Akt2, phospho-Akt, and AS160 is denoted as arbitrary units (A.U.) and represented as the fold change normalized to Caveolin-1.

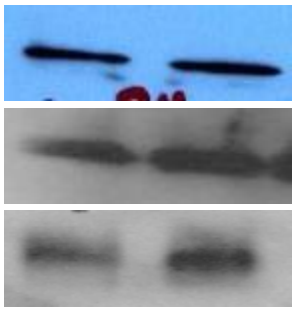

Caveolin-1

Actin

GLUT4

C.

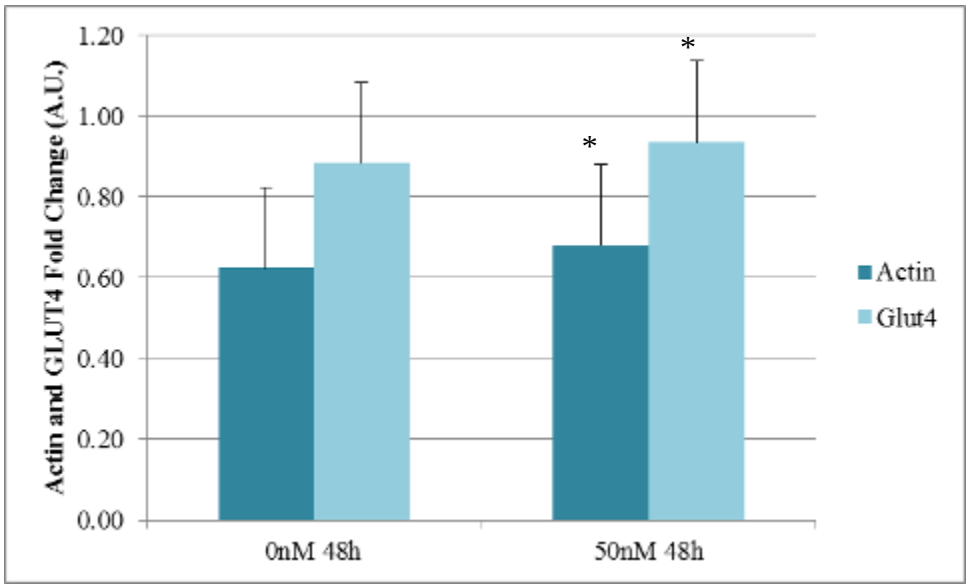

Figure 17C: Actin and GLUT4 are significantly up-regulated after *Atp10c*-silencing and acute insulin stimulation in L6-G4myc myotubes

L6-G4myc myoblasts were differentiated into myotubes. Myotubes were transfected at each concentration of siRNA (SI00906220) (0 and 50 nM), stimulated with insulin (100 nM, 30 min) and collected at designated time point (48 h). Proteins were collected from these samples and subjected to immunoblot analysis. Data shown are representative of multiple independent experiments (n = 2 to 4), all analyzed in triplicate ($^{*}P < 0.05$). The expression of Actin and GLUT4 is denoted as arbitrary units (A.U.) and represented as the fold change normalized to Caveolin-1.

In vivo data from *Atp10c* heterozygous mice fed a high-fat diet for 4 weeks show that several key PI3K pathway proteins are altered when challenged with insulin (Figure 18A-B). While not significant, there was an observed up-regulation of Actin ($P = 0.2$), which correlates to our *in vitro* experiment. However, PI3K ($P = 0.003$), Akt2 ($P = 0.006$), phospho-Akt (Ser473) ($P = 0.02$), and AS160 ($P = 0.01$) are all up-regulated significantly *in vivo*, data again which both complements and conflicts with our *in vitro* data. Data for IR-β, and IRS-2 was inconclusive for these samples due to antibody issues, and therefore, were not reported. Again, several reasons for these discrepancies exist (variation between animals, inefficient insulin dose, etc.) and future experiments should look at addressing those. Having said that, the up-regulation and activation of these proteins makes sense as this pathway is responsible the majority of glucose uptake in insulin responsive tissues. While a previous reports [87, 88, 89]have shown that high-fat feeding impairs insulin signal transduction by affecting tyrosine phosphorylation of insulin receptors and their substrates, results from other studies have shown that insulin-induced tyrosine phosphorylation of insulin receptors and their substrates is similar between animals fed a high-fat diet and those on a regular chow diet [1]. Recently, it was demonstrated that despite the development of IR, which is accompanied by reduced glucose-uptake rates in muscle cells, no changes in the phosphorylation state of Akt and AS160 were observed [4]. Our results contradict both of these observations as we seen a significant up-regulation of many important components of the PI3K and yet these animals still have issues with glucose metabolism. This suggests that something other than a defect in the PI3K pathway is causing the observed phenotype in these *Atp10c* heterozygous mice.

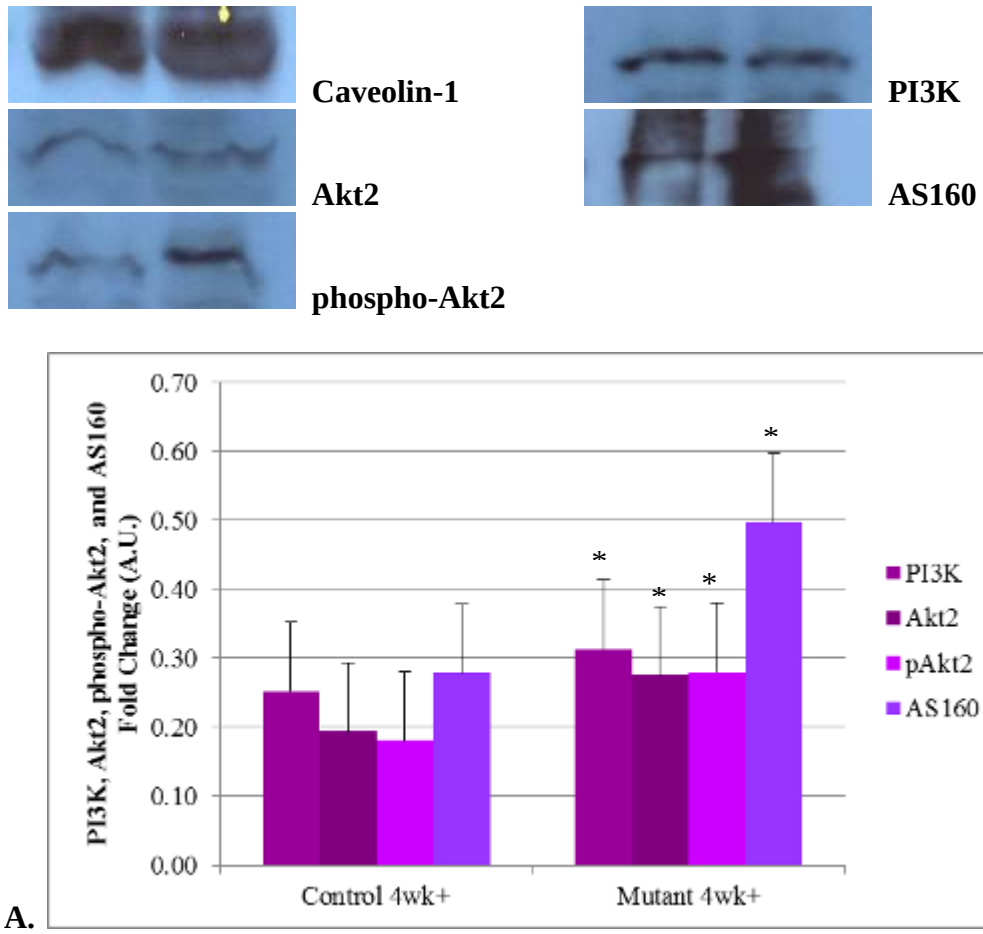

Figure 18A: PI3K proteins, PI3K, Akt2, phospho-Akt2, and AS160 are significantly up-regulated in *Atp10c*-heterzygous mutants after acute insulin-stimulation

Atp10c heterozygous mice were fed a high-fat diet for 4 weeks, and then sacrificed. Proteins were collected from these mice and subjected to immunoblot analysis. Data shown are representative of multiple independent experiments (n = 2 to 4), all analyzed in triplicate ($^{*}P < 0.05$). The expression of PI3K, Akt2, phospho-Akt, and AS160 is denoted as arbitrary units (A.U.) and represented as the fold change normalized to Caveolin-1.

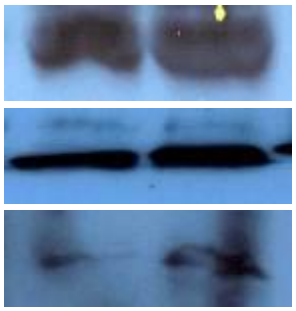

Caveolin-1

Actin

MyoD

B.

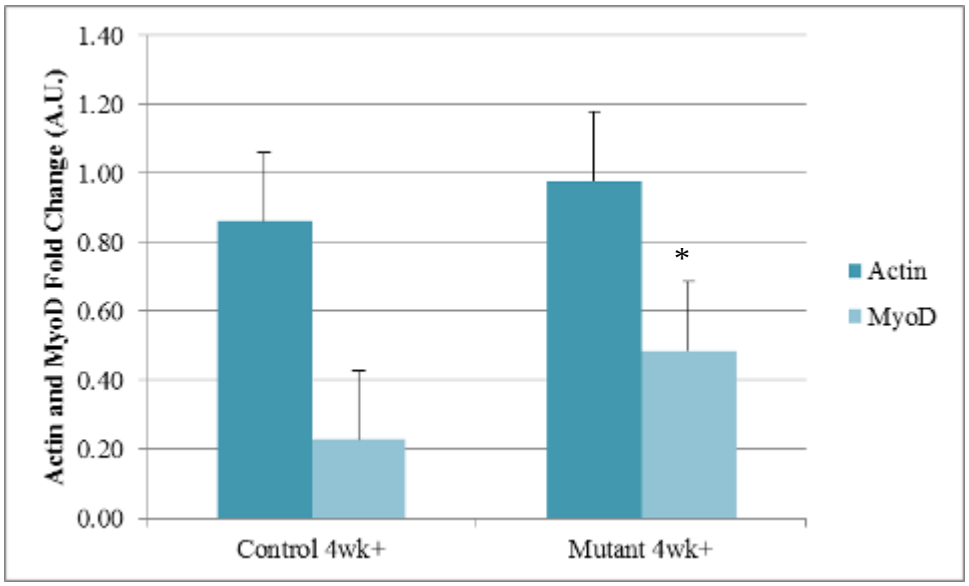

Figure 18B: MyoD is significantly altered *Atp10c*-heterzygous mutants after acute insulin-stimulation

Atp10c heterozygous mice were fed a high-fat diet for 4 weeks, and then sacrificed. Proteins were collected from these mice and subjected to immunoblot analysis. Data shown are representative of multiple independent experiments (n = 2 to 4), all analyzed in triplicate ($^{*}P < 0.05$). The expression of Actin and MyoD is denoted as arbitrary units (A.U.) and represented as the fold change normalized to Caveolin-1.

GLUT4 is essential for insulin-stimulated glucose uptake, and is expressed primarily in adipose and skeletal muscle tissues. Ideally, in response to insulin, intracellular GLUT4 vesicles move near the cell surface, fuse with the plasma membrane, and begin the process of glucose uptake. Defective uptake of glucose is a central feature of T2D, and may involve the alteration of the insulin signaling to GLUT4 vesicles, the trafficking of GLUT4 vesicles to the plasma membrane, and/or the docking and fusion of GLUT4 vesicles with the plasma membrane. As we did see a significant decrease in glucose uptake (2.5 fold), and a significant increase in GLUT4 expression ($P = 0.01$), we next wanted to investigate the effect, if any, on GLUT4 translocation when *Atp10c* is silenced in L6-G4myc myotubes. The data from immunocytochemistry experiments shows a decrease in insulin-stimulated GLUT4 translocation to the plasma membrane after 48 h post-transfection in L6-G4myc/*10c*- myotubes (Figure 19), and as such, a decrease in insulin-stimulation of these cells.

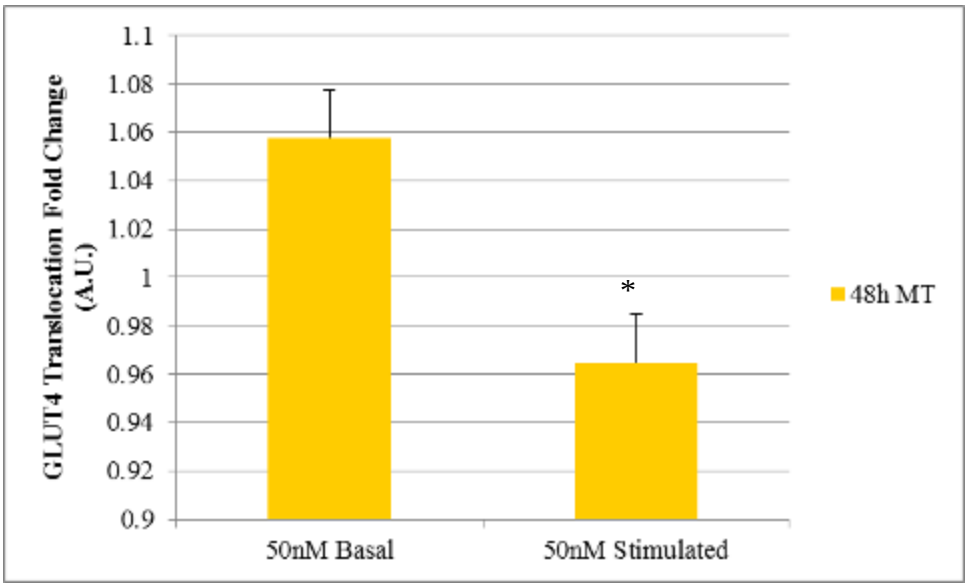

Figure 19: GLUT4 translocation in *Atp10c*-silenced L6-G4myc myotubes is decreased 48 h post-transfection

L6-G4myc myotubes were transfected at each concentration of siRNA (SI00906220) (0nM and 50 nM) at the designated time point (48 h). Cells were then stimulated with insulin (100 nM), and an immunocytochemistry assay was performed ($^{*}P < 0.05$). Data is reported as GLUT4 translocation which is expressed as the ratio of GLUT4myc intensity under basal and stimulated conditions and indicated as arbitrary units (A.U.). Data is normalized with respect to 0nM basal and stimulated controls.

To test if the observed changes in the MAPK pathway are indeed in response to *Atp10c*-silencing, and thus to confirm the involvement of p38, the inhibitor SB203580, which is specific for multiple p38 isoforms, was added to C2*10c/-* cells at a concentration of 10 μm for 60 min [90, 91]. Protein samples were subjected to immunoblot analysis with p38 and phospho-p38 antibodies (Figure 20). Our results indicate that C2*10c/-* cells treated with 10 nM SB203580 for 60 min effected the expression of both p38 ($P = 0.1$) and phospho-p38 ($P = 0.08$). While not significant, it appears that the inhibitor was able to partially restore the expression of all the proteins tested suggesting its action on the MAPK protein, p38. This was further confirmed by the glucose uptake assay performed on C2*10c/-* and MAPK-inhibited cells. Results from the assay showed that glucose uptake remained unchanged, confirming that the inhibitors are acting directly on the MAPK protein, p38, and are not affected by changes in *Atp10c* expression alone (Figure 21).

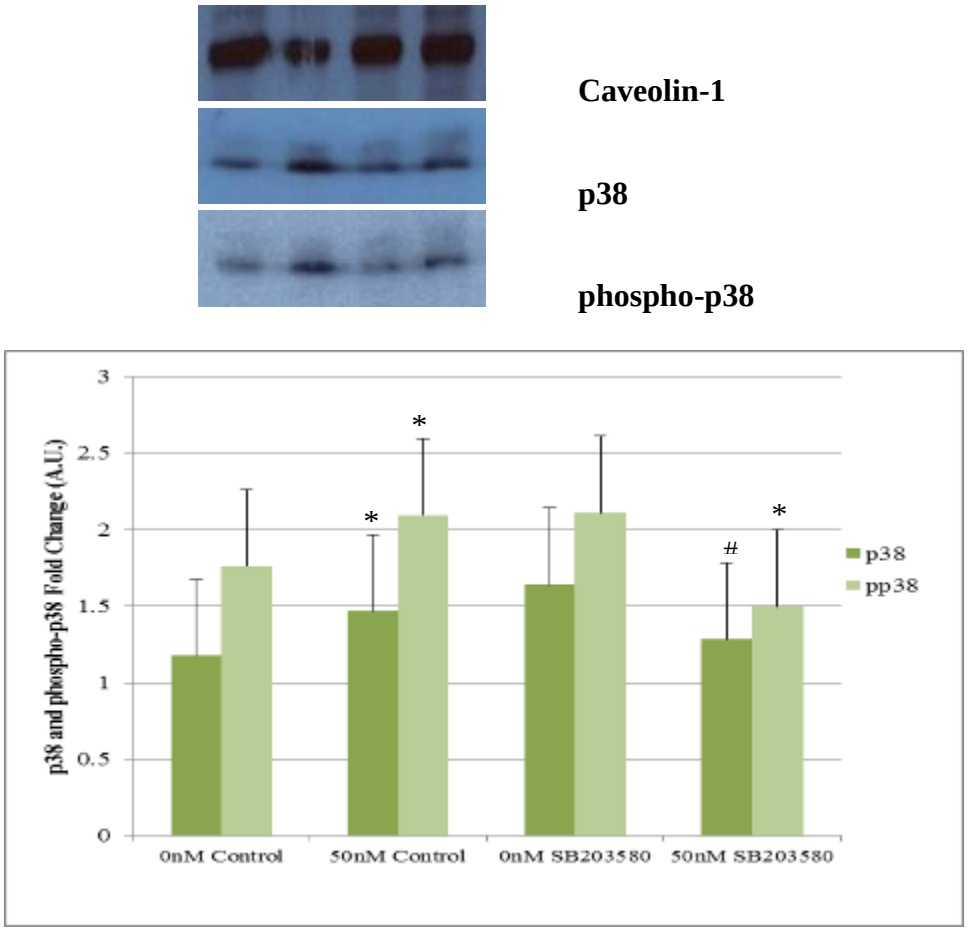

Figure 20: MAPK protein, p38, activity is partially rescued after treatment with specific inhibitor SB203580

C2C12 cells were differentiated from myoblasts to myotubes. Myotubes were transfected at each concentration of siRNA (SI00906220) (0 and 50 nM) at the designated time point (24 h). Cells were then treated with the inhibitor SB203580 (10 nM) and collected after 60 min. Proteins were collected from these samples and subjected to immunoblot analysis ($^{*}P < 0.05$, $^{\#}P < 0.1$). The expression of p38 and phospho-p38 is denoted as arbitrary units (A.U.) and represented as the fold change normalized to Caveolin-1.

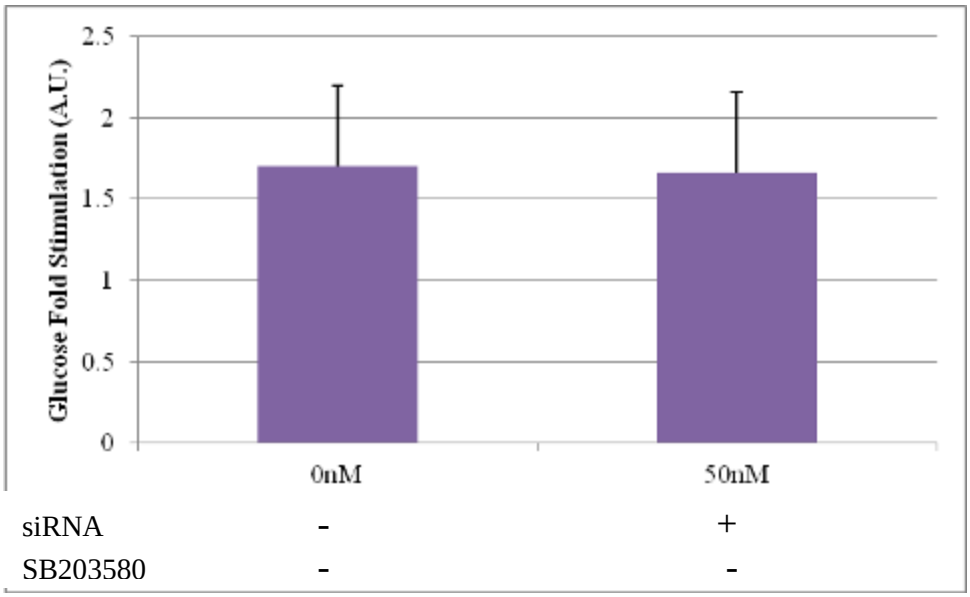

Figure 21: Glucose uptake remained unchanged, confirming that the p38 inhibitors are acting directly on the MAPK proteins and are not affected by changes in *Atp10c* expression

C2C12 cells were differentiated from myoblasts to myotubes. Myotubes were treated with the inhibitor SB203580 (10 nM) and collected after 60 min. Cells were then stimulated with insulin (100 nM, 30 min) and a 2-DOG uptake was performed. Data is reported as the glucose uptake stimulation which is expressed as the ratio of dpm/µg of total protein in presence of insulin to that in the absence of insulin and indicated as arbitrary units (A.U.).

The exact mechanism by which the MAPKs mediate glucose uptake is debatable, and as such that both *in vitro* and *in vivo* data are often times inconclusive. MAPKs, specifically, p38 and ERK1/2 proteins regulate glucose uptake via insulin-dependent and insulin-independent pathways [87, 88, 89]. Most importantly, there are many reports which show the involvement of the MAPK pathway in glucose uptake without an effect on GLUT4 translocation. Our results suggest that when myotubes become insulin resistant by *Atp10c*-silencing, there is a significant increase in the expression of both native and activated (phosphorylated) MAPK proteins. Data demonstrates that both p38 and ERK1/2 are responsive to changes in *Atp10c* with increased expression.

The importance of p38 in this process is further supported by the fact that there are significant changes in glucose transporter proteins as well. GLUT1 and GLUT4 have been demonstrated to be the key players of glucose clearance in peripheral tissues [2]. GLUT1 is responsible for glucose uptake in the basal state whereas, GLUT4 is insulin responsive. Defective uptake of glucose mediated by the GLUTs is a central feature of DIO and T2D.

Results from our *in vivo* analysis of *Atp10c* heterozygous mice demonstrate that at the protein level, the expression of key MAPK proteins are up-regulated during an IR state and remain up-regulated when challenged with exogenous insulin. As a consequence of IR, there is a shift away from GLUT4 as the main player in glucose clearance to GLUT1 as the responsible transporter. Results from several studies in addition to ours show that prolonged exposure to insulin increases basal glucose uptake and decreases acute insulin-mediated glucose transport. The latter attributed to reduced insulin-stimulated GLUT4 translocation. However, it is still possible that the insulin-

resistant state is associated with diminished GLUT4 activity as our *in vitro* data shows a significant increase in GLUT1 and no measurable change in GLUT4. Of relevance to our study, MAPK protein expression, specifically p38, has been shown to affect the expression of GLUT1 and GLUT4; which can subsequently affect glucose uptake in peripheral tissues. The MAPK protein, p38, reportedly up-regulates the expression of GLUT1, thereby altering glucose transport at the basal level, while also involved in an insulin-induced enhancement of intrinsic GLUT4 activity on the cell surface. Since, we do not see any increase in the basal glucose uptake, we strongly feel that the up-regulation of GLUT1 is more of a compensatory mechanism against IR in C2*10c/-*, since there is no change in GLUT4; the precise underlying mechanism, however, remains to be clarified. This result may prove to be the most crucial, as GLUT4 is the main player in insulin-stimulated glucose metabolism. Reports additionally indicate that the activation of p38 reduces insulin responsiveness [87, 88, 89, 90], so the exact mechanism by which the MAPK pathway is involved in glucose metabolism still remains controversial.

Up-regulation of MyoD and Actin in transfected cells (C2*10c/-)* suggests a regulatory mechanism by which the myotubes are trying to combat the stressful state of IR. As seen in the skeletal muscle tissues of the *Atp10c* mutant mice fed a high-fat diet for 12 weeks, MyoD expression is decreasing as a result of the insulin resist state and a high fat diet; this observation was not seen for these mice at 4 weeks on a high-fat diet.. As the availability of new myoblasts cells *in vivo* is not the same as *in vitro*, this result is indicative of muscle wasting and/or myotube de-differentiation. Again, this may be a compensatory effect. If the *in vitro* process continued for a longer period of time, we hypothesis that like the tissues, the expression of MyoD would also decreases as the

myotubes started reverting back to a myoblast state. By aiding with GLUT4-containing vesicle membrane movement and/or fusion, there is considerable evidence that Actin is essential for insulin-regulated glucose transport. Therefore, these cells may be up-regulating the expression of Actin acutely in preparation for insulin-stimulated glucose uptake [76].

Multiple studies on skeletal muscle from type 2 diabetics have demonstrated an altered gene/protein expression profile compared to healthy controls [71]. These changes can either be secondary to the altered metabolic state, a direct consequence of reduced insulin signaling, or as the primary cause of the disease. The defects observed in diabetic muscle biopsies were reportedly specific for the PI3K pathway, thereby leaving the MAPK pathway intact. However, unlike our study, other laboratories discovered that several of the MAPK proteins were down-regulated at the protein expression level.

Conclusions

A phenomenon known as phospholipid randomization affects the structure and function of many channels, transporters, and signal transducing proteins and has been implicated in several pathophysiology processes. Thus, maintaining the organization and activity of the lipid bilayer is essential for normal cell function. One class of proteins that performs this action is the flippases, or type 4 ATPases [7]. In yeast studies, these proteins cause the translocation of glycerophospholipids, and this movement is necessary for intracellular membrane and protein trafficking [7]. *Atp10c* is one such phospholipid translocase which encodes for a type 4 P-type ATPase. Our laboratory has demonstrated that *Atp10c* heterozygous mice are insulin resistant and have an altered insulin-stimulated

response in peripheral tissues. Our obesity mouse model is diet-induced and shows IR characterized by hyperinsulinemia, hyperglycemia, hyperlipidemia, and DIO in association with glucose intolerance [2, 36, 72]. In fact, a recent publication has sited ATP10C as a potential biomarker for obesity and related metabolic disorders [12].

The pathways involved in glucose and lipid metabolism are extremely complex and challenging to interpret. *Atp10c* is a proposed membrane bound protein with 10-11 transmembrane domains and its flippase activity has been studied extensively in yeasts. This is why we hypothesize one or more mechanisms of action on the membrane itself which can in turn affect these pathways. The activation of the PI3K pathway and its downstream kinases like Akt include the GLUT4 translocation. This insulin-dependent pathway is the one of the most important in glucose metabolism, accounting for up to 70% of glucose clearance. Numerous studies have shown Akt and its related substrates to be the key players in this pathway. Importantly, Akt, which regulates GLUT4 exocytosis, is not required for insulin regulation of GLUT4 endocytosis [92].

The significant increase of important MAPK proteins, p38 and ERK1/2, under both basal and acute insulin-stimulated conditions shows that *Atp10c*-silencing does affect these proteins and in turn, glucose metabolism via both insulin-independent and insulin-dependent manners. Results from the PI3K pathway proteins are confusing as *in vitro* data does not complement the *in vivo* data for all the proteins. For example, PI3K ($P = 0.02$), Akt2 ($P = 0.03$) and phospho-Akt (Ser 473) ($P = 0.01$) are significantly down-regulated after *Atp10c* silencing under *in vitro* conditions, but are significantly up-regulated in the *Atp10c*-heterozygous mice on a high-fat diet; PI3K ($P = 0.003$), Akt2 ($P = 0.006$) and phospho-Akt (Ser 473) ($P = 0.02$). Rationale for these conflicting results

could be that *Atp10c* could be involved with these proteins directly by a yet unknown mechanism, or as a consequence of *Atp10c*'s effect on the MAPK pathway which is significantly affected by the diet as indicated in the mice. These results are important as the activation of Akt2 plays a critical role in the PI3K pathway by further activating AS160 (phospho-Akt Ser473/Thr308). It is important to note that only 10–20% of Akt2 needs to be phosphorylated to achieve full glucose transport activation [47, 48]. IRS-2 plays a key role in transmitting signals to both intracellular pathways PI3K and MAPK. It appears as though the cells are trying to augment signaling to these pathways to compensate for inactivity (as in PI3K) or over activity (as in MAPK) in these pathways. In the case of the PI3K pathway, *Atp10c* appears to be halting the activation of PI3K (p85) and phospho-Akt2. As a result, we see up-regulation both up stream in IR-β and IRS2 and downstream in AS160. In turn, IRS-2 may be sending these compensatory signals to MAPK proteins [72]. As such, the up-regulation of p38 must be in response to shift the uptake from GLUT4 as the main player to GLUT1 as the main player as p38 has been directly implicated in the regulation of these glucose transporters. Activation of p38 significantly alters the expression of GLUT1 and GLUT4, increasing basal glucose transport and reducing insulin responsiveness [91]. As p38 up-regulation resulted in an increase in GLUT1 and an assumed decrease in GLUT4, it is highly likely that p38 is central in the regulation of glucose metabolism. Moreover, in data from others [41, 90, 91] as well as our laboratory, the pyridinylimidazole inhibitor of p38 activity, SB203580, reduced the stimulation of glucose uptake by insulin in skeletal muscle suggesting that p38 may be a component in the signaling pathway leading to the stimulation of glucose uptake.

Results from the immunocytochemistry analysis of GLUT4 translocation show that the silencing of *Atp10c* is altering normal GLUT4 regulation. At this time, it appears as though *Atp10c* most likely plays a role in GLUT4 endocytosis. Although GLUT4 exocytosis has been studied extensively, GLUT4 endocytosis and its possible regulation had remained less scrutinized. Recent studies have begun to shed light on GLUT4 endocytic mechanisms and their metabolic regulation [92]. Endocytosis involves GLUT4 molecules getting 'ready' by concentrating within a small region of the plasma membrane. Secondly, they get 'set' by interacting with specific membrane proteins and/or lipids, resulting in membrane bending and invagination. Finally, the bud is formed occluding GLUT4 from the extracellular milieu and allowing them to 'go' into the cell interior to intracellular compartments. It has been reported that the internalization of GLUT4 occurs by clathrin-mediated endocytosis [42]. Moreover, it has been argued that GSVs are formed from endosomes and that GLUT4 may be retained intracellular by an interaction between GSVs and retention machinery, or by restricting the access of GSVs to the vesicle tethering/docking/fusion apparatus at the cell surface [40, 42]. Based on our results, it is possible that ATP10C is involved in either of these steps in addition to its other effects on the metabolic pathways.

Addressing the discrepancies between *in vivo* and *in vitro* data is difficult at best as we are dealing whole animal complexities compared to cell culture homogeneity. Moreover, these metabolic pathways themselves are multifaceted in whole animal models due to the interplay of endogenous cytokines, apidokines and other nature responses in response to chronic syndromes like IR and T2D. We feel confident that our results for the most part are complementary to one another with only two major points of conflict—the

expression of PI3K, Akt2 and phospho-Akt (Ser473). These observations demonstrate the necessity of a muscle-specific *Atp10c* knockout to study these complex processes.

For the first time, our results show a direct correlation between *Atp10c*/ATP10C and glucose metabolism, at least in part via the MAPK pathway. Our results showed no significant change in the basal glucose uptake suggesting that when *Atp10c* is silenced using *Atp10c*-specific siRNA an acute state of IR is observed. Conversely, cells are insulin sensitive when normal levels of *Atp10c* are maintained; both observation shown *in vitro* as well as *in vivo*. The MAPK protein, specifically p38, is potentially influencing this system by exerting an effect on glucose transporter proteins, namely GLUT1 and GLUT4. Moreover, we showed that the MAPK pathway is essential for both insulin-independent and insulin-dependent glucose uptake; exact mechanisms of which need further study. Last, but certainly not least, we have revealed *Atp10c*'s possible role in GLUT4 endocytosis in addition to its other effects on the glucose metabolic pathway. Based on the results of the numerous studies discussed throughout this dissertation, Figure 22 presents putative *Atp10c*/ATP10C mechanisms of action and possible protein/pathway targets.

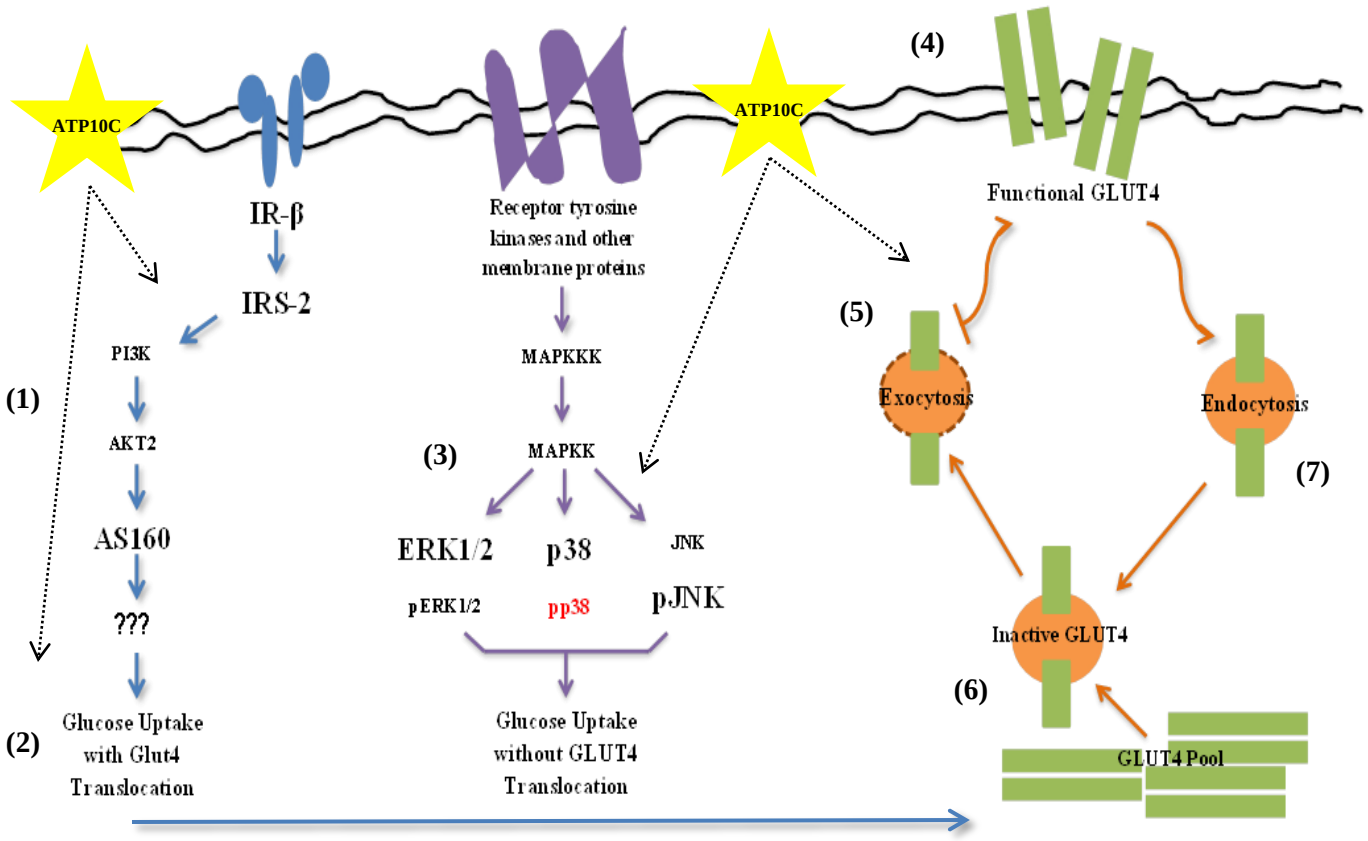

Figure 22: *Atp10c*/ATP10C in Action

ATP10C may function by activating key proteins in the PI3K pathway and influence glucose uptake in connection with GLUT4 translocation (1). Moreover, it may exert its affects downstream thus affecting glucose uptake that way (2). When normal expression levels of ATP10C are maintained, MAPK proteins should not be up-regulated and therefore normal glucose uptake both at the basal and insulin-stimulated level should occur (3) and last, but not least, ATP10C may function on the endocytosis as well as the exocytosis of GLUT4 by several machineries; (4) by maintaining lipid bilayer asymmetry and cell homeostasis, (5) as an aid in GSV formation, (6) by retaining the GSVs inside the cell, and (7) by stimulating the endocytosis of GLUT4 back inside the cell.

CHAPTER IV

OVERALL CONCLUSIONS AND FUTURE RECOMMENDATIONS

The prevalence of T2D and DIO has reached epidemic levels during recent years and shows no progress of slowing down. Moreover, it is estimated that less than half of the worldwide patient population responds to existing treatments, and as such increases the occurrence of secondary complications of the disease. The currently accessible treatments offer improvement in glycemic control, but have also been implicated with significant adverse events such as hypoglycemia, weight gain, fluid retention, congestive heart failure, loss of bone mineral density and gastrointestinal discomfort. Our research eludes to a novel protein marker that we believe is a good candidate for T2D and DIO and therefore, it's modification may play a role in expanding the treatment of T2D and other diseases associated with IR, findings of which are significant as many of the anti-diabetic drugs currently on the market have undesirable side-effects like those previously described.

Glucose metabolism is reduced in type 2 diabetics resulting in elevated levels of glucose in the bloodstream, and complications of IR and T2D can be either short term (e.g. diabetic coma) or long term (e.g. limb amputation, neuropathies, kidney failure, strokes, and other cardiovascular problems). As glucose is vitally important for animals and humans, its concentration in the blood is strictly controlled. Glucose homeostasis in the body is the responsibility of key peripheral tissues, skeletal muscle and adipose tissue, and glucose utilization is carried out by GLUTs specifically GLUT4. GLUT4 trafficking is constitutive, highly regulated, multi-compartmental and involves multiple proteins. As

this protein is the most important player in glucose homeostasis, it is feasible that defects at any of the several activation steps could alter trafficking and targeting of GLUT4. Therefore, it is critically important to elucidate the molecular mechanisms leading to GLUT4 function and how any alteration impairs translocation in response to insulin. These defects would have important implication for both treatment and prevention of T2D and other related metabolic disorders.

Atp10c/ATP10C is a putative phospholipid translocase that plays a role in the maintenance of the phospholipid asymmetry and fluidity of the plasma membrane. In view of this property of *Atp10c*/ATP10C, and the displayed phenotype in the heterozygous mice, a loss of *Atp10c*/ATP10C function might upset the normal membrane environment, and as such, perturbs glucose metabolism. Inclusion of all the studies discussed in this dissertation, we established the legitimacy of our gene as a good candidate for DIO and T2D, potentially via the disruption of glucose metabolism. In view of the data presented here and the literature discussed, we are encouraged in using this model to dissect metabolic pathways involved in glucose and lipid metabolism thus gaining a better understanding of the underlying molecular mechanisms. Additionally, we validated *Atp10c*'s possible biological function by showing its location at or around the plasma membrane, and its suggested co-localization with GLUT4 (81%). Furthermore, we validated by *Atp10c*'s increased expression in two mice models of obesity, one a genetic model and the other an environmental one.

As glucose and lipid metabolism pathways are of great importance, we have focused on two pathways, the PI3K and the MAPK. Utilizing siRNA technology to alter the expression of *Atp10c in vitro*, our laboratory measured key pathway protein

expression by both Western blot and immunofluorescence techniques. Results of both *in vitro* as well as *in vivo* studies demonstrated a key role for MAPK proteins, specifically p38, in both insulin-independent, but also insulin-dependent glucose clearance. Moreover, information gleamed from these studies show a possible mechanism by which p38 and therefore, the MAPK pathway, work in mediating glucose metabolism and thus influences IR and T2D. Function assays of 2-DOG glucose uptake and immunocytochemistry of GLUT4 translocation were also performed, results of which revealed significant decreases in acute insulin stimulated glucose uptake and GLUT translocation. We believe that the resulting decrease in translocation is the direct consequence of *Atp10c*'s role in the endocytosis of GLUT4 and not an effect on the MAPK pathway, an answer which is not surprising given the literature on MAPKs non-involvement in GLUT4 translocation. Thus, *in vitro* functional outcomes again mimicked *in vivo* ones. However, we believe future work to confirm this result needs to be performed using L6-G4myc myotubes treated with p38-specific inhibitors, and repeat the translocation of GLUT4 to see if any changes are observed. For the future of this work, from an *in vitro* standpoint, stable cell lines, either over-expressing ATP10C or with ATP10C deleted should be generated and the above mentioned experiment repeated. From an *in vivo* perspective, specific targeted experiments to generate adipose tissue and skeletal muscle-specific transgenics are necessary. Then, the assessment of protein expression of these target genes should be initiated. Tissue-specific expression of *Atp10c* transgenes will determine if *Atp10c* expressed solely in muscle or in adipocytes will complement the mutant phenotypes. These experiments will give us information about

defects associated with the heterozygous deletion of *Atp10c* in a target tissue without any interference from its expression/miss-expression in the other.

LIST OF REFERENCES

1. M. Halaby, J.C. Hibma, J. He, et al. “ATM protein kinase mediates full activation of Akt and regulates glucose transporter 4 translocation by insulin in muscle cells.” *Cellular Signaling,* 20: 1555–1563, 2008.

2. M. S. Dhar, J. S. Yuan, S. B. Elliot et al. “A type IV p-type ATPase affects insulin-mediated glucose uptake in adipose tissue and skeletal muscle in mice,” *Journal of Nutritional Biochemistry*, 17: 811–820, 2006.

3. M. Larance, G. Ramm, and D.E. James. “The GLUT4 Code.” *Molecular Endocrinology*, 22(2):226–233, 2008.

4. D. Baus, K. Heermeier, M. De Hoop, et al. “Identification of a novel AS160 splice variant that regulates GLUT4 translocation and glucose-uptake in rat muscle cells.” *Cell Signal* 2008.

5. J.T. Brozinick Jr., B.A. Berkemeier, and J.S. Elmendorf. “Acting” on GLUT4: Membrane & Cytoskeletal Components of Insulin Action.” *Curr Diabetes Rev*, 3 (2): 111–122, 2007.

6. C.C. Paulusma and R.P. Oude Elferink. “The type 4 subfamily of P-type ATPases, putative aminophospholipid translocases with a role in human disease.” *Biochim Biophys Acta,* 1741(1-2): 11-24, 2005.

7. C.C. Paulusma and R. P. J. Oude Elferink. “Diseases of intramembrane lipid transport,” *FEBS Letters*, 580: 5500–5509, 2006.

8. N. J. Hoffmann and J.S. Elmendorf. “Signaling, cytoskeletal and membrane mechanisms regulating GLUT4 exocytosis.” *Trends in Endocrinology and Metabolism*, 1–7, 2011.

9. C. Huang, R. Somwar, N. Patel, et al. “Sustained exposure of L6 myotubes to high glucose and insulin decreases insulin-stimulated GLUT4 translocation but upregulates GLUT4 activity.” *Diabetes* 51: 2090–2098, 2002.

10. I.F. Charo. “Macrophage polarization and insulin resistance: PPARg in control.” *Cell Metabolism*, 6, 2007.

11. M. V. Dodson, P. S. Mir, G. J. Hausman, et al. “Obesity, metabolic syndrome, and adipocytes.” *Journal of Lipids,* 2011.

12. F. I. Milagro, J. Campion, P. Cordero et al. “A dual epigenomic approach for the search of obesity biomarkers: DNA methylation in relation to diet induced weight loss,” *The FASEB Journal*, 25: 1378–1389, 2011.

13. M. A. O'Malley and K. Stotz. "Intervention, integration and translation in obesity research: Genetic, developmental and metaorganismal approaches." *Philosophy, Ethics, and Humanities in Medicine* 6 (2), 2011.

14. M. Frontera, B. Dickins, A. Plagge et al. "Imprinted Genes, Postnatal Adaptations and Enduring Effects on Energy Homeostasis." *Genomic Imprinting*. Austin, TX: Landes Bioscience and Springer Science+ Business Media, 2008.

15. L. Laffel and B. Svoren. "Comobidities and complications of type 2 diabetes mellitus in children and adolescents." [Cited 2012 January 05]. Available at http:// www.uptodate.com/contents/

16. V. Andres and K. Walsh. "Myogenin expression, cell cycle withdrawal, and phenotypic differentiation are temporally separable events that precede cell fusion upon myogenesis." *The Journal of Cell Biology*, 132 (4): 657-66, 1996.

17. B. Bisht and C. S. Dey. "Focal adhesion kinase contributes to insulin-induced actin reorganization into a mesh harboring glucose transporter-4 in insulin resistant skeletal muscle cells," *BMC Cell Biology*, 9: 48-60, 2008.

18. K. Hayata, K. Sakano, and S. Nishinaka. "Establishment of new highly insulin-sensitive cell lines and screening of compounds to facilitate glucose consumption," *Journal of Pharmacological Sciences*, 108: 348–354, 2008.

19. J. Laskshmanan, J.S. Elmendorf, and S. Ozcan. "Analysis of insulin-stimulated glucose uptake in differentiated 3T3-L1 adipocytes." *Diabetes Mellitus Methods and Protocols: Methods in Molecular Medicine.* Ed. S. Ozcan. Totowa, NJ: Humane Press, 2003, 97-99.

20. T. Nedachi and M. Kanzaki. "Regulation of glucose transporters by insulin and extracellular glucose in C2C12 myotubes," *American Journal of Physiology: Endocrinology and Metabolism*, 291: E817–E828, 2006.

21. T. Nedachi, H. Fujita, and M. Kanzaki. "Contractile C2C12 myotube model for studying exercise-inducible responses in skeletal muscle." *Am J Physiol Endocrinol Metab.* 295(5):E1191-204, 2008.

22. W. Niu, P. J. Bilan, S.Ishikura, et al. *Am J Physiol Endocrinol Metab* 298:1058-1071, 2010.

23. T.Kobayashi, Y. Akiyama, N. Akiyama, et al. "Irbesartan enhances GLUT4 translocation and glucose transport in skeletal muscle cells." *European Journal of Pharmacology*, 649: 23–28, 2010.

24. T. Pomorski, J.C. M. Holthuis, A. Herrmann et al. “Tracking down lipid flippases and their biological functions.” *Journal of Cell Science* 117: 805-813, 2004.

25. T.R.Graham. “Flippases and vesicle-mediated protein transport.” *Trends in Cell Biology*, 14(12): 670-7, 2004.

26. S. Bryde, H. Hennrich, P.M. Verhulst et al. “CDC50 proteins are critical components of the human class-1 P4-Atpase transport machinery.” *JBC Papers*, 2010.

27. D. L. Daleke. “Phospholipid flippases.” *J Biol Chem,* 282(2): 821-5, 2007.

28. X. Zhou and T. R. Graham. “Reconstitution of phospholipid translocase activity with purified Drs2p, a type-IV P-type ATPase from budding yeast.” PNAS, 106(39): 16586–16591, 2009.

29. Z. Hua, P. Fatheddin, and T. R. Graham. “An essential subfamily of Drs2p-related P-type ATPases is required for protein trafficking between golgi complex and endosomal/ vacuolar system.” *Molecular Biology of the Cell,* 13: 3162–3177, 2002.

30. D.E. Folmer, R.P.J. Oude Elferink, and C.C. Paulusma. “P4-type ATPases–lipid flippases and their role in disease.” *Biochimica et Biophysica Acta,* 2009.

31. M.I. Sigurdsson, N. Jamshidi, J.J. Jonsson, et al. “Genome-scale network analysis of imprinted human metabolic genes.” *Epigenetics* 4(1): 43-46; 2009.

32. C. Kato, M. Tochigi, J. Ohashi, et al. “Association study of the 15q11-q13 maternal expression domain in Japanese autistic patients.” *American Journal of Medical Genetics Part B (Neuropsychiatric Genetics),* 147B: 1008–1012, 2008

33. A.J. DuBose , K. A. Johnstone , E.Y. Smith, et al. “Atp10a, a gene adjacent to the PWS/AS gene cluster, is not imprinted in mouse and is insensitive to the PWS-IC.” *Resnick Neurogenetics*, 11:145–151, 2010.

34. E.L. Nurmi, T. Amin, L.M. Olson, et al. “Dense linkage disequilibrium mapping in the 15q11–q13 maternal expression domain yields evidence for association in autism.” *Molecular Psychiatry*, 8: 624–634, 2003.

35. S.J. Kim, L.B. Herzing, J. Veenstra-VanderWeele, et al. “Mutation screening and transmission disequilibrium study of ATP10C in autism.” *Am J Med Genet*, 114: 137–143, 2002.

36. M. S. Dhar, L. S. Webb, L. Smith et al. “A novel ATPASE on mouse chromosome 7 is a candidate gene for increased body fat,” *Physiological Genomics,* 4: 93–100, 2000.

37. M. Broydell, D.M. Mazzuca, P.A. Kudo, et al. “The role of the GLUT 4 transporter in regulating rat myoblast glucose transport processes.” *Biochimica et Biophysica Acta,* 1371: 295–308, 1998.

38. E. L. Baker, R.G. Dennis, and L.M. Larkin. “Glucose transporter content and glucose uptake in skeletal muscle constructs engineered *in vitro*.” *In Vitro Ceil. Dev. Biol.--Animal* 39:434-439, 2003.

39. N. J. Bryant, R. Govers and D. E. James. “Regulated transport of the glucose transport GLUT4.” *Molecular Cell Biology*, 3, 2002.

40. L.J. Foster and A. Klip. “Mechanism and regulation of GLUT-4 vesicle fusion in muscle and fat cells.” *Am J Physiol Cell Physiol* 279:C877-C890, 2000.

41. M. Bazuine, F. Carlotti, M. J. W. E. Rabelink, et al. “The p38 mitogen-activated protein kinase inhibitor SB203580 reduces glucose turnover by the glucose transporter-4 of 3T3-L1 adipocytes in the insulin-stimulated state.” *Endocrinology* 146(4):1818–1824, 2005.

42. S. Huang, L.M. Lifshitz, C. Jones, et al. “Insulin stimulates membrane fusion and GLUT4 accumulation in clathrin coats on adipocyte plasma membranes.” *Molecular and Cellular Biology,* 27(9): 3456–3469, 2006.

43. R.L. Lo´pez-Marque´s, L.R. Poulsen, S. Hanisch, et al. “Intracellular targeting signals and lipid specificity determinants of the ALA/ALIS P4-ATPase complex reside in the catalytic ALA _-subunit.” *Molecular Biology of the Cell,* 21: 791–801, 2010.

44. J. M. Muretta, I. Romenskaia, and C.C. Mastick. “Insulin releases Glut4 from static storage compartments into cycling endosomes and increases the rate constant for Glut4 exocytosis.” The Journal of Biological Chemistry, 283 (1): 311–323, 2008.

45. R.L. Adochio, J.W. Leitner, K. Gray, et al. “Early responses of insulin signaling to high-carbohydrate and high-fat overfeeding.” *Nutrition & Metabolism,* 6:37, 2009.

46. T. Saito, C. C. Jones, S. Huang, et al. “The Interaction of Akt with APPL1 is required for insulin-stimulated Glut4 translocation.” The Journal of Biological Chemistry, 282(44): 32280–32287, 2007.

47. R. Somwar, S. Koterski, G.Sweeney, et al. “A Dominant-negative p38 MAPK mutant and novel selective inhibitors of p38 MAPK reduce insulin-stimulated glucose uptake in 3T3-L1 adipocytes without affecting GLUT4 translocation.” *The Journal of Biological Chemistry*, 277(52): 50386–50395, 2002.

48. R. Somwar, D.Y., Kim, G. Sweeney, et al. “GLUT4 translocation precedes the stimulation of glucose uptake by insulin in muscle cells: potential activation of GLUT4 via p38 mitogen-activated protein kinase.” *Biochem. J. 359*, 639±649, 2001.

49. C. J. Carlson and C.M. Rondinone. “Pharmacological inhibition of p38 MAP kinase results in improved glucose uptake in insulin-resistant 3T3-L1 adipocytes.” *Metabolism Clinical and Experimental* 54: 895– 901, 2005.

50. S. Boldt, U.H.Weidle and W. Kolch. “The role of MAPK pathways in the action of chemotherapeutic drugs.” *T Carcinogenesis* 23(11): 1831–1838, 2002.

51. C. Cabane, W. Englaro, K. Yeow, et al. “Regulation of C2C12 myogenic terminal differentiation by MKK3/p38alpha pathway.” *Am J Physiol Cell Physiol* 284:658-666, 2003.

52. H.F. Kramer and L.J. Goodyear. “Exercise, MAPK, and NF-_B signaling in skeletal muscle.” *J Appl Physiol*, 103: 388–395, 2007.

53. J.F. Schindler, J.B. Monahan and W.G. Smith “p38 pathway kinases as anti-inflammatory drug targets.” *J Dent Res*, 86: 800, 2007.

54. C. Vantaggiato, I. Formentini, A. Bondanza, et al. “ERK1 and ERK2 mitogen-activated protein kinases affect Ras-dependent cell signaling differentially.” *Journal of Biology*, 5:14, 2006.

55. D. Prusty, B.H. Park, K.E. Davis, et al. “Activation of MEK/ERK signaling promotes adipogenesis by enhancing peroxisome proliferator-activated receptor (PPAR) and C/EBP gene expression during the differentiation of 3T3-L1 preadipocytes.” *The Journal of Biological Chemistry*, 277(48): 46226–46232, 2002.

56. A. Tomas, B. Yermen, L.Min, et al. “Regulation of pancreatic-cell insulin secretion by actin cytoskeleton remodeling: role of gelsolin and cooperation with the MAPK signaling pathway.” *Journal of Cell Science*, 119: 2156-2167, 2006.

57. A. Cuenda and P. Cohen. “Stress-activated protein kinase-2/p38 and a rapamycin-sensitive pathway are required for C2C12 myogenesis.” The Journal of Biological Chemistry, 274(7): pp4341-4346, 1999.

58. K. Bismuth and F. Relaix. “Genetic regulation of skeletal muscle development.” *Experimental Cell Research*, 316: 3081-3086, 2010.

59. C. Chang, J. W. Yoo, S.W.Hong, et al. “Asymmetric shorter-duplex siRNA structures trigger efficient gene silencing with reduced nonspecific effects.” *Mol Ther.* 17(4): 725–732, 2009.

60. T. A. Brown. *Gene Cloning and DNA Analysis: An Introduction.* 5 Ed. Hoboken NJ: Wiley-Blackwell, 2006.

61. S. Okada, M. Mori, and J.E. Pessin. “Introduction of DNA into 3T3-L1 adipocytes by electroporation. “ *Diabetes Mellitus Methods and Protocols: Methods in Molecular Medicine.* Ed. S. Ozcan. Totowa, NJ: Humane Press, 2003, 93.

62. G. Kummer and N. Klocker. “Transfection of epithelial and fibroblast cell lines using Metafectene.” [Cited 05 January 2012]. Available at https://biontex-usa.com

63. L. Baldi, N. Muller, S. Picasso, et al. “Transient gene expression in suspension HEK-293 cells: Application to large-scale protein production.” *Biotechnol. Prog.* 21: 148–153, 2005.

64. Y. Durocher, S. Perret, and Kamen, A. “High-level and high-throughput recombinant protein production by transient transfection of suspension-growing human 293-EBNA1 cells.” *Nucleic Acids Res.* 30: E9, 2002.

65. S. Roshwalb, S. Gorman, S. Hurst et al. “mRNA expression of canine ATP10C, a P4-type ATPase, is positively associated with body condition score,” *The Veterinary Journal*, 190(1): 174–175, 2010.

66. A. L. Peretich, M. Cekanova, S. Hurst, et al. “PPAR agonists down regulate the expression of atp10c mRNA during adipogenesis,” *The Open Obesity Journal*, 1: 41–54, 2009.

67. M. Pfaffl. “A new mathematical model for relative quantification in quantitative RT-PCR,” *Nucleic Acids Research*, 29(9): e45, 2001.

68. “Turbofectin.” OriGene Technologies, Inc. [Cited 05 January 2012]. Available at www.origene.com

69. M. Hance, M. S. Dhar, and H. K. Plummer III. “Tobacco carcinogens stimulate different signaling pathways in breast cancer,” *Breast Cancer: Basic and Clinical Research,* 1: 25–34, 2008.

70. N. Kumar and C. S. Dey. “Development of insulin resistance and reversal by thiazolidinediones in C2C12 skeletal muscle cells,” *Biochemical Pharmacology,* 65: 249–257, 2003.

71. J. Palsgaard, C. Brøns, M. Friedrichsen, et al. “Gene expression in skeletal muscle biopsies from people with type 2 diabetes and relatives: Differential regulation of insulin signaling pathways.” PLoS ONE 4(8): e6575, 2009.

72. M. S. Dhar, C. S. Sommardahl, T. Kirkland et al. “Mice heterozygous for atp10c, a putative amphipath, represent a novel model of obesity and type 2 diabetes,” *The Journal of Nutrition,* 134: 799–805, 2004.

73. M. Meguro, A. Kashiwagi, K. Mitsuya et al. “A novel maternally expressed gene, ATP10C, encodes a putative aminophopholipid translocase associated with Angelman syndrome,” *Nature Genetics,* 28: 19–20, 2001.

74. G. Lenoir and J. C. M. Holthuis. “The elusive flippases.” *Current Biology,* 14(21): R912-13, 2004.

75. B. Bisht, H. L. Goel, and C. S. Dey. “Focal adhesion kinase regulates insulin resistance in skeletal muscle,” *Diabetologia,* 50: 1058–1069, 2007.

76. A. McCarthy, K.O. Spisak, J.T. Brozinick et al. “Loss of cortical actin filaments in insulin-resistant skeletal muscle cells impairs GLUT4 vesicle trafficking and glucose transport,” *American Journal of Physiology Cell Physiology*, 291(5): 860-868, 2006.

77. Johnson, D.K., et al., “Molecular analysis of 36 mutations at the mouse pink-eyed dilution (p) locus*”*. *Genetics*, 141(4): 1563-71, 1994.

78. Russell, L.B., et al., “Complementation analyses for 45 mutations encompassing the pink-eyed dilution (p) locus of the mouse”. *Genetics*, 141(4): 1547-62, 1995.

79. T. N. Lui, C. W Tsao, S. Y. Huang et al. “Activation of imidazoline I2b receptors is linked with AMP kinase pathway to increase glucose uptake in cultured C2C12 cells,” *Neuroscience Letters,* 474(3): 144–147, 2010.

80. T. Shimokawa, M. Kato, O. Ezaki et al. “Transcriptional regulation of muscle-specific genes during myoblast differentiation,” *Biochemical and Biophysical Research Communications,* 246: 287–292, 1998.

81. E. B. Katz, R. Burcelin, T. S.Tsao et al. “The metabolic consequences of altered glucose transporter expression in transgenic mice,” *Journal of Molecular Medicine,* 74: 639–652, 1996.

82. R. T. Watson, M. Kanzaki, and J. E. Pessin. “Regulated membrane trafficking of the insulin responsive glucose transporter 4 in adipocytes,” *Endocrine Reviews,* 25(2): 177–204, 2004.

83. G. I. Shulman. “Cellular mechanisms of insulin resistance,” *Journal of Clinical Investigation,* 106(2): 171–176, 2000.

84. R. T. Watson and J. E. Pessin. “Intracellular organization of insulin signaling and GLUT4 translocation,” *Recent Progress in Hormone Research,* 56: 175–193, 2001.

85. P. R. Shepherd and B. B. Kahn. “Glucose transporters and insulin action: implications for insulin resistance and diabetes mellitus,” *New England Journal of Medicine*, 341(4): 248–257, 1999.

86. H. Wallberg-Henriksson and J. R. Zierath. “GLUT4: a key player regulating glucose homeostasis? Insights from transgenic and knockout mice,” *Molecular Membrane Biology,* 18: 205–2011, 2001.

87. M. Fujishiro, Y. Gotob, H. Katagiri et al. “MKK6/3 and p38 MAPK pathway activation is not necessary for insulin-induced glucose uptake but regulates glucose transporter expression,” *The Journal of Biological Chemistry,* 276(23): 19800–19806, 2001.

88. N. Kumar and C. S. Dey. “Gliciazide increases insulin receptor tyrosine phosphorylation but not p38 phosphorylation in insulin-resistant skeletal muscle cells,” *The Journal of Experimental Biology,* 205: 3739–3746, 2002.

89. N. Wijesekara, F. S. L. Thong, C. N. Antonescu et al. “Diverse signals regulate glucose uptake into skeletal muscle,” *Canadian Journal of Diabetes*, 30(1): 80–88, 2006.

90. M. Koistinaho and J. Koistinaho. “Role of p38 and p44/42 mitogen-activated protein kinases in microglia,” *Glia*, 40(2): 175–183, 2002.

91. H. Wang, Q. Xu, F. Xiao et al. “Involvement of the p38 mitogen-activated protein kinase α, β isoforms in myogenic differentiation,” *Molecular Biology of the Cell*, 19: 1519–1528, 2008.

92. S. Ishikura, C.N. Antonescu, and A.Klip. “Documenting GLUT4 exocytosis and endocytosis in muscle cell monolayers.” *Curr. Protoc. Cell Biol.* 46:15.15.1-15.15.19, 2010.

VITA

Sarah Elizabeth Hurst was born in Maryville, TN on December 14, 1981. She graduated from Maryville College with a Bachelor of Arts degree in Biochemistry with an emphasis on Instrumental Analysis and Analytical Techniques in May 2004. In 2008, after two years of work at a small research and development company and two years in the healthcare industry, Sarah attended the University of Tennessee-Knoxville, where she received a Doctorate of Philosophy (Ph.D.) in Comparative and Experimental Medicine in May 2012. She is currently working on starting her own biotechnology company as well as looking for post-doctoral opportunities. She is excited to be finishing this chapter of her life and opening a new chapter towards her future dreams and goals.